

**REGULATION OF DNA REPLICATION INITIATION AND THE DNA
DAMAGE RESPONSE**

by
Lei Wei

A Dissertation presented to the Faculty of the Louis V. Gerstner, Jr.
Graduate School of Biomedical Sciences,
Memorial Sloan-Kettering Cancer Center
in Partial Fulfillment of the Requirements for the Degree of
Doctor of Philosophy

New York, NY

May, 2016

Xiaolan Zhao PhD
Dissertation Mentor

Date

Copyright © by Lei Wei 2016

DEDICATION

I dedicate this thesis to my parents, Jianrong Du and Xiaojiang Wei, who gave me the most precious thing I have ever owned, the joy of life. My parents have a heart as warm as spring, a dream as passionate as summer, and a home as cozy as autumn. Without their unconditional love, this work would not have been possible.

ABSTRACT

Genome stability relies on proper DNA replication initiation and ability to respond to DNA damage. Many regulatory mechanisms have evolved to promote the accuracy of these processes. Such regulatory mechanisms often converge on central enzymes and proteins that are required for multiple pathways. My thesis research examines three of these central regulatory targets, including the replicative DNA helicase MCM, DNA polymerase epsilon, and ssDNA binding protein RPA. Specifically, I have been using budding yeast as a model system to examine how MCM and polymerase epsilon are regulated during DNA replication initiation and how RPA sumoylation is connected to the DNA damage response.

First, I demonstrated a new MCM sumoylation cycle. I found that each of the six MCM subunits undergoes sumoylation upon loading at origins in G1 before MCM phosphorylation. MCM sumoylation levels then decline as MCM phosphorylation levels rise, thus suggesting an inhibitory role of MCM sumoylation for replication initiation. Indeed, increasing MCM sumoylation impairs replication initiation, partly through promoting the recruitment of a phosphatase that decreases MCM phosphorylation and activation. These data suggest that MCM sumoylation counterbalances kinase-based regulation, thus ensuring accurate control of replication initiation.

Second, I examined the N-terminal unique domain (NUD) of Pol2, the catalytic subunit of polymerase epsilon. This domain is highly conserved among Pol2 homologs but is not shared with other B family polymerases. Taking advantage of naturally occurring point mutations in the NUD that are found in cancer patients, I demonstrated that NUD mutations blocked replication by impairing the formation of the pre-loading complex that is required for replisome assembly. These data suggest that

the NUD is critical for replication initiation. I also found that Pol2 is sumoylated during replication and this modification occurs at a single lysine in the NUD. Mutating this lysine to arginine exacerbated the replication defects of an NUD mutant, suggesting that Pol2 sumoylation also can contribute to replication.

Last, I identified four sumoylation sites on Rfa1 and one on Rfa2 under DNA damage conditions. Mutation of these sites led to 90% reduction of Rfa1 and Rfa2 sumoylation. RPA sumoylation deficient mutants suppressed the DNA damage sensitivity of mutants with persistent Mec1-, but not Tel1- mediated checkpoint activation. This suppression correlated with a reduction of Mec1 checkpoint activity, suggesting that RPA sumoylation promotes Mec1 checkpoint activation. In addition, the combination of a RPA sumoylation deficient mutant with another Rfa1 mutant that itself barely had any defects, resulted in strong sensitivity to the topoisomerase poison camptothecin (CPT), but not to other types of genotoxins. This sensitivity is unlikely because of DNA repair defects, as indicated by the assays that we have done so far. These data suggest that sumoylated RPA may promote Mec1 checkpoint activation.

In summary, my studies revealed an essential function of the NUD domain of Pol2 in replication initiation, and a positive effect on this function by its sumoylation. I also revealed a new sumoylation cycle of MCM during replication and found that this cycle contributed to timely replication initiation by inhibiting MCM activation during G1, likely to prevent premature replication. Last, I have gathered evidence that RPA sumoylation promotes Mec1 mediated checkpoint activation, suggesting that there is a crosstalk between checkpoint and the DNA damage induced sumoylation response.

BIOGRAPHICAL SKETCH

Lei Wei was born in a quaint southern town, Changle, in Fujian province, China. Changle means long-lived happiness. Bestowed by this auspicious meaning and the care of his parents and grand parents, Wei had a joyful childhood. He graduated from the Changle Shiyuan primary school, Huaqiao middle school, and then Changle No.1 high school. He then left his hometown and entered Tsinghua University in Beijing. He completed his undergraduate research under the mentorship of Professor Zihe Rao, a prominent structure biologist. Wei's undergraduate research focused on the crystallization of SARS non-structural proteins 2, 3, and the delta-endotoxin insecticidal Cry8Ea1. After the acquirement of a Bachelor in Science (BS) in Biological Science, Wei continued to acquire a Master degree in the same lab. On July 15th, 2009, Wei landed in New York and began his pursuit of PhD at the Louis V. Gerstner, Jr. Graduate School of Biomedical Sciences at Memorial Sloan-Kettering Cancer Center. Subsequently, he joined Professor Xiaolan Zhao's laboratory and focused on studying the regulation of two critical processes in genome maintenance, DNA replication and DNA repair.

ACKNOWLEDGMENT

I would love to express my gratitude to those people who have helped, influenced, and shaped me. These include my teachers, parents, colleagues and friends.

My thesis mentor Xiaolan is a generous, warm and kind person, who nurtured me in almost every aspect of my graduate student life. Her passionate lectures during my first year opened the gate of molecular biology and yeast genetics for me. I am mesmerized by the puzzles of DNA replication and repair and Xiaolan showed me the way to solve them. Among many precious things that she gave or taught me, I value two of them the most. First is her time. Despite time being the most valuable possession for every person, she is most generous with it. Her door is always open, and no question, be it a scientific or personal one, is too trivial for her to give you her full attention. The amount of time she shared with me is the key for my growth as a graduate student. Second is her attitude towards mistakes. She sees them as opportunities to learn, to grow, and to be better. This attitude not only contributes to her academic achievements, but also her big heart. I thank her for all her time, her mentoring, and her enthusiasm.

I would love to thank my thesis committee members, Ken and Scott, for their guidance and advice over the past few years. They used their logic, rigorousness, and the pursuit for pure scientific perfection to set the best examples for me to learn. I also would like to thank Ken for being an excellent Dean and pouring his precious time to the graduate school and graduate students. I would like to thank Scott for recruiting such wonderful people in his lab, with many of whom I have spent much joyful time. In addition, I thank Scott for his witty humor. I am very grateful to Lorraine, my external examiner, for her precious time to read my thesis and her suggestions. I also would like to thank Jayanta to chair my thesis exam.

I owe much to my undergraduate mentor, Zihe Rao, for his encouragement and persuasion for me to pursue science. I owe all my knowledge to my teachers, from kindergarten till today. I will always carry a piece of their dreams and expectations wherever I go.

I would like to thank my graduate school, the most nurturing and interactive place I have experienced. I am very fortunate to be a part of it. I would love to thank the unsung heroes for my thesis study, Linda, Iwona, Maria, and Ivan, who have made tremendous efforts to ensure my smooth study. I would like to thank Iwona for helping format this dissertation.

I thank my parents for their unconditional love and support. I thank their dedication for each other, the loving home they have created for me, and their support for my education. I thank them for helping me prepare my chemistry lab during my high school years. These creative and joyful experiences have fueled my curiosity and passion for science. I owe everything to my loving parents.

I have been most fortunate to have many wonderful colleagues and friends in and out of the lab. I thank Jackie and Nalini for their valuable suggestions to my manuscripts and thesis writing. I thank Bingbing for being the most responsible and caring friend, who carries such a passion for science. I thank Michael for insightful discussions. I thank Shelly for her kindness. I enjoyed their presence in the lab. For the past lab members, I thank my dear friend Prabha for teaching me when I joined the lab and for being such a loving person. I cherish all the laughter we shared. I am very grateful to Lisa for her most kind heart and for helping me through difficult times. I thank Inn for her lively giggles, which bring smiles to my face every time I hear them. I am also

grateful to other past lab members, including Koyi, Catherine and Yan, for their contribution to the lab and friendship. For friends out of the lab, I thank all the lovely RRL 9th floor residents for creating this wonderful atmosphere. I would like to thank Isabel for her help with R language, thesis writing tips, and the laughs we shared. I would like to thank Yuanyuan, my dearest friend, without his encouragement, I would have entered a different life trajectory in 2008. I thank Liangliang, Yu, Wei, Xiao, Danming, Jia, Weiran, Qi, Zijing, Ke, and many other friends for touching my life in Tsinghua. I thank all my classmates in the year of 2009. I believe we are going to share a life-long friendship. I am grateful to Yuchen, Weiran, Yilong, Rui, Dayong, Sheng, Yifan, and many others for entering my life and making it shine.

TABLE OF CONTENTS

| | |
|--|-----|
| LIST OF TABLES..... | xv |
| LIST OF FIGURES | xvi |
| LIST OF ABBREVIATIONS | xix |
| Chapter 1 | 1 |
| Introduction | 1 |
| 1.1 Overview of DNA replication initiation in yeast..... | 1 |
| Origin licensing..... | 2 |
| Origin firing..... | 3 |
| Multiple mechanisms to prevent re-replication..... | 7 |
| Outstanding questions to be addressed in replication initiation | 10 |
| 1.2 Overview of the DNA damage response (DDR) and two key posttranslational modifications (PTMs) that function in the DDR | 10 |
| Activation of the apical checkpoint kinases Mec1 and Tel1 | 13 |
| Transduction of checkpoint signaling by Mec1 and Tel1 | 14 |
| Termination of the Mec1 and Tel1 checkpoints | 14 |
| Summary of the Mec1 and Tel1 checkpoint activation and termination..... | 16 |
| 1.3 Overview of DNA damage induced sumoylation (DDIS)..... | 17 |
| Siz2 mediated DDIS branch..... | 17 |
| The interplay between DDIS and the Mec1 mediated checkpoint activation | 19 |
| Summary of the two branches of DDR and questions to be addressed | 20 |
| 1.4 The SUMO system..... | 20 |
| SUMO E1, E2 and E3 enzymes and sumoylation..... | 21 |
| Desumoylation enzymes and the removal of SUMO | 22 |
| The function of sumoylation and desumoylation | 23 |
| 1.5 Thesis objective | 24 |

| | |
|--|----|
| Chapter 2 | 31 |
| A new MCM modification cycle regulates DNA replication initiation | 31 |
| Introduction | 31 |
| Results | 33 |
| Detection of MCM-subunit sumoylation during normal growth..... | 33 |
| MCM sumoylation on chromatin requires its loading at origins..... | 35 |
| MCM sumoylation levels peak in G1 and decline in S phase | 35 |
| MCM sumoylation loss in S phase requires DDK and GINS..... | 36 |
| Mcm6 sumoylation loss coincides with origins firing | 38 |
| Mcm6-SuOn (SUMO on) increases MCM sumoylation..... | 38 |
| Mcm6-SuOn impairs replication initiation | 40 |
| Increasing MCM sumoylation levels compromises CMG formation (Cdc45-MCM-GINS) | 41 |
| Removing a PP1 (Protein phosphatase 1) cofactor rescues defects of Mcm6-SuOn cells | 42 |
| Mcm6-SuOn shows increased association with PP1 | 43 |
| Discussion..... | 44 |
| MCM sumoylation negatively regulates origin firing..... | 44 |
| The reversal of MCM sumoylation | 45 |
| The potential effect of Mcm6-SuOn in diploid cells | 46 |
| Other potential roles for MCM sumoylation | 46 |
| Methods and Materials..... | 48 |
| Chapter 3 | 78 |
| Function and modification of Pol2 N-terminal unique domain (NUD) | 78 |
| Introduction | 78 |
| Results | 80 |

| | |
|--|-----|
| Pol2-NUD and cancer mutations in this domain | 80 |
| Pol2-NUD is essential for viability | 81 |
| The Pol2-NUD mutant <i>pol2-REL</i> is defective in replication..... | 82 |
| <i>pol2-REL</i> impairs CMG formation and replisome assembly | 82 |
| <i>pol2-REL</i> is defective in pre-LC formation | 84 |
| Pol2 is sumoylated during DNA replication | 85 |
| Pol2 sumoylation occurs on a single lysine on the NUD..... | 86 |
| <i>pol2-sd</i> (sumoylation deficient) exacerbates the growth defects of <i>pol2-REL</i> | 86 |
| <i>pol2-sd</i> exacerbates the replisome assembly defect in <i>pol2-REL</i> | 87 |
| Discussion..... | 88 |
| Pol2 NUD is essential? | 88 |
| The paradox of the essential NUD within the dispensable Pol2 N-terminus..... | 88 |
| The effect of <i>pol2-REL</i> on Dpb11 binding | 89 |
| Pol2 NUD mutations in cancer | 91 |
| Pol2 sumoylation on the NUD contributes to replisome assembly..... | 92 |
| Molecular mechanisms of the function of Pol2 sumoylation | 93 |
| Multiple functions of sumoylation in replication initiation..... | 94 |
| Methods and materials..... | 96 |
| Chapter 4 | 115 |
| Interplay between RPA sumoylation and the Mec1 checkpoint..... | 115 |
| Introduction | 115 |
| Results | 118 |
| Detection of Rfa1 and Rfa2 sumoylation..... | 118 |
| Rfa1 sumoylation occurs under genotoxin treatments that activate Mec1..... | 119 |
| Confirming two major sites for Rfa1 sumoylation..... | 120 |
| K133 and K494 are not responsible for Rfa1 sumoylation..... | 121 |

| | |
|---|-----|
| Rationale for identifying candidate sites for residual Rfa1 sumoylation | 121 |
| Identification of two additional sites of Rfa1 sumoylation..... | 123 |
| Determining Rfa2 sumoylation sites..... | 124 |
| Properties of RPA sumoylation sites..... | 124 |
| <i>rfa1-4KR</i> rescues <i>srs2Δ</i> defects caused by persistent Mec1 checkpoint..... | 125 |
| <i>rfa1-4KR</i> augments suppression of <i>srs2Δ</i> by another Rfa1 allele..... | 126 |
| <i>rfa1-5KR</i> leads to reduced Rad53 phosphorylation levels in <i>srs2Δ</i> cells | 127 |
| Rfa2 sumoylation deficient mutant behaves similarly to <i>rfa1-4KR</i> | 128 |
| Loss of Rad52 and Rad59 sumoylation do not confer <i>srs2Δ</i> suppression..... | 129 |
| <i>rfa1-5KR</i> does not affect DNA end resection | 129 |
| Discussion..... | 130 |
| Potential mechanisms by which RPA sumoylation regulates the Mec1 checkpoint | 130 |
| Generate new Rfa2 and Rfa3 sumoylation deficient alleles..... | 131 |
| Why do <i>rfa1-4KR</i> and <i>rfa1-K494R</i> specifically cause CPT sensitivity? | 132 |
| Multiple functions of RPA sumoylation..... | 133 |
| Strategies for identification of sumoylation sites | 134 |
| Methods and Materials..... | 136 |
| Chapter 5 | 148 |
| Conclusions and Perspectives..... | 148 |
| Summary and conclusions..... | 148 |
| Emerging roles for SUMO-based regulation of DNA replication | 148 |
| Inhibitory effects of sumoylation on replication initiation | 148 |
| A positive role for sumoylation on replication initiation..... | 150 |
| SUMO and replication progression | 150 |
| Low levels of sumoylation can lead to robust biological effects | 152 |

| | |
|---|-----|
| Crosstalk between sumoylation and other types of PTMs | 154 |
| The function of Pol2 in replication initiation | 156 |
| Conclusions and future perspectives | 157 |
| REFERENCES | 160 |

LIST OF TABLES

| | |
|---|-----|
| Table 1. Strains used in chapter 2 | 54 |
| Table 2. Strains and plasmids used in chapter 3 | 100 |
| Table 3. Strains and plasmids used in chapter 4 | 138 |

LIST OF FIGURES

| | |
|--|----|
| Figure 1-1. Replication initiation in eukaryotic cells | 25 |
| Figure 1-2. Activation of the Mec1 mediated checkpoint | 26 |
| Figure 1-3. Activation of the Tel1 mediated checkpoint | 27 |
| Figure 1-4. Reversal of the Mec1 and Tel1 mediated checkpoints | 28 |
| Figure 1-5. Siz2 mediated DNA damage induced sumoylation (DDIS) branch | 29 |
| Figure 1-6. The SUMO conjugation cycle and its biological effects | 30 |
| Figure 2-1. Sumoylation of six MCM subunits occurs on chromatin and depends on MCM loading at replication origins | 57 |
| Figure 2-2. Detection of MCM subunit sumoylation under normal growth conditions | 59 |
| Figure 2-3. Examination of MCM subunits in the absence of Cdc6, DDK, and GINS | 60 |
| Figure 2-4. Sumoylation levels of MCM subunits oscillate during the cell cycle | 61 |
| Figure 2-5. Mcm2-6 sumoylation loss at the G1-S transition requires DDK, GINS and replication initiation | 63 |
| Figure 2-6. Examination of Mcm6-SuOn effects on sumoylation and MCM complex levels | 65 |
| Figure 2-7. Increasing sumoylation of Mcm6-SuOn slows growth and this defect is suppressed by a <i>ubc9</i> mutant | 66 |
| Figure 2-8. Genetic examination of Mcm6-SuOn sumoylation | 68 |

| | |
|--|-----|
| Figure 2-9. Mcm6-SuOn impairs replication initiation | 69 |
| Figure 2-10. Genome-wide profiles of copy number changes in Mcm6-SuOn and Mcm6-ctrl cells. | 71 |
| Figure 2-11. Mcm6-SuOn cells exhibit low levels of the Cdc45-MCM-GINS (CMG) complex formation and phosphorylation of Mcm4 that can be suppressed by <i>rif1</i> Δ | 72 |
| Figure 2-12. Examination of Mcm6-SUMO fusion and Glc7-Mcm6 association | 74 |
| Figure 2-13. <i>rif1</i> Δ suppresses Mcm6-SuOn growth defects and Mcm6-SuOn leads to enhanced association between Mcm6 and the Glc7 phosphatase | 75 |
| Figure 2-14. Examination of Mcm4 sumoylated form, MCM desumoylation, and verification of Mcm3 protein levels | 77 |
| Figure 3-1. Pol2 is the hub of the interaction network during pre-LC formation | 102 |
| Figure 3-2. The N-terminal unique domain (NUD) of Pol2 is essential for cell growth | 103 |
| Figure 3-3. Mutations in the Pol2 NUD cause temperature sensitivity and slow S phase progression | 105 |
| Figure 3-4. <i>pol2-REL</i> is defective in CMG formation and replisome assembly | 106 |
| Figure 3-5. <i>pol2-REL</i> diminishes Pol2-Dpb11 interaction | 108 |
| Figure 3-6. Pol2 sumoylation correlates with DNA replication and occurs at a single lysine on the NUD | 110 |
| Figure 3-7. Pol2 sumoylation deficient mutation exacerbates the replisome assembly defects caused by <i>pol2-REL</i> | 112 |

| | |
|--|-----|
| Figure 3-8. A working model of the function of the NUD and Pol2 sumoylation | 114 |
| Figure 4-1. Characterization of the sumoylation status of Rfa1 and Rfa2 | 140 |
| Figure 4-2. Determination of the sumoylation sites on Rfa1 | 141 |
| Figure 4-3. The domain composition and structure of the RPA complex | 142 |
| Figure 4-4. The Rfa1 sumoylation deficient mutant is defective in Mec1 mediated checkpoint activation | 143 |
| Figure 4-5. The K494 residue of Rfa1 contacts DNA | 144 |
| Figure 4-6. <i>rfa1-5KR</i> has decreased phosphorylation of Rad53 under CPT treatment conditions | 145 |
| Figure 4-7. Rfa2 sumoylation deficient mutant phenocopies Rfa1 sumoylation deficient mutant | 146 |
| Figure 4-8. <i>rfa1-5KR</i> mutant shows proficient DSB resection, and exacerbates the CPT sensitivity of mutants specifically defective in CPT repair pathway | 147 |

LIST OF ABBREVIATIONS

- AID:** IAA-inducible degron
- CDK:** Cyclin-dependent kinase
- CMG:** Cdc45-MCM-GINS
- CMGE:** Cdc45-MCM-GINS-Pol ϵ
- CPT:** Camptothecin
- Ctrl:** Control
- DDIS:** DNA damage induced sumoylation
- DDK:** Dbf4-dependent kinase
- DDR:** DNA damage response
- DSB:** Double stranded break
- FACS:** Fluorescence-activated cell sorting
- HA:** Hemagglutinin
- HF:** Hexa-histidine (His6)-Flag
- HR:** Homologous recombination
- HU:** Hydroxyurea
- IAA:** Indole-3-acetic acid
- IP:** Immunoprecipitation
- iPOND:** Isolation of protein on nascent DNA chains
- MMS:** Methyl methanesulfonate
- NEM:** N-Ethylmaleimide
- Ni-NTA:** Nickel-nitrilotriacetic acid
- NUD:** N-terminal unique domain
- OriDB:** DNA Replication Origin Database
- PD:** Pull down

pre-LC: pre-Loading complex

PTM: Posttranslational modification

SCA1: Spinocerebellar ataxia type 1

sd: Sumoylation deficient

SIM: SUMO interacting motifs

ssDNA: Single stranded DNA

SUMO: Small Ubiquitin-like Modifier

SuOn: SUMO on

TCA: Trichloroacetic acid

Ts: Temperature sensitivity

WH domain: Winged helix domain

YPD: Yeast peptone dextrose

Y2H: Yeast two hybrid

2D gel: Two-dimensional agarose gel electrophoresis

3AT: 3-amino-1,2,4-triazole

5-FOA: 5-fluoroorotic acid

Chapter 1

Introduction

DNA replication and the DNA damage response (DDR), two critical processes for proper genome maintenance, are tightly regulated at spatial and temporal levels through multilayered mechanisms. A wealth of genetic and biochemical studies in several organisms has revealed major roles of post-translational modifications (PTMs) in the control of these two processes. Kinase-mediated phosphorylation is the best-demonstrated class of PTMs that has been shown generally to confer positive regulation of these processes. More recently, genetic studies have hinted at a role for the small ubiquitin-like modifier (SUMO) as a key PTM involved in these two processes. My thesis research investigated the mechanisms by which SUMO provides regulatory mechanisms for DNA replication initiation and DNA damage checkpoint activation. I used the budding yeast as a model system because both processes have been well characterized in this organism in addition to the availability of powerful genetic and biochemical tools. In this introduction, I first describe the DNA replication initiation process and its regulation by phosphorylation as characterized in yeast. I also introduce the DDR in yeast, including the classical kinase-based checkpoint activation and DNA damage induced sumoylation (DDIS). Lastly, I summarize the SUMO pathway and delineate my thesis objectives and my main findings.

1.1 Overview of DNA replication initiation in yeast

Eukaryotic organisms initiate DNA replication at hundreds of genomic sites called origins. Current work suggests that the activation of each replication origin requires two temporally separated steps, origin licensing and origin firing (Diffley et al. 1994; Kelly

and Brown 2000; Bell and Dutta 2002; Sclafani and Holzen 2007; Remus and Diffley 2009; Wei and Zhao 2016b) (Figure 1-1). These two steps are centered on the loading and activation of the replicative helicase MCM (Mini-Chromosome Maintenance), respectively. In this subsection, I first introduce how MCM is loaded onto the replication origins during the origin-licensing step. Then, I describe how loaded MCM is activated during the origin-firing step, I focus on the mechanisms by which two kinases activate the loaded MCM. In addition, the phosphatases that counteract these two kinases during replication initiation are also introduced. Lastly, I discuss how deleterious re-replication and premature replication events are prevented.

Origin licensing

As shown in Figure 1-1, origin licensing occurs during late M to G1 phase and entails the loading of replicative helicase MCM onto the origins. MCM is composed of the Mcm2-7 subunits, each with an ATPase domain and two regulatory domains. MCM loading onto origins depends on several protein factors in yeast (Kelly and Brown 2000; Bell and Dutta 2002; Sclafani and Holzen 2007; Remus and Diffley 2009). The first factor is the origin recognition complex (ORC), a hexameric ATPase complex composed of the Orc1-6 subunits (Bell and Stillman 1992; Diffley and Cocker 1992). ORC recognizes and binds to origin sequences, thereby determining the sites of subsequent MCM loading (Rao and Stillman 1995; Rowley et al. 1995; Bell and Kaguni 2013; Costa et al. 2013). The second factor involved in MCM loading is the ATPase Cdc6 protein that physically interacts with ORC and MCM, and serves as a recruitment factor for MCM loading to ORC-bound origins (Liang et al. 1995; Cocker et al. 1996; Speck et al. 2005; Fernández-Cid et al. 2013; Sun et al. 2013). The concerted ATP hydrolysis of ORC and Cdc6 enables MCM loading (Klemm et al. 1997; Klemm and Bell 2001; Randell et al. 2006). It has been shown that the Mcm3 C-terminal tail directly binds the ORC-Cdc6 complex and

stimulates its ATPase activity (Frigola et al. 2013); however, the detailed mechanism remains to be elucidated. The MCM subunits that are first loaded onto the origin are in an inactive, double hexameric form and will be referred to as loaded MCM hereafter.

Origin firing

Loaded MCM cannot initiate replication until S phase when it is converted to the active, single hexamer form. The process of MCM activation is called origin firing (Gambus et al. 2006; Moyer et al. 2006b; Pacek et al. 2006; Ilves et al. 2010; Kang et al. 2012) (Figure 1-1). Origin firing occurs in a temporal order such that some origins fire early in S phase, while others in mid or late S phase (Masai et al. 2010). Regardless of the timing, origin firing requires the formation of an active replicative helicase composed of a single MCM hexamer and two accessory factors, namely Cdc45 and the GINS complex (Gambus et al. 2006; Moyer et al. 2006b; Pacek et al. 2006; Ilves et al. 2010; Kang et al. 2012). The complex formed between MCM, Cdc45 and GINS, called CMG, is capable of DNA unwinding. There are extensive interactions among the three protein entities such that each contacts the other two factors at multiple interfaces (Costa et al. 2011; Sun et al. 2015; Yuan et al. 2016). Both Cdc45 (containing DNA-binding activity) and GINS (composed of four subunits, Psf1-3 and Sld5) appear to play a structural role (Costa et al. 2011). Previous biochemical studies using purified MCM subunits show that the interaction between Mcm2 and Mcm5 is weaker than that of other MCM subunit pairs (Crevel et al. 2001; Davey et al. 2003; Bochman et al. 2008). A gap between Mcm2/5 subunits has been proposed to be critical to load MCM onto DNA and the closure of the gate is critical for its helicase activity (Samel et al. 2014). Indeed, the gate between Mcm2 and Mcm5 can be observed in electronic microscopy (Costa et al. 2011; Costa et al. 2014). Importantly, biochemical and structural studies have shown that Cdc45 and

GIN5 mainly help to stabilize MCM on DNA by sealing this gate between Mcm2 and Mcm5 subunits (Moyer et al. 2006a; Costa et al. 2011).

The recruitment of Cdc45 and GINS to loaded MCM requires two essential and conserved kinases, DDK (Dbf4-dependent kinase) and CDK (cyclin-dependent kinase), as well as DNA polymerase Pol ϵ and three scaffolding proteins, Sld2, Sld3, and Dpb11 (Gambus et al. 2006; Moyer et al. 2006b; Pacek et al. 2006; Ilves et al. 2010; Kang et al. 2012)(Figure 1-1). DDK phosphorylates the MCM subunits, and the phosphorylated peptide in Mcm4 binds to Sld3, recruiting Sld3 and its binding partner Cdc45 to loaded MCM (Sheu and Stillman 2006; Sheu and Stillman 2010; Deegan et al. 2016). Subsequently, CDK phosphorylates Sld2 and Sld3, which work together with Dpb11 and Pol ϵ to recruit GINS to loaded MCM (Tanaka et al. 2007; Zegerman and Diffley 2007). These two recruitment events allow the formation of CMG. Subsequently, more than a dozen additional proteins are recruited leading to the formation of the replisome that can initiate DNA synthesis (Gambus et al. 2006; Morohashi et al. 2009). The Sld2-Dpb11-Sld3 scaffold proteins are finally dissociated from CMG by binding to ssDNA (single-stranded DNA) at origins and do not travel with the replisome (Bruck and Kaplan 2011; Kanter and Kaplan 2011; Dhingra et al. 2015)(Figure 1-1).

During the multi-step replisome formation summarized above, DDK and CDK-regulated events serve as triggers for origin firing. As replication needs to be tightly coupled with other events of S phase and to ensure each DNA locus is replicated once and only once per cell cycle, replisome assembly is also subjected to negative regulation to prevent re-replication events. Some of the known negative regulation is partly achieved by direct reversal of DDK and CDK phosphorylation through the action of specific phosphatases. In the sections below, I describe in more detail the roles of DDK

and CDK, their counteracting phosphatases, as well as the roles of the scaffold proteins during CMG formation.

The role of DDK in CMG formation

How does DDK target loaded MCM and promote Cdc45 recruitment? Elegant genetic and biochemical studies during the past decade have addressed some of the detailed mechanisms. DDK physically associates with the loaded MCM via binding to Mcm2 and Mcm4 subunits (Sheu and Stillman 2006; Bruck and Kaplan 2009; Ramer et al. 2013; Bruck and Kaplan 2014). It has been shown that the main DDK phosphorylation targets among the MCM subunits are Mcm4 and Mcm6 (Lei et al. 1997; Francis et al. 2009; Randell et al. 2010). These MCM subunits contain N-terminal serine/threonine rich domains (NSD) that harbor the DDK consensus sites S/T-D/E and S/T-S/T-P/Q (Randell et al. 2010)(where the first S/T is targeted by DDK). Among these consensus sites, a dozen serines and threonines on Mcm4 are the most critical for replication initiation. Expression of Mcm4 phospho-mimetic mutants with these sites changed to acidic amino acids, or removal of the amino acids 74-174 of the Mcm4 NSD, bypasses the DDK requirement for CMG formation, suggesting that DDK-mediated phosphorylation at these sites alleviates the inhibitory effect of Mcm4 NSD on initiation (Sheu and Stillman 2006; Randell et al. 2010; Sheu and Stillman 2010). What is the inhibitory effect of Mcm4 NSD and how does MCM phosphorylation alleviate it? A recent study has shown that the DDK-mediated phosphorylation of Mcm4 and Mcm6 appears to enable the recruitment of Sld3 and its binding partner Cdc45 to the loaded MCM (Deegan et al. 2016). It has been shown that Sld3 directly binds DDK-phosphorylated Mcm4 and Mcm6 and abrogation of these interactions leads to lethality (Deegan et al. 2016). Therefore, Sld3

serves as an essential reader of DDK-phosphorylated MCM and recruits Cdc45. These observations suggest that the inhibitory effect of Mcm4 NSD is to prevent Sld3 binding.

CDK-mediated formation of the preloading complex (pre-LC) and CMG

The delivery of the third component of CMG, GINS to loaded MCM requires CDK. In budding yeast, the key CDK substrates for CMG formation are the scaffold proteins Sld2 and Sld3 (Tanaka et al. 2007; Zegerman and Diffley 2007) (Figure 1-1). These phosphorylation events enable recruitment of GINS to loaded MCM through a two-step process. First, CDK phosphorylation of Sld2 at site T84 enables the formation of a 10-protein preloading complex (pre-LC) (Masumoto et al. 2002; Tak et al. 2006; Muramatsu et al. 2010). Pre-LC contains phosphorylated Sld2 (Sld2-p), GINS, Pol ϵ (Pol2-Dpb2-Dpb3-Dpb4) and Dpb11 (Figure 1-1). Pre-LC can be isolated biochemically independent of chromatin after crosslinking, suggesting it likely represents a transient step (Muramatsu et al. 2010). Dpb11 contains two pairs of tandem BRCT domains in the N and C-terminus, respectively. Phosphorylated Sld2 interacts with the C-terminal BRCT repeats (Tanaka et al. 2007; Zegerman and Diffley 2007). The Pol2 and Dpb2 subunits of Pol ϵ are essential for pre-LC formation by binding to Dpb11, Sld2, and GINS (Muramatsu et al. 2010) (Figure 1-1). This function of Pol ϵ appears to account for its essential roles, and is distinct from its role in DNA polymerization.

Second, CDK phosphorylates Sld3 at residues T600 and S622 (Zegerman and Diffley 2007). Phosphorylated Sld3 (Sld3-p) binds to the N-terminal BRCT repeats of Dpb11, thus providing a linkage between pre-LC and loaded MCM (Tanaka et al. 2007; Zegerman and Diffley 2007) (Figure 1-1). This results in the formation of an unstable complex between pre-LC and MCM-Sld3(p)-Cdc45, which is rapidly converted to the

active replicative helicase CMG complex (Figure 1-1). It is proposed that Pol ϵ remains bound to CMG, and such a complex has been termed as CMGE (Cdc45-MCM-GINS-Pol ϵ) that is a part of the replisome and traverses the leading strand (Langston et al. 2014; Sun et al. 2015).

Multiple mechanisms to prevent re-replication

If the origin licensing and firing step could occur at the same cell cycle phase, then the MCM complex could be loaded onto origins that have already been fired and lead to re-replication. In order to duplicate the genome only once per cell cycle, the cells need to prevent re-replication events. One important factor that prevents re-replication is separation of the licensing and firing steps, such that loaded MCM cannot be activated during origin licensing and loading of additional MCM proteins is blocked once origin firing starts (Blow and Dutta 2005; Arias and Walter 2007). Here I list two mechanisms that separate the origin licensing and firing steps (Figure 1-1). First, protein phosphatase 1 dephosphorylates DDK substrates and prevents activation of loaded MCM during the origin-licensing step. Second, CDK blocks MCM loading during the origin-firing step.

De-phosphorylation of DDK substrates via Protein Phosphatase 1

Although DDK is essential to trigger MCM activation during S phase, it may also trigger potentially dangerous replication outside of S phase. It has been shown that DDK activity appears in late G1 phase (Tanaka et al. 2011). It is thus logical that the DDK activity should be restricted such that it does not prematurely initiate CMG assembly during G1 phase. One means of achieving this is through protein phosphatase 1 (PP1) (Figure 1-1). PP1 binds DDK via its cofactor, Rif1. Two N-terminal motifs of Rif1, SILK and RVXF, mediate interaction with PP1, while the C-terminal tail of Rif1 mediates DDK interaction

(Davé et al. 2014; Hiraga et al. 2014; Mattarocci et al. 2014). It is not clear whether the association with DDK is sufficient to target the PP1-Rif1 complex to loaded MCM or whether additional mechanisms are involved. Importantly, it is known that in the absence of PP1 or Rif1, DDK can trigger MCM phosphorylation in G1 phase, suggesting a role for the PP1-Rif1 complex in counteracting untimely DDK activity (Davé et al. 2014; Hiraga et al. 2014; Mattarocci et al. 2014; Poh et al. 2014). The biological implication of PP1-Rif1-mediated events is deduced from genetic suppression and genome-wide replication profiling. Deleting Rif1 or mutating the Rif1 domains involved in PP1 binding increase Mcm4 phosphorylation and suppress the replication initiation defects of *cdc7-4* mutants (Davé et al. 2014; Hiraga et al. 2014; Mattarocci et al. 2014). In CDC7 wild-type cells, *rif1* Δ advances the replicating timing of more than one hundred late replication origins and shortens the duration of S phase (Hayano et al. 2012). Thus, the function of PP1-Rif1 is twofold: 1) to restrict DDK activity during G1 phase and 2) to establish a proper order of origin firing during S phase.

One question raised by the PP1-Rif1 mediated inhibition of DDK is: How is DDK activated during S phase? It turns out that when S phase starts, the PP1-Rif1 mediated inhibition of Mcm4 phosphorylation begins to weaken because an increase in DDK protein levels. This is achieved by increased transcription of DDK subunits and blocking the degradation of the Dbf4 subunit of DDK (Chapman and Johnston 1989; Cheng et al. 1999; Oshiro et al. 1999; Ferreira et al. 2000). Higher DDK levels can directly augment Mcm4 phosphorylation and also remove the PP1-mediated inhibition by modification of Rif1. Both DDK and CDK phosphorylate Rif1 at regions surrounding its SILK and RVXF motifs, weakening its association with PP1 (Davé et al. 2014; Hiraga et al. 2014). This results in a positive feed-forward mechanism for DDK-dependent phosphorylation.

Similar to negative regulation of DDK mediated phosphorylation by PP1, studies in yeast show that the Cdc14 phosphatase can reverse a myriad of CDK-mediated phosphorylation events in mitosis, including phosphorylated Sld2 (Visintin et al. 1998; Bloom and Cross 2007) (Figure 1-1). However, It is not clear if Cdc14 mediated de-phosphorylation of Sld2-p contributes to prevention of re-replication.

*CDK blocks MCM loading via three redundant mechanisms**

CDK is essential to prevent re-replication because it blocks MCM loading onto origins once they fire (Figure 1-1). CDK employs three mechanisms to achieve this by targeting three key factors involved in MCM loading (Nguyen et al. 2001). These mechanisms are redundant, such that only elimination of all three can generate a detectable re-replication event. First, CDK interacts with and phosphorylate Cdc6 in late G1 phase and S phase, leading to its recognition by SCF^{Cdc4} ubiquitin ligase and degradation (Elsasser et al. 1996; Drury et al. 1997; Elsasser et al. 1999; Sánchez et al. 1999; Calzada et al. 2000; Drury et al. 2000; Perkins et al. 2001). Second, CDK phosphorylation of Mcm3 triggers MCM export after MCM loading is completed but before origin firing starts (Labib et al. 1999; Nguyen et al. 2000; Liku et al. 2005). Lastly, CDK phosphorylates two subunits of the ORC complex, namely Orc2 and Orc6. The phosphorylation of these two proteins diminishes recruitment of MCM to origins (Nguyen et al. 2001; Wilmes et al. 2004; Chen and Bell 2011).

**Adapted from: Springer, The Initiation of DNA Replication in Eukaryotes, Editors: Kaplan, Daniel L., Chapter 18: Role of Posttranslational Modifications in Replication Initiation, 2016, Wei, L. & Zhao, X., Springer International Publishing, ISBN 978-3-319-24696-3, with permission from Springer*

Outstanding questions to be addressed in replication initiation

As described above, our understanding of eukaryotic replication initiation has greatly advanced owing to elegant genetic and biochemical studies *in vitro*. Although much progress has been made, several key mechanisms underlying replication initiation remain ambiguous. In particular, two outstanding questions are relevant to my study.

1. Considering the regulation of loaded MCM is at a central position in replication initiation, could any other type of PTMs contribute to regulation of loaded MCM?

In chapter 2, I describe that loaded MCM is sumoylated and this modification restrains MCM activation.

2. Given that Pol ϵ is critical for pre-LC formation, how does it execute this function?

In chapter 3, I describe that a unique N-terminal domain in the largest subunit of Pol ϵ plays an essential role in pre-LC formation.

1.2 Overview of the DNA damage response (DDR) and two key posttranslational modifications (PTMs) that function in the DDR

Aside from DNA replication, another important process for maintenance of genome integrity is the DDR. The DDR detects DNA lesions generated by intrinsic or extrinsic sources and coordinates cellular programs that promote recovery from damage. The DDR relies heavily on various forms of PTMs that can quickly and reversibly change many protein properties and affect multiple cellular processes at once. The best understood PTM in the DDR are the apical checkpoint kinases Mec1/ATR and Tel1/ATM mediated phosphorylation processes (Figures 1-2 and 1-3). In budding yeast, Mec1 is the primary checkpoint kinase and Tel1 has a minor role. Several other PTMs have been shown to be involved in DDR and one is DNA damage induced sumoylation (DDIS)

(Cremona et al. 2012; Psakhye and Jentsch 2012; Chung and Zhao 2015). In the sections below, I will first summarize the three steps of canonical checkpoint kinase activation, namely the recognition of DNA lesion, activation of checkpoint kinase and transduction of checkpoint signaling. Then I describe the termination of DNA damage checkpoint activation. Lastly, I summarize the findings related to DDIS, and the crosstalk between phosphorylation based checkpoint activation and DDIS in yeast, as well as outstanding questions addressed in my thesis.

Activation of the Mec1 and Tel1 mediated checkpoint

Recognition of DNA lesions by the DNA damage sensor proteins

As shown in Figures 1-2 and 1-3, both Mec1 and Tel1 mediated checkpoint is initiated by DNA damage sensor proteins that recognize common DNA structures (such as ssDNA or double strand break (DSB)) arising from DNA lesions or replication stress. One of the main DNA damage sensor proteins is the highly conserved ssDNA binding protein RPA, which is composed of subunits Rfa1-3 (Zou and Elledge 2003). The N-terminus of Rfa1 interacts with Ddc2 (yeast homolog of ATRIP) (Ball et al. 2007). Ddc2 associates with Mec1 and recruits the complex to the ssDNA region. RPA also helps to recruit two factors that can activate the kinase activity of Mec1, namely the trimeric ring complex Rad17-Mec3-Ddc1 (9-1-1) and the helicase-endonuclease Dna2 (Bae et al. 2001; Bae et al. 2003; Yang and Zou 2006; Zhou et al. 2015). These multiple roles make RPA-coated ssDNA an essential platform to trigger Mec1 checkpoint activation.

A long stretch of ssDNA coated by RPA can be generated through replicative stress (Figures 1-2). Uncoupling of MCM and DNA polymerases when a lesion on the template strand blocks the latter, but not the former, can cause ssDNA generation. Moreover, dNTP depletion or DNA gaps left behind replication forks are also sources of

ssDNA (Sogo et al. 2002; Byun et al. 2005; Feng et al. 2006). In many situations, such ssDNA structures are accompanied by ss- and ds-DNA junctions. These junctions can be recognized by 9-1-1, a complex important for sensing DNA damage and for activating Mec1 (Yang and Zou 2006). It has been proposed that components of the replisome, such as DNA polymerases and helicases, could also promote checkpoint activation (Navas et al. 1995; Labib et al. 2001; Sheu et al. 2014). However, it remains unclear how these factors serve as damage sensors.

Another important DNA damage sensor is the trimeric Mre11-Rad50-Xrs2 complex (MRX) that binds to DSB ends (Nakada et al. 2003; Falck et al. 2005; Lee and Paull 2005) (Figures 1-2 and 1-3). MRX recruits Tel1 to DSB and activates Tel1 (Figure 1-3). In yeast, Tel1 plays a minor role in checkpoint activation. This is partly caused by the efficient conversion of a DSB to ssDNA by end resection and Tel1 recruitment depends on a DSB (Lisby et al. 2004; Clerici et al. 2006; Gobbin et al. 2015). During resection, MRX and Sae2 perform end-clipping by removing 100-300 nucleotides from the 5' end of a DSB (Lobachev et al. 2002; Clerici et al. 2005; Deng et al. 2005; Neale et al. 2005; Lengsfeld et al. 2007; Mimitou and Symington 2008; Zhu et al. 2008; Nicolette et al. 2010; Cannavo and Cejka 2014). This is followed by extensive resection of a DSB to generate long 3' ssDNA overhang through two redundant pathways mediated by the Exo1 nuclease and the DNA helicase/nuclease Sgs1 and Dna2 (Mimitou and Symington 2008; Zhu et al. 2008). Here, RPA helps establish the polarity of Dna2 in DNA degradation, promotes duplex unwinding by Sgs1 helicase, as well as prevents 3' overhang degradation and inappropriate annealing that can generate MMEJ (microhomology-mediated end joining) products (Cejka et al. 2010; Niu et al. 2010; Nimonkar et al. 2011; Chen et al. 2013; Deng et al. 2014). Whether these multiple roles of RPA can be functionally separated from each other remains to be seen.

Activation of the apical checkpoint kinases Mec1 and Tel1

Upon recruiting Mec1-Ddc2 to DNA lesions by DNA damage sensor proteins, Mec1 is activated by several activation factors, such as 9-1-1 and Dpb11 (Zou 2013) (Figure 1-2). Furthermore, Mec1 can phosphorylate the Ddc1 subunit of 9-1-1 at site T602 (Puddu et al. 2008; Navadgi-Patil and Burgers 2009). The phosphorylated Ddc1 can then recruit Dpb11 (Puddu et al. 2008). Similar to 9-1-1, Dpb11 was shown to stimulate Mec1 activity directly (Mordes et al. 2008; Navadgi-Patil and Burgers 2008). Note that this role of Dpb11 is separable from its role in replication initiation (Mordes et al. 2008; Navadgi-Patil and Burgers 2008).

Two other proteins that have the ability to stimulate Mec1 activity *in vitro* are the helicase-endonuclease Dna2 and Mrc1 (Chen and Zhou 2009; Kumar and Burgers 2013) (Figure 1-2). Both proteins appear to only activate Mec1 during DNA replication (Chen and Zhou 2009; Kumar and Burgers 2013). Dna2 also acts in the maturation of Okazaki fragments by removing the flaps while Mrc1 is an intrinsic member of the replisome. The close proximity of these factors to the replication fork likely contributes to their ability to stimulate Mec1.

On the other hand, Tel1 kinase activity is directly activated by its recruiter MRX and does not seem to require additional activating factors (Lee and Paull 2004; Fukunaga et al. 2011) (Figure 1-3).

Transduction of checkpoint signaling by Mec1 and Tel1

Activated Mec1 and Tel1 kinases can transduce the checkpoint response by phosphorylating several downstream kinases, the main one being the effector kinase Rad53 (Harrison and Haber 2006). Phosphorylation of Rad53 is facilitated by the mediator protein Rad9 under DNA damage conditions (Weinert and Hartwell 1988; Schwartz et al. 2002; Harrison and Haber 2006) (Figure 1-2). Rad9 is a scaffold protein that can bind to and promote the accumulation of Rad53 at DNA lesions (Gilbert et al. 2001). During replication, Mrc1 helps Mec1 to phosphorylate Rad53 through a poorly defined scaffolding role (Alcasabas et al. 2001; Osborn and Elledge 2003) (Figure 1-2). Mrc1 does not seem to have a role in promoting Tel1 mediated phosphorylation of Rad53.

Phosphorylation of Rad53 by Mec1 and Tel1 activates its kinase activity (Lee et al. 2003b). Together with other kinases, Rad53 triggers the phosphorylation of numerous substrates involved in various cellular processes, including mitosis, DNA replication and DNA repair, etc (Harrison and Haber 2006) (Figures 1-2 and 1-3). For example, Rad53 can phosphorylate Sld3 and the Dbf4 subunit of DDK (Lopez-Mosqueda et al. 2010; Zegerman and Diffley 2010). Dbf4 phosphorylation diminishes DDK activity (Weinreich and Stillman 1999), while Sld3 phosphorylation diminishes its binding to Dpb11 and Cdc45 (Lopez-Mosqueda et al. 2010; Zegerman and Diffley 2010). As such, Rad53 inhibits CMG formation, and consequently, prolongs S phase to give cells more time to cope with replicative stress.

Termination of the Mec1 and Tel1 checkpoints

After successful repair or relief of replicative stress, the Mec1 or Tel1 mediated checkpoints need to be turned off to allow cell cycle progression and survival. Several

regulatory steps to terminate Mec1 and Tel1 checkpoint activity have been described and are summarized below (Figure 1-4).

Reversal of Mec1 checkpoint by elimination of RPA coated ssDNA

Elimination of ssDNA-RPA is an important way to reduce Mec1 checkpoint (Figure 1-4, left). ssDNA can be removed as a natural consequence of DNA repair and completion of replication under situations of genotoxic stress. A contribution of the DNA helicase Srs2 that can remove the recombinase Rad51 from DNA has also been noted (Harrison and Haber 2006; Yeung and Durocher 2011). It has been proposed that as Rad51 avidly binds to ssDNA, it can protect ssDNA from being degraded and consequently allow ssDNA-RPA to persist longer (Yeung and Durocher 2011). Srs2 is important to strip Rad51 from DNA thus facilitate the elimination of ssDNA-RPA (Yeung and Durocher 2011) (Figure 1-4, left). Furthermore, it has been shown that the DNA damage sensitivity of *srs2* Δ can be accounted for by the persistence of the Mec1-mediated checkpoint caused by the accumulation of ssDNA bound by Rad51 and RPA (Vaze et al. 2002; Yeung and Durocher 2011).

Termination of Tel1 checkpoint by Sae2

Tel1 is recruited to a DSB by the sensor protein complex MRX (Figure 1-4, right). MRX leaves the DNA lesion site after the end-clipping step mediated by MRX and Sae2 (Lisby et al. 2004; Clerici et al. 2006; Gobbini et al. 2015). Therefore, Sae2 is critical to remove MRX and Tel1 from DSB and to terminate the Tel1-dependent checkpoint (Figure 1-4, right). Recent studies show that the DNA damage sensitivities of *sae2* Δ are due to a persistently activated Tel1-mediated checkpoint (Clerici et al. 2006; Gobbini et al. 2015).

Dampening Rad9 mediated phosphorylation of Rad53

Another means to dampen checkpoint signaling is to reduce Rad9 function, which facilitates Rad53 phosphorylation (Harrison and Haber 2006) (Figure 1-4, left). Rad9 is recruited to DNA lesion sites *via* its binding to Dpb11 and phosphorylated H2AX (Hammet et al. 2007; Granata et al. 2010; Pfander and Diffley 2011) (a product of Mec1/Tel1 phosphorylation). It has been shown that the Slx4-Rtt107 complex competes with Rad9 for binding to Dpb11 and phosphorylated H2AX, thereby dampening checkpoint activation (Ohouo et al. 2013) (Figure 1-4, left). Consequently, DNA damage sensitivities of *slx4* Δ or *rtt107* Δ cells are due to persisting Mec1 checkpoint generated by enhanced engagement of Rad9 at lesion sites (Ohouo et al. 2013).

Reversal of Mec1 and Tel1 checkpoint by phosphatases

Besides removal of DNA damage sensor and mediator proteins from DNA, four major serine/threonine phosphatases can reverse checkpoint activation by direct dephosphorylation of the checkpoint kinases themselves and their substrates (Leroy et al. 2003; Guillemain et al. 2007; O'Neill et al. 2007; Szyjka et al. 2008; Bazzi et al. 2010) (Figure 1-4). These include the PP4 phosphatase, Pph3-Psy2; two PP2C phosphatases, Ptc2 and Ptc3; and the PP1 phosphatase, Glc7. These phosphatases can inactivate both Mec1 and Tel1 checkpoints by dephosphorylating Rad53.

Summary of the Mec1 and Tel1 checkpoint activation and termination

As described above, successful checkpoint activation relies on the coordination of DNA lesion sensors, checkpoint kinases, checkpoint kinase activation factors, mediator proteins and effector kinases to transduce a cascade of phosphorylation events and modulate various cellular processes under DNA damage and replicative stress

conditions. In addition, negative regulation of checkpoint response is equally critical for cell survival, and cells employ several down regulation pathways to ensure this. In the next section, I will describe DNA damage induced sumoylation (DDIS) that is also critical for the DDR and cell survival.

1.3 Overview of DNA damage induced sumoylation (DDIS)

DDIS refers to the phenomenon where, in response to DNA damage and replication stress, a large number of proteins become sumoylated to promote DNA repair and survival of cells (Cremona et al. 2012). The number of substrates in DDIS is comparable to those involved in phosphorylation based DNA damage checkpoint activation (Cremona et al. 2012). The sumoylation of most of the substrates is conserved from yeast to human, indicating that sumoylation constitutes a critical means of regulation upon DNA damage (Golebiowski et al. 2009; Cremona et al. 2012; Tammsalu et al. 2014). It is proposed that recruitment of SUMO ligases to DNA lesions is critical to transduce DDIS signaling (Cremona et al. 2012; Chung and Zhao 2015). There are three mitotic SUMO ligases in yeast, Siz1, Siz2 and Mms21, and the recruitment of each SUMO ligases to DNA lesions may constitute a different branch of DDIS. Thus far, the only well understood pathway is mediated by Siz2, as described below.

Siz2 mediated DDIS branch

Recent studies have shown that one branch of DDIS is through the recruitment of Siz2 (Chung and Zhao 2015) (Figure 1-5). In this case, RPA coated ssDNA is the platform to recruit SUMO ligase Siz2 to initiate DDIS (Figure 1-5). The C-terminal winged helix (WH) domain of the Rfa2 subunit binds Siz2 directly and recruits it to DNA lesion sites. Siz2 subsequently mediates the sumoylation of three major substrates, including RPA itself

and two proteins involved in homologous recombination repair, Rad52 and Rad59 (Psakhye and Jentsch 2012; Chung and Zhao 2015) (Figure 1-5). The major sumoylation sites of RPA, Rad52, and Rad59 have been mapped by mass spectrometry (Sacher et al. 2006; Psakhye and Jentsch 2012). It has been proposed that sumoylation of these proteins has redundant roles in promoting homologous recombination (HR), such that loss of sumoylation of a single protein does not affect HR at non-repetitive regions (Psakhye and Jentsch 2012). This phenomenon has been termed 'protein group modification', and emphasizes the redundant nature of the group modification (Psakhye and Jentsch 2012). It has been reported that SUMO interacting motifs (SIMs) are found in RPA, Rad59 and other proteins involved in homologous recombination (Psakhye and Jentsch 2012). It is likely that sumoylation of RPA, Rad59 and Rad52 promotes the binding with each other. However, Rad52 sumoylation itself has been shown to affect HR at repetitive rDNA region, indicating that 'protein group modification' is a context dependent event (Torres-Rosell et al. 2007). Interestingly, this effect of Rad52 sumoylation appears to be negative, since mutating Rad52 sumoylation sites results in elevated HR at repetitive regions (Torres-Rosell et al. 2007). It is not known how Rad52 sumoylation has both positive and negative roles in HR under different circumstances.

RPA sumoylation is conserved in human, and the sumoylation sites are mapped to be residues K449 and K577, which are not the same sumoylation sites mapped in yeast (Dou et al. 2010; Psakhye and Jentsch 2012). Mutating these sites to arginines leads to defective HR (Dou et al. 2010). Sumoylated RPA binds to Rad51 better than non-modified RPA and contributes to HR (Dou et al. 2010). Whether the same mechanism is true in yeast is unknown. The effects of sumoylation of RPA, Rad52, and Rad59 have not been examined outside of HR.

The interplay between DDIS and the Mec1 mediated checkpoint activation

One outstanding question in the study of the DDR is whether DDIS and DNA damage checkpoint activation affect each other. DDIS and Mec1 checkpoint activation are largely independent in yeast (Cremona et al. 2012). Deletion of Mec1 does not diminish DDIS, instead it increases sumoylation of certain substrates, presumably because of elevated levels of DNA lesions when the Mec1 mediated checkpoint is absent (Cremona et al. 2012). On the other hand, reducing sumoylation leads to a delay of Mec1 checkpoint activation but does not abolish it (Cremona et al. 2012). Our genetic data also show that deletion of Mec1 and reduction of sumoylation have additive or synergistic effects on cell survival, depending on different DNA damaging conditions (Cremona et al. 2012). These findings indicate that both the Mec1 checkpoint and DDIS are critical for the DDR, and DDIS promotes optimal Mec1 checkpoint activation. Interestingly, the effects of DDIS on ATR checkpoint activation seem to be conserved in human (Wu et al. 2014). It has been reported that the ATR binding partner ATRIP is sumoylated at sites K234 and K289 (Wu et al. 2014). Mutation of ATRIP sumoylation sites to arginines leads to defective ATR checkpoint activation but does not abolish it (Wu et al. 2014). An ATRIP sumoylation defective mutant exhibits diminished binding of ATRIP to other proteins involved in checkpoint activation, e.g. ATR and RPA (Wu et al. 2014). Importantly, fusion of a SUMO chain to this ATRIP sumoylation defective mutant rescues its binding to ATR and RPA, and also partially restores ATR checkpoint activation (Wu et al. 2014). These data indicate that ATRIP sumoylation augments ATR checkpoint activation. The yeast homolog of ATRIP, Ddc2, is not found to be sumoylated (Cremona et al. 2012). Therefore, in yeast the substrate(s) of DDIS that augment the Mec1 checkpoint is still a mystery. Several checkpoint proteins in yeast contain SIM and bind to SUMO. For example, Mec1 contains two SIMs, and synthetic peptides containing these SIMs bind SUMO (Psakhye and Jentsch 2012). The endonuclease Dna2, which stimulates Mec1

kinase activity, also binds SUMO (Makhnevych et al. 2009). These findings reveal potential mechanisms by which DDIS influences the Mec1 checkpoint activation.

Summary of the two branches of DDR and questions to be addressed

In the above sections, I have described two examples of PTM mediated DDR, namely the Mec1 mediated checkpoint and Siz2 mediated DDIS. Although these two processes are not dependent on each other, DDIS does promote optimal checkpoint activation, indicating a cross talk between the two. An outstanding question is how DDIS promotes checkpoint activation. Because RPA is the key in promoting both processes, and RPA itself is a substrate in DDIS (Zou and Elledge 2003; Psakhye and Jentsch 2012; Chung and Zhao 2015), I studied if RPA sumoylation promotes checkpoint activation and the crosstalk between these two processes. In chapter 4, I present my findings supporting this hypothesis. In the final section of introduction, I summarize the SUMO system, including the enzymes involved in the SUMO conjugation and deconjugation processes, and the potential biological effects of sumoylation on its substrates.

1.4 The SUMO system

SUMO (Small Ubiquitin-like Modifier) belongs to the ubiquitin family of protein modifiers, and is conserved in eukaryotic cells. SUMO is essential in almost all organisms tested, including budding yeast and humans (Johnson 2004). Though SUMO and ubiquitin have similar sequence and structures, their surface charge distributions are completely different thus contributing to their interaction with different motifs (Bayer et al. 1998; Mossessova and Lima 2000a). Also SUMO contains an N-terminal 20 amino acid tail that contributes to SUMO chain formation that is important for meiosis in yeast (Bylebyl

et al. 2003; Sabate et al. 2012; Klug et al. 2013). The budding yeast has only one form of SUMO, called Smt3, which is 101 amino acid long.

SUMO E1, E2 and E3 enzymes and sumoylation

Similar to ubiquitination, sumoylation requires three enzymes to conjugate SUMO to the lysine residue of a substrate, resulting in a branched molecule (Johnson 2004) (Figure 1-6). The three enzymes are the SUMO activating (E1) and conjugating (E2) enzymes, and the E3 ligase (Figure 1-6). In most organisms, there are only one E1 and E2 enzymes and multiple E3 ligases. SUMO E1 is a heterodimer (Aos1/Uba2 in budding yeast) that activates SUMO by formation of a thioester bond between a conserved cysteine residue in Uba2 and SUMO C-terminal double glycine tail in an ATP dependent manner (Gareau and Lima 2010). This high energy E1~SUMO thioester bond is then transferred to the E2 enzyme Ubc9 and becomes a high energy E2~SUMO thioester bond (Gareau and Lima 2010). Then the SUMO moiety is transferred to the ϵ -amino group of a lysine residue of the substrate (Gareau and Lima 2010). This step is usually facilitated by E3 SUMO ligases (Gareau and Lima 2010). There are four known E3 SUMO ligases in yeast, namely Siz1, Siz2, Mms21 and Zip3 (Johnson and Gupta 2001; Takahashi et al. 2001; Zhao and Blobel 2005a; Cheng et al. 2006a) (Figure 1-6). These E3 enzymes are responsible for the sumoylation of hundreds of substrates and often have redundancy in their substrates.

The sites of sumoylation in many cases are determined by Ubc9 and confined to the consensus [Ψ KX(D/E)] or reverse consensus [(D/E)XK Ψ] sites that interact with Ubc9 (Gareau and Lima 2010), Ψ represents a hydrophobic amino acid, K is lysine, X is any amino acid and D/E is either aspartate or glutamate (Gareau and Lima 2010;

Lamoliatte et al. 2014). As not all these sites are sumoylated, more requirements exist for defining sumoylation sites. It has been noted that sumoylation tends to occur in less structured loop region of a protein (Gareau and Lima 2010). It is likely that a flexible loop region is more amenable for proper alignment and local conformation change required for the productive contact of the E2~SUMO thioester bond and the acceptor lysine. This principle also helps to explain that though the homologs of a protein are sumoylated, their sumoylation sites usually vary from one another.

Desumoylation enzymes and the removal of SUMO

The reverse reaction of sumoylation is desumoylation, which is catalyzed by two non-redundant SUMO isopeptidases Ulp1 and Ulp2 in budding yeast (Hickey et al. 2012) (Figure 1-6). These two enzymes have different substrate preferences, activities and subcellular localizations (Li and Hochstrasser 1999; Li and Hochstrasser 2000; Strunnikov et al. 2001; Panse et al. 2003; Kroetz et al. 2009). Ulp1 is additionally required in SUMO maturation by cleaving the tail of the precursor SUMO molecule, exposing the double glycine residues (Li and Hochstrasser 1999), while Ulp2 prefers to remove the SUMO chain from its substrates (Li and Hochstrasser 2000). Ulp1 deletion is lethal, which is very poorly rescued by overexpression of mature SUMO, indicating that the roles of Ulp1 SUMO maturation and desumoylation are both critical for cell fitness (Li and Hochstrasser 1999). Ulp2 deletion results in viable but sick cells that are extremely sensitive to various genotoxins, indicating that accumulation of SUMO chain is toxic to cells (Li and Hochstrasser 2000; Schwartz et al. 2007). This defect is suppressed to a large degree by mutating the lysines on SUMO, thus preventing SUMO chain formation. Ulp1 and Ulp2 exhibit different subcellular localizations: Ulp1 primarily associates with the nuclear pore complex, whereas Ulp2 is nuclear (Panse et al. 2003; Kroetz et al.

2009). Consistent with these observations, Ulp1 and 2 also have different substrates (Li and Hochstrasser 2000).

The function of sumoylation and desumoylation

Protein sumoylation and desumoylation has been implicated in a myriad of biological processes, including transcription, nuclear transport and DNA repair. The addition and removal of SUMO from proteins can have different effects, including altering protein-protein interactions, influencing protein solubility and DNA binding activity (Sarangi and Zhao 2015) (Figure 1-6). Before my thesis work, there was no evidence that sumoylation and desumoylation were directly involved in DNA replication, although our lab and others have shown that a dozen proteins involved in DNA replication are sumoylated in yeast and humans (Golebiowski et al. 2009; Cremona et al. 2012). In particular, the helicase MCM complex and leading strand polymerase epsilon (Pol ϵ) are sumoylated, which could provide an entry point to examine whether and how sumoylation regulates DNA replication. The study of DDIS is also at an early stage, the research on several substrates affecting DNA repair, such as PCNA, Sae2 and Rad1, has provided some general ideas of the effects of sumoylation (Sarangi and Zhao 2015). In the case of PCNA, the processivity factor of replicative polymerases, its sumoylation at K164 promotes interaction with the DNA helicase Srs2, leading to the removal of Rad51 filament from DNA, and consequently preventing HR at the replication fork (Papouli et al. 2005; Armstrong et al. 2012). In the case of Sae2, which is involved in DNA end resection, sumoylation at K97, which is located in a region involved in Sae2 oligomerization, helps it to become soluble upon DNA damage (Sarangi et al. 2015). In the case of Rad1, a structure specific nuclease for cleaving flap structures during HR and nucleotide excision repair, sumoylation at K32 reduces its DNA binding activity and

likely promotes recycling of this enzyme at lesion sites (Sarangi et al. 2014b). These examples show that sumoylation is extensively involved in multiple DNA repair processes and has diverse effects on substrate functions.

1.5 Thesis objective

My thesis study focused on three questions: 1) How does MCM sumoylation affect DNA replication initiation? 2) How does Pol2 sumoylation contribute to replication? 3) And what is the basis for cross talk between sumoylation and the DNA damage checkpoint?

Based on previous work from our lab and others I know that MCM and Pol ϵ sumoylation is conserved from yeast to human, but the effects of their sumoylation were not known. In addition, the role of Pol ϵ in replication initiation was poorly understood. In chapter 2, I show that MCM is sumoylated specifically after its loading on to origins and the extent of this modification declines as replication initiates. I show that MCM sumoylation is inhibitory to replication initiation partly by recruiting a phosphatase to counteract DDK mediated activation of MCM. In chapter 3, I first studied the function of Pol2 in replication initiation and revealed a surprising function for its N-terminal unique domain in the pre-LC formation during replication initiation. I further showed that Pol2 is sumoylated on this domain and this modification contributes to the domain's function in replication initiation. In chapter 4, I provide genetic and physical evidence that RPA sumoylation promotes Mec1-mediated checkpoint activation, enabling a crosstalk between checkpoint activation and sumoylation.

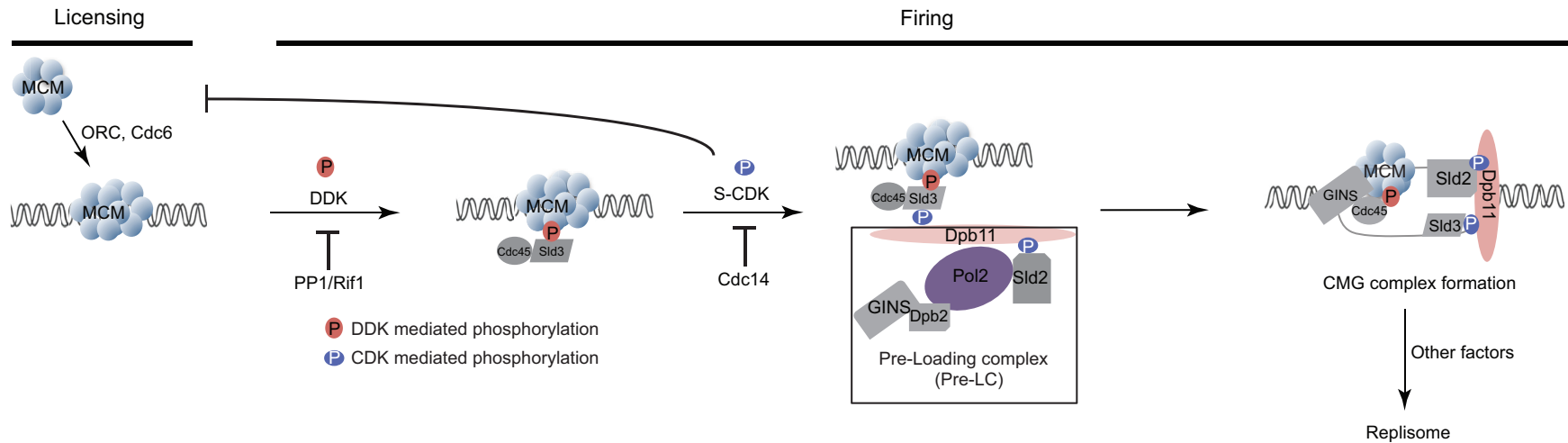


Figure 1-1 The initiation of chromosome replication in budding yeast.

During the origin licensing step (late M to G1 phase), free MCM is loaded onto replication origins as a double hexamer. This process depends on several loading factors, including the ORC complex and Cdc6. During the origin firing step (S phase), the essential kinases DDK and CDK activate the loaded MCM. DDK-mediated phosphorylation of loaded MCM recruits Sld3 and its binding partner Cdc45. CDK-mediated phosphorylation of Sld2 promotes the formation of the pre-LC, composed of Pol ε, GINS, Sld2, Sld3, and Dpb11. In addition, CDK-mediated phosphorylation of Sld3 fosters an interaction between Sld3-p and Dpb11, leading to recruitment of the GINS complex to the loaded MCM. Cdc45, MCM, and the GINS complex form the active replicative helicase CMG. The subsequent recruitment of additional protein factors results in formation of the replisome. Two phosphatases, the PP1/Rif1 complex and Cdc14, can reverse the effects of DDK and CDK, respectively. CDK is critical for preventing re-replication events by inhibition of the loading of MCM. Three major targets of CDK are MCM, ORC, and Cdc6. The phosphorylation of MCM by CDK leads to its nuclear export, ORC phosphorylation reduces MCM loading, and Cdc6 phosphorylation leads to its degradation.

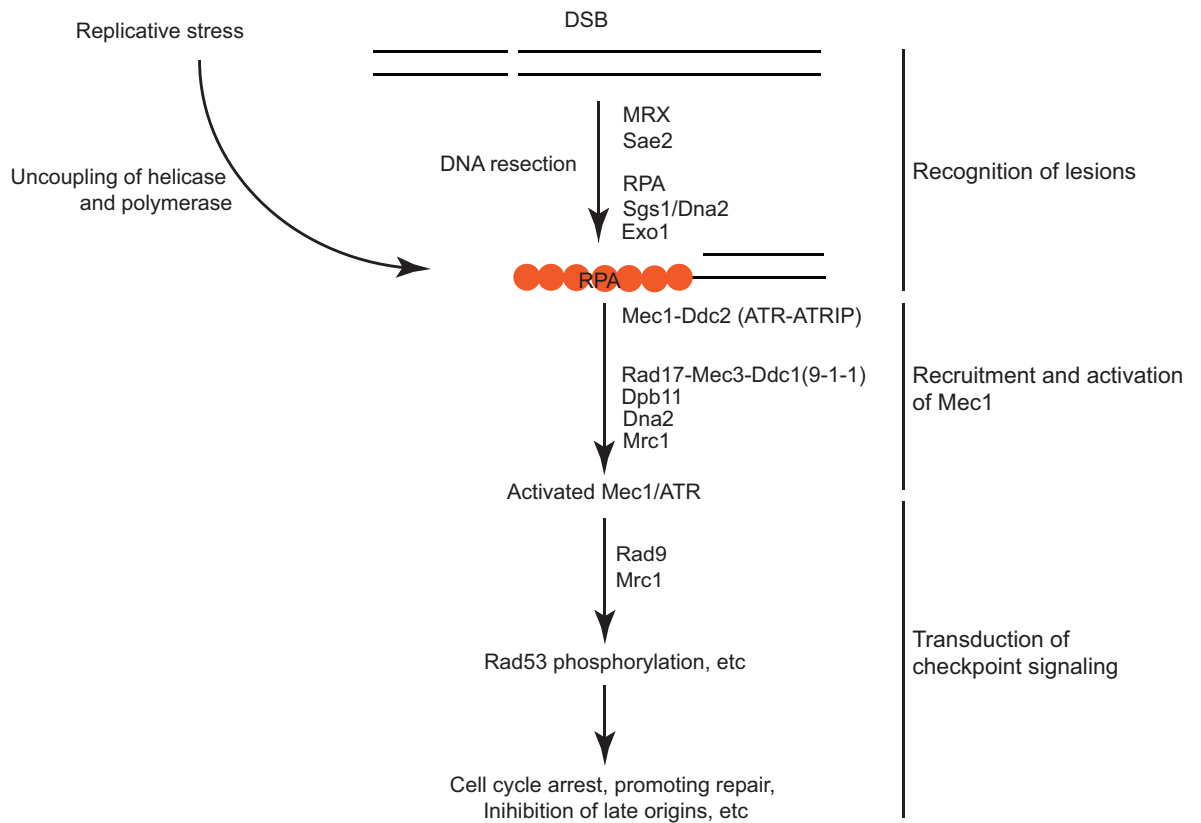


Figure 1-2 Activation of the Mec1 mediated checkpoint in budding yeast. The Mec1 checkpoint can be triggered by replicative stress or DSBs. The Mec1 checkpoint comprises three steps: Recognition of lesions, recruitment and activation of the Mec1 kinase, and transduction of checkpoint signaling. In replicative stress conditions, ssDNA is generated by the uncoupling of the replicative helicase and polymerase. Alternatively, a DSB can be processed to generate a 3' ssDNA overhang by the DNA resection process, which is mediated by several factors, including MRX, Sae2, and RPA. RPA-coated ssDNA recruits the Mec1 kinase complex, Mec1-Ddc2 (ATR-ATRIP in human). Mec1-Ddc2 is subsequently activated by several factors, including Rad17-Mec3-Ddc1 (the 9-1-1 complex in human), Dpb11, Dna2, and Mrc1. In the transduction of checkpoint signal step, the key effector kinase Rad53 is phosphorylated by the active Mec1 kinase, resulting in extensive cellular responses, including cell cycle arrest.

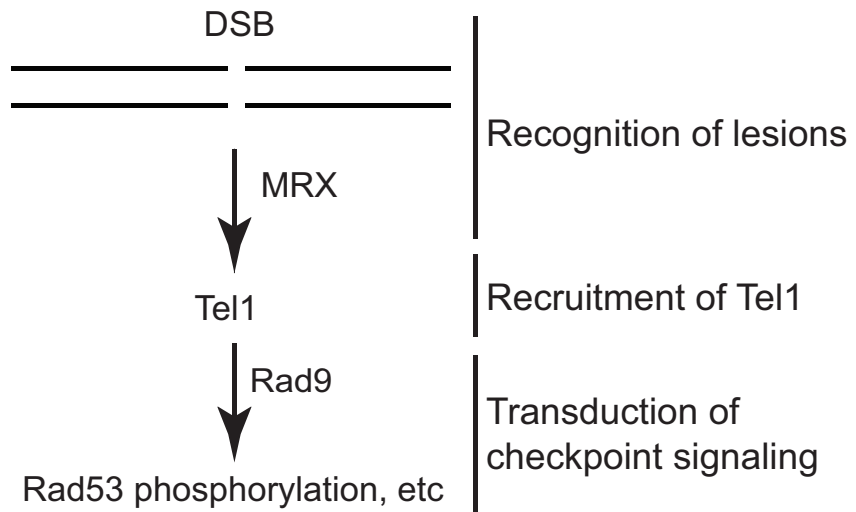


Figure 1-3 Activation of the Tel1 mediated checkpoint.

The Tel1 mediated checkpoint is triggered by a DSB and has three steps, including lesion recognition, recruitment of the Tel1 kinase, and transduction of checkpoint signaling. A DSB can be recognized by the MRX complex, which recruits the Tel1 kinase. The Tel1 kinase activates the effector kinase Rad53 to transduce checkpoint signaling.

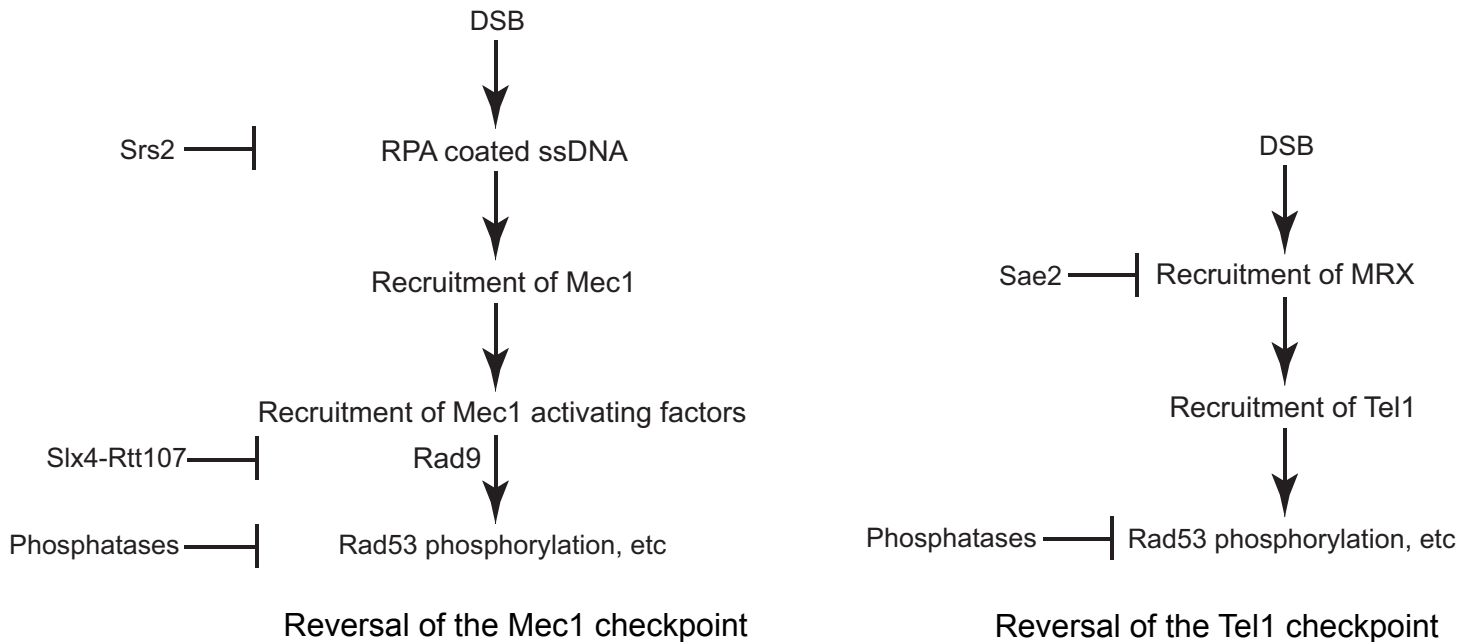


Figure 1-4 Reversal of the Mec1 and Tel1 mediated checkpoints.

The Mec1 and Tel1 checkpoints can be reversed by multiple mechanisms. (Left) There are three mechanisms to reverse the Mec1 checkpoint. First, Srs2 helicase can remove Rad51 from residual ssDNA, consequently promoting degradation of ssDNA. Second, the scaffold protein complex Slx4-Rtt107 can reduce the interactions between Rad9 and Dpb11 and phosphorylated H2AX, consequently reducing Rad53 phosphorylation. Third, several phosphatases can dephosphorylate and inactivate the Rad53 kinase. (Right) There are two mechanisms to reverse the Tel1 checkpoint. First, DNA resection of a DSB, mediated by Sae2, terminates the engagement of the MRX complex and the Tel1 kinase at the lesion site. Second, several phosphatases can dephosphorylate and inactivate Rad53.

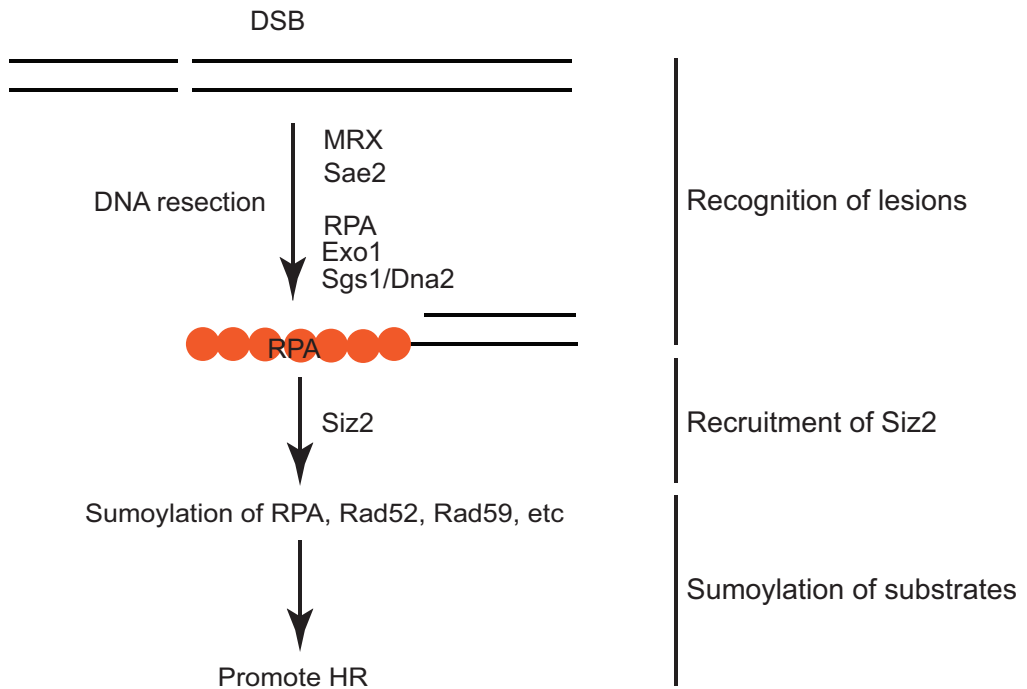


Figure 1-5 Schematic representation of the Siz2-mediated branch of DDIS. Siz2-mediated DDIS is composed of three steps: Lesion recognition, Siz2 recruitment, and sumoylation signaling transduction. A DSB is first resected to generate 3' ssDNA overhang. RPA coated ssDNA recruits the Siz2 SUMO E3 ligase, which promotes sumoylation of several substrates involved HR, including RPA, Rad52, and Rad59. The sumoylation of RPA, Rad52, and Rad59 collectively promotes HR.

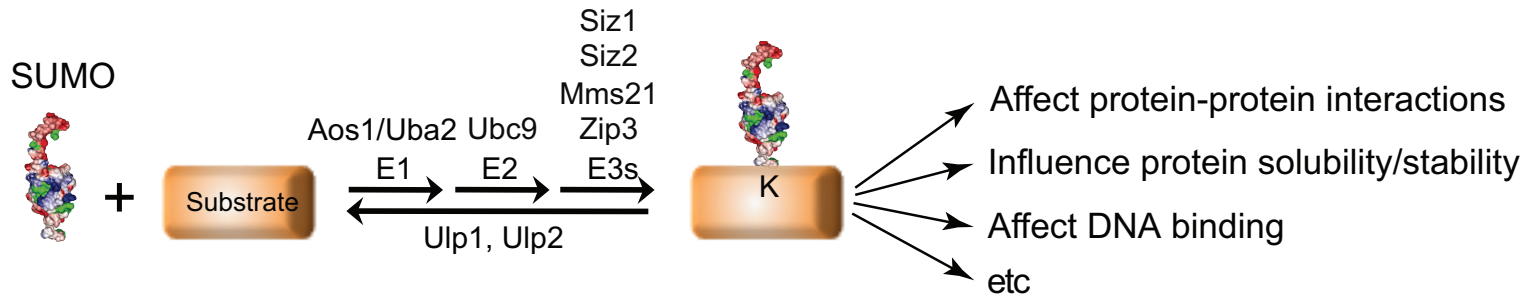


Figure 1-6 The SUMO conjugation cycle and its biological effects.

The SUMO conjugation process requires E1, E2, and E3 enzymes to transfer a SUMO molecule to a lysine residue of a substrate. The budding yeast E1, E2 and E3 enzymes are indicated. Sumoylation of a substrate can have several biological effects, as indicated. Sumoylation can be reversed by SUMO isopeptidases. Ulp1 and Ulp2 are the two SUMO isopeptidases in budding yeast.

Chapter 2

A new MCM modification cycle regulates DNA replication initiation*

Introduction

The initiation of DNA replication is tightly controlled to ensure that duplication of every locus occurs once and only once per cell cycle and to establish specific replication programs unique to an organism or cell type. Impairment in regulation of replication initiation can lead to various forms of genomic changes and instability, and consequently to human diseases and cancers (Nguyen et al. 2001; Tanaka et al. 2007; Zegerman and Diffley 2007; Sheu and Stillman 2010; Jackson et al. 2014). Previous studies have revealed multiple forms of regulation at both local and global levels, including several pathways targeting a key replicative enzyme, the DNA helicase MCM (Sheu and Stillman 2006; Francis et al. 2009; Randell et al. 2010; Sheu and Stillman 2010; Davé et al. 2014; Hiraga et al. 2014; Maric et al. 2014; Mattarocci et al. 2014).

The MCM complex is composed of Mcm2–7 subunits and is highly conserved in eukaryotes. Among its many roles during replication, MCM is critical for replisome assembly. MCM, in complex with cofactor Cdt1, is the first replisome component to arrive at replication initiation sites (or origins). In budding yeast, MCM loading at origins is mediated by Cdc6 and the origin recognition complex (ORC, comprising Orc1–6) in late mitosis and G1 phase, in a process called origin licensing (Fig. 2-1a) (Sclafani and Holzen 2007; Remus and Diffley 2009). A subset of loaded MCM then initiates stepwise replisome assembly in a process termed origin firing. This begins with the recruitment of two cofactors: Cdc45 and the heterotetrameric GINS complex (Fig. 2-1a). Recruitment of

* Reprinted from Wei, L. & Zhao, X. (2016) A new MCM modification cycle regulates DNA replication initiation. *Nat Struct Mol Biol.*, **23**, 209-216

both factors requires kinases. Dbf4-dependent kinase (DDK, composed of Cdc7 and Dbf4) primarily phosphorylates Mcm4, thereby recruiting Cdc45; subsequent phosphorylation of non-MCM proteins by the S-phase cyclin-dependent kinase complex (S-CDK) recruits GINS (Fig. 2-1a) (Heller et al. 2011; Yeeles et al. 2015).

The Cdc45, MCM and GINS (CMG) complex serves as the replicative helicase (Scalfani and Holzen 2007; Remus and Diffley 2009). After CMG formation, more than a dozen additional replisome members assemble in a highly ordered yet still poorly understood manner before replication is initiated (Gambus et al. 2006; Morohashi et al. 2009). Throughout this intricate replisome-assembly process, MCM and CMG are kept inactive to prevent premature DNA unwinding.

The precision of many biological processes depends on the balance between positive and negative regulation. It is conceivable that the tightly controlled transition from inactive to active MCM states also requires additional regulation besides the known kinase-based positive regulation. Recent studies have indeed revealed other chemical modifications of MCM. In particular, proteomic screens in yeast, humans and plants have shown that MCM subunits are sumoylated, thus revealing another highly conserved MCM modification (Golebiowski et al. 2009; Elrouby and Coupland 2010; Cremona et al. 2012). Sumoylation entails the conjugation of the small protein modifier SUMO to lysine residues on target proteins. This modification is reversible through desumoylation, and the cycle of sumoylation and desumoylation is highly dynamic in cells. The addition and removal of SUMO exert a range of effects on protein function, such as altering protein-protein interactions or enzymatic activities, and influence a variety of cellular processes (Geiss-Friedlander and Melchior 2007b; Sarangi and Zhao 2015). Although SUMO is known to affect genome maintenance, its roles in this arena

have been examined primarily under genome damaging situations (Galanty et al. 2009; Morris et al. 2009; Cremona et al. 2012; Psakhye and Jentsch 2012; Sarangi et al. 2014a; Chung and Zhao 2015); how SUMO influences the normal replication program is largely unanswered.

To understand how sumoylation of MCM subunits pertains to normal replication programs, I first examined spatial and temporal patterns of this modification in budding yeast. I found that sumoylation of the six MCM subunits occurred exclusively on chromatin. Moreover, MCM sumoylation levels oscillated during the cell cycle in a manner opposite to those of MCM phosphorylation, suggesting that MCM sumoylation is an inhibitory marker for replication. The MCM sumoylation cycle depended on key MCM loaders and activators, suggesting that it is integral to MCM functions. Importantly, increased MCM sumoylation impaired replication initiation and decreased CMG levels. Mechanistically, these effects were linked to enhanced recruitment of the phosphatase PP1, which counteracts DDK functions. Together, my findings suggest that MCM sumoylation enables a form of negative regulation during replication initiation. I propose that the dual control of MCM by two modifications ensures precise replication initiation and enables flexible control of genome duplication under different cellular contexts.

Results

Detection of MCM-subunit sumoylation during normal growth

In search of additional means of MCM regulation, I investigated MCM sumoylation, which has been found in proteomic screens in multiple organisms (Golebiowski et al. 2009; Elrouby and Coupland 2010; Cremona et al. 2012). To detect sumoylation, I followed a well-established method wherein denaturing conditions throughout protein

preparation minimizes desumoylation (Ulrich and Davies 2009). In this method, the endogenous yeast SUMO (Smt3) is replaced with a hexa-histidine (His₆)-Flag-tagged version (HF-Smt3) at its genomic locus, such that sumoylated forms containing HF-Smt3 are enriched by Ni-NTA resin (referred to herein as Ni PD). Although unmodified forms of proteins show nonspecific histidine-mediated binding to Ni-NTA, they can be distinguished from sumoylated forms upon western blotting for a particular protein on the basis of two criteria: (i) sumoylated forms are detected only in the presence of HF-Smt3 but not untagged Smt3, whereas unmodified forms are detectable regardless of the presence of HF-Smt3, and (ii) mono-sumoylated forms show an ~20-kDa upshift compared to the unmodified forms.

In my tests, I tagged Mcm2–7 proteins with hemagglutinin (HA) at their endogenous loci and verified that cell growth was fully supported by the tagged proteins. In the presence of HF-Smt3, but not untagged Smt3, I detected a modified form of each MCM subunit with anti-HA antibodies through western blotting (Fig. 2-1b). In each case, the modified form exhibited an ~20-kDa upshift from the unmodified form of the protein (Fig. 2-1b). Consistently with their being the sumoylated species, these modified forms showed a smaller upshift when SUMO was tagged with a smaller tag (Fig. 2-2a). I also observed sumoylated forms of each MCM subunit when examining immunoprecipitated protein by western blotting with SUMO-specific antibodies (Fig. 2-2b). In all cases, the detected levels of MCM sumoylation were not abundant, consistently with the dynamic nature of this modification. After showing through two approaches that a fraction of each MCM subunit was sumoylated during normal growth, I used the Ni PD method in subsequent tests.

MCM sumoylation on chromatin requires its loading at origins.

Because MCM is subject to tight spatial regulation and can function only upon chromatin loading, I asked whether the chromatin-bound or soluble fraction of MCM was sumoylated. Sumoylated MCM subunits were detectable exclusively in the chromatin-bound fraction (Figure 2-1c). Consistently with this finding, MCM-subunit sumoylation was absent when MCM loading onto chromatin was prevented by Cdc6 depletion in G1 cells (Fig. 2-1d and Fig. 2-3a). These results suggest that MCM-subunit sumoylation occurs on chromatin after the complex is loaded at origins.

MCM sumoylation levels peak in G1 and decline in S phase

Next, I examined the temporal regulation of MCM sumoylation during the cell cycle. Cells were arrested in G1 and then allowed to synchronously progress through the cell cycle (Fig. 2-4a, fluorescence-activated cell sorting (FACS)). Using Mcm6 as an example, I observed an oscillation in sumoylation levels: Sumoylation of Mcm6 peaked in G1 phase, coinciding with its chromatin loading, declined during S phase and reappeared in M phase, concurrently with the next loading cycle (Fig. 2-4a). Examination of chromatin-bound Mcm6 also showed a high sumoylation level in G1 and a low level in S phase (Fig. 2-3b).

I observed similar patterns for Mcm2–5, detecting sumoylation in G1 when DDK activity, as indicated by Mcm4 phosphorylation, and CDK activity, as indicated by Orc6 phosphorylation, were low (Fig. 2-4b). As expected, CMG levels were also low in G1, as evidenced by the low amount of the GINS subunit Psf1 associated with Mcm4 (Fig. 2-4b) in coimmunoprecipitation assay. As cells entered S phase, DDK and CDK activities, as well as CMG levels, rose (Fig. 2-4b), whereas Mcm2–5 sumoylation levels

decreased (Fig. 2-4b). In G2-M phase, when DDK and CDK activities, as well as CMG levels fell, sumoylation levels of Mcm2–5 rose again (Fig. 2-4b). The Mcm7 sumoylation pattern was somewhat different. Like other MCM subunits, Mcm7 showed sumoylation in G1; however, unlike that of other MCM subunits, Mcm7 sumoylation persisted throughout most of S phase, then decreased in late S phase and reappeared in G2-M phase (Fig. 2-4b). Because among all MCM subunits, only Mcm7 subunit has been shown to be involved in replication termination (Maric et al. 2014; Priego Moreno et al. 2014), the difference in sumoylation patterns between Mcm2–6 and Mcm7 may reflect distinct regulation and functions of these subunits.

Together, sumoylation levels of Mcm2–6 oscillate during the cell cycle in a pattern opposite to those of DDK- and CDK-mediated phosphorylation events. I also visualized this phenomenon by plotting the relative ratio of sumoylated or phosphorylated Mcm4 versus unmodified Mcm4 proteins (Fig. 2-4c). This temporal pattern suggests that in contrast to phosphorylation, MCM sumoylation is an inhibitory marker of replication initiation.

MCM sumoylation loss in S phase requires DDK and GINS

To gain a detailed understanding of the changes in Mcm2–6 sumoylation at the G1-S transition, I examined the roles of two key MCM regulators, DDK and GINS. To test the role of DDK, I arrested cells containing the temperature-sensitive *cdc7-4* allele and HA-tagged MCM subunits in G1 at a permissive temperature (24 °C) and then shifted them to a non-permissive temperature (37 °C) before releasing them into S phase (Fig. 2-5a). I confirmed *cdc7-4* inactivation upon temperature shift, on the basis of the lack of Mcm4 phosphorylation (Fig. 2-3c). I found that sumoylation of Mcm2–6 still occurred in G1

when DDK was inactivated and that the Mcm6 sumoylation level was similar to that in wild-type cells (Fig. 2-5a). Thus, bulk MCM sumoylation in G1 did not require DDK. However, DDK inactivation prevented the loss of Mcm2–6 sumoylation when G1 cells were released into S phase (Fig. 2-5a). This effect was not due to indirect alteration of CDK activity (as monitored by Orc6 phosphorylation) or DNA damage checkpoint activity (monitored by Rad53 phosphorylation) (Fig. 2-3c). Thus, DDK is required for loss of Mcm2–6 sumoylation when cells enter S phase.

To test the role of GINS, I used an indole-3-acetic acid (IAA)-inducible degron (or aid) method to acutely deplete the GINS subunit Psf2 (Nishimura et al. 2009; Havens et al. 2012). I arrested Psf2-aid and control cells in G2-M phase, and Psf2-aid was degraded after IAA addition (Fig. 2-5b; Fig. 2-3d-3e). Next, I released cells into G1 arrest in the presence of IAA and subsequently allowed them to enter S phase (Fig. 2-5b; efficient Psf2-aid degradation, proper cell cycle arrest and release, and lethality caused by Psf2 degradation are shown in Figure 2-3d-3f). As in the case for DDK, Psf2 loss did not affect Mcm2–6 sumoylation in G1 but prevented Mcm2–6 sumoylation loss (Fig. 2-5b). The observed effects were not because of a lack of CDK and DDK activities or abnormal checkpoint activation (Fig. 2-3e).

Together, these results show that DDK and GINS are not required for Mcm2–6 sumoylation in G1; instead, they are required for the loss of this modification at the beginning of S phase. These findings, in conjunction with the cell-cycle pattern of Mcm2–6 sumoylation, suggest that the modification takes place before DDK- and GINS-mediated events and then decreases in a DDK- and GINS-dependent manner upon S-phase entry.

Mcm6 sumoylation loss coincides with origins firing

Next I addressed how the change in Mcm2–6 sumoylation status at the G1-S transition is related to early and late origin firing. Releasing G1 cells into medium containing 200 mM hydroxyurea (HU) for a short time (for example, 60 min) allows limited DNA synthesis from early origins (Crabbe et al. 2010). The number of fired origins greatly increases when checkpoint-mediated inhibition of late origins is removed by mutating the phosphorylation sites on the DDK subunit Dbf4 and the replisome-assembly factor Sld3 (*dbf4-4A sld3-A*) (Zegerman and Diffley 2010). Thus, releasing G1 cells into HU-containing medium for a short time allows the assessment of the influence of firing of only early origins (in wild-type cells) versus both early and late origins (in *dbf4-4A sld3-A* cells).

Using this experimental setup, I found that 40 min after release into HU, the Mcm6 sumoylation level was reproducibly decreased by approximately 30% in wild-type and 65% in *dbf4-4A sld3-A* cells, relative to the level in G1-arrested cells (Fig. 2-5c). These results suggest that loss of Mcm6 sumoylation coincides with the firing of both early and late origins. Because wild-type and *dbf4-4A sld3-A* cells do not experience replication termination under this treatment (Maric et al. 2014), the observed Mcm6 sumoylation loss is not associated with replication termination.

Mcm6-SuOn increases MCM sumoylation

The correlation of Mcm2–6 sumoylation loss with origin firing led us to hypothesize that this modification inhibits replication initiation. An important prediction of this hypothesis is that increasing MCM sumoylation should impair replication initiation. To test this prediction, I used a tagging strategy that utilizes the high-affinity SUMO interaction

region from a catalytically inactive SUMO protease domain to promote sumoylation of its fusion partner and subunits of the same complex, presumably by increasing the local SUMO concentration (Almedawar et al. 2012) (Fig. 2-6a). I fused this tag, referred to as SuOn (denoting SUMO on), to Mcm6. As a control, I fused Mcm6 to the same tag containing a point mutation of a key residue required for SUMO interaction (Mcm6-ctrl) (Mossessova and Lima 2000b; Almedawar et al. 2012). Both fusions were expressed from the endogenous MCM6 locus and tagged with the V5 epitope.

Compared with Mcm6-ctrl, Mcm6-SuOn showed an increase of at least approximately four-fold in a modified form of the protein in both G1 and S phases (Fig. 2-7a). This form exhibited the characteristic ~20-kDa upshift of mono-SUMO modification and was increased in Mcm6-SuOn cells, thus suggesting that it was the sumoylated form (Fig. 2-7a). I validated this conclusion with two additional tests. I found that first, compared with untagged SUMO, HF-Smt3 led to a further upshift of this form (Fig. 2-6b). Second, immunoprecipitation of Mcm6-SuOn or Mcm6-ctrl and subsequent western blotting showed that this form was recognized by a SUMO-specific antibody (Fig. 2-6c). Together, these findings demonstrated that the modified form represented the sumoylated form. Mcm6-SuOn also increased sumoylation levels of three other MCM subunits (Mcm2, 4 and 7) and thus is an effective tool to increase MCM sumoylation (Fig. 2-6d).

Subsequent tests showed that Mcm6-SuOn did not affect the general behavior of MCM or modification of other replication factors: (i) Mcm6-SuOn mimicked Mcm6-ctrl with regard to protein level or MCM-complex formation (Fig. 2-7a and Fig. 2-6e); (ii) Mcm6-SuOn and Mcm6-ctrl exhibited a normal distribution between chromatin and cytosol fractions, thus suggesting proficient chromosomal loading (Fig. 2-7b); (iii)

Sumoylated Mcm6-SuOn was detected in the chromatin fraction in a Cdc6-dependent manner (Fig. 2-7b-7c); (iv) Mcm6-SuOn did not affect sumoylation of several other DNA-replication factors (Fig. 2-6f); and (v) Mcm6-SuOn did not show abnormal DNA damage checkpoint activation (Fig. 2-7a). These results suggest that the increased MCM sumoylation caused by Mcm6-SuOn obeys the rules of MCM sumoylation and does not perturb general MCM behavior or other replication and checkpoint protein modifications.

Mcm6-SuOn impairs replication initiation

Next, I examined how increased MCM sumoylation by Mcm6-SuOn affected replication and growth. Mcm6-SuOn grew slowly, whereas Mcm6-ctrl supported normal growth (Fig. 2-7d and Fig. 2-8a). Importantly, this defect was ameliorated when the SUMO E2 Ubc9 was mutated (Fig. 2-7e). Thus, although tagging per se did not interfere with protein functions, Mcm6-SuOn impaired growth in a sumoylation-dependent manner.

I next examined the kinetics of S-phase progression. To avoid chronic defects caused by Mcm6-SuOn, I constructed diploid cells homozygous for *cdc7-4*, containing either Mcm6-SuOn or Mcm6-ctrl and an Mcm6-aid allele. I synchronized cells grown at the permissive temperature for *cdc7-4* (24 °C) in G2-M and then depleted Mcm6-aid by IAA addition (Figure 2-9a). Next, I released cells from G2-M arrest and synchronized them at the G1-S boundary by raising the temperature to 37 °C to inactivate *cdc7-4*. Finally, I released cells from this arrest by bringing the temperature back to 24 °C to reactivate *Cdc7-4*. FACS profiles showed that cells containing Mcm6-SuOn or Mcm6-ctrl entered S phase after the final release, but Mcm6-SuOn cells exhibited a slower replication profile than that of Mcm6-ctrl cells (Fig. 2-9a). Quantification of DNA content from the FACS

analyses suggested that Mcm6-SuOn cells moved through S phase about half as quickly as the control (Fig. 2-9b).

To understand whether the slow replication seen in Mcm6-SuOn cells was because of replication initiation defects, I subjected the samples collected in the above tests to two-dimensional agarose gel electrophoresis (2D gel). Using probes specific to an early origin (ARS305) and a late origin (ARS609), I detected replication-firing events as bubble DNA structures, as shown previously (Fig. 2-9c-9d). Whereas Mcm6-ctrl cells showed robust origin-firing signals at both loci at the expected times, Mcm6-SuOn cells showed weaker signals, thus indicating impaired replication initiation (Fig. 2-9c-9d).

From deep-sequencing analysis of samples from *cdc7-4* arrest (0 min) and 30 min after release, I deduced copy-number changes and genome-wide replication profiles (Hawkins et al. 2013; Murakami and Keeney 2014). This analysis showed that Mcm6-SuOn cells, compared with Mcm6-ctrl cells, exhibited decreased replication at nearly all the origins annotated in the DNA Replication Origin Database (OriDB) (Fig. 2-9e and Fig. 2-10). Together, these results demonstrate that increased MCM sumoylation levels impair genome-wide replication from both early and late origins.

Increasing MCM sumoylation levels compromises CMG formation

To gain insight into the molecular basis of the replication initiation defects associated with Mcm6-SuOn, I examined CMG formation, because it is critical for replisome assembly. CMG formation can be assessed by measuring the amount of Cdc45 or a GINS subunit (for example, Psf1) that coimmunoprecipitates with Mcm6. Using the samples obtained from experiments depicted in Figure 2-9a, I found that Mcm6-SuOn,

compared to Mcm6-ctrl, co-purified lower amounts of both Cdc45 and Psf1, at 30 and 40 min after S phase entry (Fig. 2-11a). This finding suggested that Mcm6-SuOn interfered with CMG formation. This conclusion was substantiated by the observation that Mcm4 phosphorylation was reduced in Mcm6-SuOn compared with Mcm6-ctrl cells in G1 and S phases (Fig. 2-11b, lane 1-8). In addition, I found that mimicking constitutive sumoylation by using an Mcm6-SUMO fusion led to similar defects as those observed for Mcm6-SuOn; i.e., lower amounts of Cdc45 and Psf1 were associated with Mcm6-SUMO than with the control (Fig. 2-12a). Consistently with these results, Mcm6-SUMO fusion strains grew poorly and showed slower replication profiles (Fig. 2-12b-12c). Our findings that increasing MCM sumoylation through two strategies resulted in similar molecular and phenotypic defects support a negative role for MCM sumoylation in controlling replication initiation at a step involving CMG formation.

Removing a PP1 cofactor rescues defects of Mcm6-SuOn cells

Because Mcm4 phosphorylation is a prerequisite for CMG formation, I determined whether low Mcm4 phosphorylation might be responsible for the observed Mcm6-SuOn defects. I tested this idea genetically by removing Rif1, a binding partner of phosphatase PP1 (Glc7, essential in budding yeast), because disruption of this complex increases Mcm4 phosphorylation in both G1 and S phases (Davé et al. 2014; Hiraga et al. 2014; Mattarocci et al. 2014). Rif1 loss in Mcm6-SuOn increased Mcm4 phosphorylation without affecting the Mcm6 sumoylation level in both cell-cycle phases (Fig. 2-11b, lanes 5-12).

Importantly, Rif1 loss improved Mcm6-SuOn growth, as assessed by spore-clone sizes and spotting assays (Fig. 2-13a). Control cells showed wild-type levels of Mcm4 phosphorylation, which were increased by *rif1* Δ , as expected (Fig. 2-12d). In

addition, I observed no growth defects for Mcm6-ctrl or Mcm6-ctrl *rif1* Δ cells (Fig. 2-13a). I also compared *rif1* Δ with two other mutations, *mcm5-bob1* and *mcm4* Δ^{2-174} , known to improve replication when Mcm4 phosphorylation is dampened (Hardy et al. 1997; Sheu and Stillman 2010). While the lethality of Mcm6-ctrl *mcm4* Δ^{2-174} precluded testing this allele (Fig. 2-8b), I found that *mcm5-bob1* did not suppress *cdc7-4* as potently as did *rif1* Δ (Fig. 2-8c) and failed to suppress Mcm6-SuOn growth defects (Fig. 2-8d), thus suggesting that suppression of Mcm6-SuOn requires maximal bypass of Mcm4 phosphorylation defects. The observed *rif1* Δ suppression of Mcm6-SuOn cells supports the notion that reduced Mcm4 phosphorylation is partly responsible for the replication defects in these cells.

Mcm6-SuOn shows increased association with PP1

The above findings, in conjunction with a previously detected interaction between Glc7 and SUMO (Sung et al. 2013), raised the possibility that the decreased Mcm4 phosphorylation caused by MCM hypersumoylation may be due to increased recruitment of Glc7 to MCM. To test this possibility, I examined the Glc7-Mcm6 association in G1 cells by coimmunoprecipitation. I detected a slight but reproducible enrichment of Glc7 in the immunoprecipitated fraction when Mcm6 was pulled down (Fig. 2-13b). Importantly, I found a two-fold-greater enrichment of Glc7 in the immunoprecipitated fraction of Mcm6-SuOn cells, compared to that of Mcm6-ctrl cells, both in G1 and upon release into S phase (Fig. 2-13b and Fig. 2-12e). Because the level of association of Glc7 with Mcm6-SuOn was not affected in cells lacking Rif1 (Fig. 2-12f), Rif1 probably has additional roles in promoting Glc7 functions. Together, my results suggest that MCM sumoylation promotes Glc7 recruitment to MCM, thereby disfavoring MCM phosphorylation.

Discussion

MCM sumoylation negatively regulates origin firing

Proper control of replication initiation is important for cell survival and for the prevention of human diseases. While positive regulation promotes origin licensing and replisome assembly, negative regulation is needed to prevent premature initiation or re-replication, and to ensure the proper sequence of events in the assembly of a functional replisome. Many of these regulatory targets are subunits of MCM due to its central role in multiple aspects of replication. While phosphorylation was the only known chemical modification on MCM that regulates replication initiation thus far, other modifications have recently been identified through studies such as proteomic screens. Here we examined a highly conserved MCM modification by SUMO and demonstrated its strict temporal and spatial regulation in cells (summarized in Fig. 2-13c). For each MCM subunit, a fraction of the protein showed sumoylation upon Cdc6-mediated MCM loading onto chromatin, prior to bulk Mcm4 phosphorylation (Fig. 2-1 and -4). As cells entered S phase, Mcm2–6 sumoylation levels greatly reduced (Fig. 2-4). This loss was associated with replication initiation from both early and late origins (Fig. 2-5c). That the pattern of MCM sumoylation was opposite to that of replication activity suggested that this modification played a negative role in replication. We tested this model by increasing MCM sumoylation through the use of Mcm6-SuOn or mimicking the modification by Mcm6-SUMO fusion (Fig. 2-7 and -12a-12c). In both cases, cell growth and replication were impeded and CMG levels were reduced, providing strong evidence for this model (Figs. 2-7d, -9a-9e, -10, -11a, and -12a-12c). In addition, the growth defect of Mcm6-SuOn was rescued either by reducing sumoylation or diminishing protein phosphatase 1 (PP1) function, which restored Mcm4-phosphorylation (Figs. 2-7e, -11b, and -13a). Finally, our data suggest that MCM sumoylation promotes the association of PP1 with MCM (Fig. 2-

13b and -12e), providing a mechanism for targeting the phosphatase specifically to chromatin-loaded MCM in G1 phase (model in Fig. 2-13c).

The reversal of MCM sumoylation

Our results also suggest that the reversal of MCM sumoylation is important. The loss of Mcm2–6 sumoylation required DDK and GINS (Fig. 2-5a-5b), thus suggesting that an active desumoylation process may occur to remove this replication-inhibition marker. Consistently with the proposal of an active role of DDK in MCM sumoylation loss, artificially increasing DDK effects by removing Rif1 decreased the sumoylation of Mcm2 and Mcm6 proteins (Fig. 2-14a), although this effect was masked in Mcm6-SuOn cells (Fig. 2-11b). Because sumoylated forms of Mcm4 did not appear to be phosphorylated (Fig. 2-14b), DDK is unlikely to affect desumoylation via modulating Mcm4 phosphorylation. Instead, DDK may affect this process by modulating the desumoylation enzymes. In depletion studies of the two desumoylation enzymes in yeast, I found that acute depletion of Ulp2, but not Ulp1, increased the sumoylation levels of Mcm4 and 6 on chromatin (Fig. 2-14c-14e), thus supporting a role of this enzyme in removal of MCM sumoylation. Thus, although my study focuses on MCM sumoylation and reveals a role for this modification in counteracting DDK-mediated phosphorylation in G1, the reverse is likely to be true during S phase. Such dual regulation may ensure the precise deployment of each regulatory module during replication initiation. Such dynamic nature of sumoylation and desumoylation in cells, as well as potential sumoylation loss during extraction probably explain the low levels of sumoylation observed for each MCM subunit, as for most other substrates. Notably, my data suggest that even a low level of MCM sumoylation is sufficient to achieve a biological effect, either because sumoylation promotes the recruitment of an enzyme, a small amount of which can catalyze multiple

reactions, or because sumoylation of multiple MCM subunits may have redundant roles.

The potential effect of Mcm6-SuOn in diploid cells

Since MCM hyper-sumoylation recruits the PP1 enzyme to inhibit origin firing, one would expect that Mcm6-SuOn acts dominantly regarding origin firing in diploid cells that contain both Mcm6 and of Mcm6-SuOn. While I have not tested replication initiation in such diploid cells, I observed that these cells grew normally, unlike the slow growth exhibited by the Mcm6-SuOn haploid cells. In other words, Mcm6-SuOn was recessive in terms of cell growth. Currently we do not fully understand why Mcm6/Mcm6-SuOn diploid cells grow normally, but we consider two possibilities. First, in Mcm6/Mcm6-SuOn diploid cells, it is likely that a mixture of Mcm6 and Mcm6-SuOn are loaded at origins. As such, the extend of MCM sumoylation may be less than that in Mcm6-SuOn haploid cells. Consequently, PP1 recruitment may not be as enhanced in the diploid cells as in in Mcm6-SuOn haploid cells. Due to these reasons, the diploid cells may have less inhibition of origin firing than seen in Mcm6-SuOn haploid cells. It is possible that moderate reduction of origin firing may not lead to noticeable cell growth. Second possibility is that when competing with Mcm6, Mcm6-SuOn may not be efficiently loaded onto origins, thus reducing its inhibitory effects on origin firing. These hypotheses make testable predictions that we plan to examine the future.

Other potential roles for MCM sumoylation

Our findings suggest one role of MCM sumoylation in replication regulation and do not exclude other possible functions. For example, because Rif1 removal only partially rescues the Mcm6-SuOn growth defect (Fig. 2-13a), it is possible that MCM sumoylation may have other roles in inhibiting replication. One probable scenario is that MCM sumoylation may disfavor the recruitment of Cdc45 or GINS downstream of the DDK-

mediated Mcm4 phosphorylation step (Fig. 2-13c). In addition, sumoylation of each MCM subunit may have distinct roles. For example, unlike Mcm2–6, Mcm7 sumoylation persisted throughout most of S phase (Fig. 2-4a-4b). Given that Mcm7 is the only ubiquitinated MCM subunit that enables MCM removal during replication termination (Maric et al. 2014; Priego Moreno et al. 2014), its sumoylation may be relevant to this event. Our findings regarding one effect of MCM sumoylation should stimulate future studies to uncover the full scope of the biological effects of this modification.

In summary, my findings reveal that a new SUMO-based regulation exerts a negative influence on MCM activation, thus adding to the known positive regulation conferred by MCM phosphorylation. This dual modulation can expand the range of regulation, allowing for flexible integration of multiple biological cues, including those related to chromatin structure and developmental stages, and providing precision and flexibility in replication regulation. Given that MCM sumoylation is highly conserved, my work may stimulate the elucidation of the range of effects of this modification in higher organisms.

Methods and Materials

Yeast strains and techniques. Standard procedures were used in cell growth and medium preparation. Strains are isogenic to W1588-4C, a RAD5 derivative of W303, (MATa ade2-1 can1-100 ura3-1 his3-11,15 leu2-3,112 trp1-1 rad5-535) (Zhao and Blobel 2005b). Strains and their usage are listed in Table 2. Proteins were tagged at their endogenous loci by standard methods and correct tagging was verified by sequencing. Each MCM subunit was tagged with 3HA at the C-terminus, except Mcm3, which was tagged at its N-terminus and expressed from the ADH1 promoter. As shown in Figure 2-14f, P_{ADH1} -Mcm3-HA expression level was about half that of Mcm7-HA, consistent with their endogenous protein level ratio (Donovan et al. 1997) and indicating normal protein levels. Mcm5 was additionally tagged with the strep tag II at its C-terminus in Figure 2-1d and 2-5b. Aid-tagging has been described previously (Nishimura et al. 2009; Havens et al. 2012). In brief, Psf2 was fused with a 3V5 tag-IAA7 module at its C-terminus, and Mcm6 was fused with IAA17-3Flag at its C-terminus. Mcm6-SuOn and -ctrl were constructed as described with minor modifications (Almedawar et al. 2012). Both tags and a 3xV5 linker were fused to the C-terminus of Mcm6. SuOn is composed of the catalytically dead Ulp1 protease domain (418-621aa; with C580S abolishing the activity) (Mossessova and Lima 2000b; Almedawar et al. 2012). The control tag has the F474A mutation that disrupts SUMO interaction (Mossessova and Lima 2000b; Almedawar et al. 2012). I note that SuOn is different from the canonical SUMO-interacting motif (SIM) as it interacts with the C-terminal tail of SUMO through a distinct large interface and has strict orientation requirements (Mossessova and Lima 2000b). Yeast dissection and spotting assays were performed using standard procedures. All genetic and biochemical experiments were performed using two different spore clones for each genotype.

Synchronization procedures. For experiments that entailed α -factor arrest, cells were treated for 2.5 hours with 5 $\mu\text{g/ml}$ (for BAR1 cells) or 100 ng/ml (for *bar1* Δ cells) α -factor. For experiments involving G2/M arrest, cells were grown in media containing 1% DMSO to early log phase and treated with 15 $\mu\text{g/ml}$ nocodazole for 3 hours. In all cases, cell morphology was checked to confirm the arrest. Experiments in Figure 2-1d and 7c were performed as described previously (Desdouets et al. 1998). In brief, cultures grown in YP-Galactose at 24°C were arrested in G2-M and split into two, one of which received 2% glucose for 1 hour. Subsequently, cells were released into the same media containing α -factor for 2.5 hours before harvesting. For the experiment in Figure 2-5a, cells were arrested by α -factor at 24°C, then temperature was shifted to 37°C for 1 hour. Subsequently, cultures were split into two, only one of which was released from α -factor into S phase. Samples were taken from both cultures 40 minutes afterwards. For experiments in Figure 2-5b, cells were arrested in G2-M phase at 24°C, IAA was added to a final concentration of 1 mM. After 1 hour, cells were released into media containing α -factor and 1 mM IAA for 3 hours, and then released into media containing 1 mM IAA for 60 min. For the experiment in Figure 2-5c, α -factor arrested cells were released into YPD media containing 300 $\mu\text{g/ml}$ pronase and 200 mM HU at 24°C for 40 minutes. For experiments in Figure 2-9 and 11a, diploid cells containing Mcm6-SuOn or Mcm6-ctrl and a Mcm6-aid degron allele and homozygous for *cdc7-4* were used. Cells were grown at the permissive temperature for *cdc7-4* (24°C) and synchronized in G2-M. Then Mcm6-aid was depleted with the addition of 1 mM IAA for 1 hour. Subsequently, cells were released from G2-M arrest and synchronized at the G1-S boundary by raising the temperature to 37°C to inactivate *cdc7-4*. Finally, cells were released by rapid cooling to 24°C.

Detection of protein sumoylation. Unless otherwise indicated, standard Ni-NTA pull down method was used as described (Ulrich and Davies 2009). Smt3 was tagged with HF (6His-Flag) at its N terminus and expressed from its endogenous promoter (Takahashi et al. 2008). Cell extracts prepared by 55% trichloroacetic acid (Shanbhag et al.) precipitation were dissolved in Buffer A (6 M Guanidine HCl, 100 mM sodium phosphate, pH 8.0, 10 mM Tris-HCl, pH 8.0) with rotation at room temperature. Cleared supernatant was then incubated with Ni-NTA resin (Qiagen) after the addition of Tween 20 (0.05% final concentration) and imidazole (4.4 mM final concentration) overnight at room temperature. Beads were then washed twice with Buffer A containing 0.05% Tween 20 and four times with Buffer C (8 M urea, 100 mM sodium phosphate, pH 6.3, 10 mM Tris-HCl, pH 6.3) containing 0.05% Tween 20. HU buffer (8 M urea, 200 mM Tris-HCl, pH 6.8, 1 mM EDTA, 5% SDS, 0.1% bromophenol blue, 1.5% DTT, 200 mM imidazole) was used to elute proteins from the beads before loading on to a 3-8% gradient Tris-Acetate gel (Life Technologies). Western blots were probed with antibodies recognizing the tagged substrates detecting both sumoylated and unmodified bands. The latter is due to non-specific binding to the Ni-NTA beads and is not enriched when using HF-Smt3. Our previous work using a protein immunoprecipitation method showed sumoylation of two MCM subunits under normal growth conditions (Cremona et al. 2012) and Fig. 2-2b demonstrates the sumoylation of additional MCM subunits by using this method. As desumoylation cannot be efficiently prevented during this procedure, low abundant sumoylation forms are difficult to detect. However, the use of both untagged and HF-SUMO allowed better assessment of sumoylation because of the different sizes of sumoylated forms in the two situations (Fig. 2-2b).

Two-dimensional agarose gel electrophoresis (2D gel). 2D gel analyses were performed as previously described (Friedman and Brewer 1995). Genomic DNA was

extracted from spheroplasts and purified by standard CsCl centrifugation at 90 krpm for 9 hours at 15°C. DNA was digested by EcoRI and separated by agarose gel electrophoresis in two dimensions. DNA was transferred to Hybond-XL membrane (GE Healthcare) and analyzed by Southern blot hybridization using probes specific for ARS305 or ARS609 as described previously (Hang et al. 2015). Primers used for amplification of the probes are available upon request.

Whole genome sequencing and copy number calculation. Both procedures were carried out as previously described (Hawkins et al. 2013; Murakami and Keeney 2014). Mcm6-ctrl and Mcm6-SuOn cells were collected at 0 and 30 min as described in Figure 2-9a. 1.5 µg genomic DNA from each sample was used to generate libraries using the KAPA's library kit (iGO facility, MSKCC) and sequenced using HiSeq 2500 (Illumina). At least 10 million 50 bp paired-end reads were generated per sample. Reads were mapped to the S288c reference genome (SGD, SacCer2) excluding repetitive sequences, and summed in 1 kb bins using Genome Browser. Bins containing fewer than 600 reads were excluded. Custom R script was used to analyze the value for each locus. In brief, for each strain, the binned reads from the 30 min sample at a locus were divided by those from 0 min sample, and normalized to the ratio of total reads to give a genome-wide mean value of 1. This number was adjusted by the relative DNA content at 30 min in FACS fitting curve (Fig. 2-9b) to derive a relative copy number of the particular locus. The map of adjusted copy numbers were further smoothed with the “loess” function and shown in Figure 2-9e and Figure 2-10. Detailed methods and data for calculating the relative copy number based on the whole genome sequencings are included in the GEO database (GSE70407).

Protein extraction and immunoprecipitation (IP). For Fig. 2-4b, 11a, cells was resuspended in IP buffer (100 mM HEPES/KOH pH 7.9, 100 mM KOAC, 2 mM MgOAC, 1 mM ATP, 1% Triton X-100, 2 mM NaF, 0.1 mM Na₃VO₄, 20 mM β-glycerophosphate, 1 mM PMSF, 10 mM Benzamidine HCl, 10 μg/ml leupeptin, 1 μg/ml pepstatin A) containing 1x protease inhibitor (EDTA-free, Roche) and 20 mM N-Ethylmaleimide (NEM). Cells were disrupted by bead beating. Benzonase was added to cell lysates, which were incubated for one hour at 4°C. After centrifugation for 20 min at 15,000 rpm at 4°C, the supernatant was collected and incubated with prewashed HA or V5 conjugated beads (A7345, sigma) for 2 hours at 4°C. For Figure 2-13b, minor changes were made to the IP buffer, 50 mM HEPES/KOH pH 7.9, 150 mM KOAC were used and glycerol was added at a final concentration of 10%.

Immunoblotting analysis and antibodies. Protein samples were resolved by 3%-8% or 4%-20% gradient gels (Life Technologies and Bio-Rad) and transferred to a 0.2 μm nitrocellulose membrane (G5678144, GE). Antibodies used are: anti-HA (F-7, Sc-7392, Santa Cruz Biotechnology), anti-V5 (R960-25, Invitrogen), anti-myc (9E10, Bio X cell), PAP (P1291, Sigma), anti-flag (M2, Sigma), anti-Rad53 (yC-19, sc-6749, Santa Cruz Biotechnology), anti-Orc2 (SB46, Abcam), anti-Pgk1 (22C5D8, Invitrogen), anti-Cdc6 (9H8/5, Abcam), anti-Strep tag II (A01732, Genscript), anti-Psf1, anti-Mcm6 (both are gifts from Karim Labib) (Gambus et al. 2006), anti-Orc6 and α-Cdc45 (both are gifts from Bruce Stillman) (Sheu and Stillman 2010) and anti-SUMO (Zhao and Blobel 2005b). Validation of these antibodies are either provided on the manufacturer's website or from the cited references. For quantification purpose, membranes were scanned with Fujifilm LAS-3000 luminescent image analyzer, which has a linear dynamic range of 10⁴. Quantification of blots was done using Photoshop and ImageGauge.

Lambda phosphatase treatment. After immunoprecipitation on HA (Fisher, 26182) or Ni-NTA beads (Qiagen), the beads were washed three times with wash buffer (50 mM K-HEPES pH7.9, 150 mM KOAC, 2 mM MgOAC, 10 µg/ml pepstatin, 10 µg/ml leupeptin, 0.5 mM PMSF, 1 mM benzamidine and 20 mM NEM). Beads were then resuspended in Lambda phosphatase reaction buffer (1x NEBuffer for PMP, 1 mM MnCl₂ and 10 µg/ml pepstatin, 10 µg/ml leupeptin, 0.5 mM PMSF, 1 mM benzamidine and 20 mM NEM). In control tests, the beads were incubated with reaction buffer and phosphatase inhibitors (50 mM EDTA, 50 mM NaF and 10 mM Na₃VO₄). 80 U of lambda phosphatase (NEB, P0753S) was added, and incubated at 30°C for 30 min. Laemmli buffer was added to stop the reaction and the proteins were eluted by boiling at 95°C for five min before SDS-PAGE and western blotting analysis.

Other methods. Chromatin fractionation was performed as described previously with minor modifications (Schepers and Diffley 2001). In brief, spheroplasts were lysed in lysis buffer containing 1% Triton-X-100 and laid upon a 30% sucrose cushion and centrifuged at 13,000 rpm for 20 min to separate the supernatant and chromatin fractions. The chromatin-bound fraction was washed once with lysis buffer and re-suspended in the same buffer. Equal volumes of samples from lysate, supernatant and chromatin fractions were precipitated with 20% TCA, and resuspended in Laemmli buffer with the addition of 2M Tris to neutralize TCA. Flow cytometry was performed as previously described using FACSCalibur flow cytometer, and data were analyzed with FlowJo Software. To calculate the relative DNA content in Figure 2-9a, the distance between 1N and 2N DNA peaks were considered as 2 and the position of 1N peak as 1. Then the distance between DNA peaks at each time point and the 1N DNA peak in G1 cells was measured and scaled between 1 and 2 and plotted.

Table 1: Strains used in this study

All strains are isogenic to W1588-4C (a RAD5 derivative of W303: MATa ade2-1 can1-100 his3-11,15 leu2-3,112 trp1-1 ura3-1). One strain is listed for each genotype, and two were used in experiments.

| Strain | Genotype |
|--------------|--|
| X3544-4D | MATa HF-Smt3::LEU2 |
| T1834-1 | MATa Mcm2-3HA::HIS3 HF-Smt3::LEU2 |
| T1839-1 | MATa P _{ADH1} -3HA-Mcm3::NatNT2 HF-Smt3::LEU2 |
| T1840-1 | MATa Mcm4-3HA::HIS3 HF-Smt3::LEU2 |
| T1841-1 | MATa Mcm5-3HA::HIS3 HF-Smt3::LEU2 |
| T1797-1 | MATa Mcm6-3HA::HIS3 HF-Smt3::LEU2 |
| T1842-1 | MATa Mcm7-3HA::HIS3 HF-Smt3::LEU2 |
| X6525-1c | MATa Mcm2-3HA::HIS3 |
| X6223-2c | P _{ADH1} -3HA-Mcm3::NatNT2 |
| X6526-3d | MATa Mcm4-3HA::HIS3 |
| X6527-3a | Mcm5-3HA::HIS3 |
| X6528-7a | MATa Mcm6-3HA::HIS3 |
| X6529-10d | Mcm7-3HA::HIS3 |
| X6629-6c | MATa cdc6Δ::Gal-Cdc6::TRP1 bar1Δ::HphMX3 Mcm2-3HA::HIS3 HF-Smt3::LEU2 |
| X6660-7b | MATa cdc6Δ::Gal-Cdc6::TRP1 bar1Δ::HphMX3 P _{ADH1} -3HA-Mcm3::NatNT2 HF-Smt3::LEU2 |
| X6628-8c | MATa cdc6Δ::Gal-Cdc6::TRP1 bar1Δ::HphMX3 Mcm4-3HA::HIS3 HF-Smt3::LEU2 |
| X6659-14c | MATa cdc6Δ::Gal-Cdc6::TRP1 bar1Δ::HphMX3 Mcm5-Strep::HIS3 HF-Smt3::LEU2 |
| X6630-8b | MATa cdc6Δ::Gal-Cdc6::TRP1 bar1Δ::HphMX3 Mcm6-3HA::HIS3 HF-Smt3::LEU2 |
| X6631-15d | MATa cdc6Δ::Gal-Cdc6::TRP1 bar1Δ::HphMX3 Mcm7-3HA::HIS3 HF-Smt3::LEU2 |
| X6525-2d | MATa cdc7-4 Mcm2-3HA::HIS3 HF-Smt3::LEU2 |
| X6623-3b | MATa cdc7-4 P _{ADH1} -3HA-Mcm3::NatNT2 HF-Smt3::LEU2 |
| X6526-5,6-6b | MATa cdc7-4 Mcm4-3HA::HIS3 HF-Smt3::LEU2 |
| X6527-1c | MATa cdc7-4 Mcm5-3HA::HIS3 HF-Smt3::LEU2 |
| X6528-7b | MATa cdc7-4 Mcm6-3HA::HIS3 HF-Smt3::LEU2 |
| X6646-2c | MATa Psf2-3V5-IAA7::KAN GPD1-TIR::LEU2 Mcm2-3HA::HIS3 HF-Smt3::LEU2 |
| X6622-9a | MATa Psf2-3V5-IAA7::KAN GPD1-TIR::LEU2 P _{ADH1} -3HA-Mcm3::NatNT2 HF-Smt3::LEU2 |
| X6647-2,3-6b | MATa Psf2-3V5-IAA7::KAN GPD1-TIR::LEU2 Mcm4-3HA::HIS3 HF-Smt3::LEU2 |
| X6648-11a | MATa Psf2-3V5-IAA7::KAN GPD1-TIR::LEU2 Mcm5-Strep::HIS3 HF-Smt3::LEU2 |

| | |
|----------------|---|
| T1874-1 | MATa Psf2-3V5-IAA7::KAN GPD1-TIR::LEU2 Mcm6-3HA::HIS3 HF-Smt3::LEU2 |
| X6576-15d | MATa GPD1-TIR::LEU2 Mcm6-3HA::HIS3 HF-Smt3::LEU2 |
| X6696-1-16d | MATa dbf4-4A::HIS3 sld3-A-10his-13myc::KAN Mcm6-3HA::HIS3 HF-Smt3::LEU2 |
| T1462-1a | MATa Mcm6-3V5-SuOn::KAN |
| T1464-7d | MATa Mcm6-3V5-ctrl::KAN |
| X6661-1d | MATa cdc6Δ::Gal-Cdc6::TRP1 bar1Δ::HphMX3 Mcm6-3V5-SuOn::KAN HF-Smt3::LEU2 |
| X6662-13b | MATa cdc6Δ::Gal-Cdc6::TRP1 bar1Δ::HphMX3 Mcm6-3V5-ctrl::KAN HF-Smt3::LEU2 |
| T1462-2 | Mcm6-3V5-SuOn::KAN/+ |
| T1464-2 | Mcm6-3V5-ctrl::KAN/+ |
| X6714 | Mcm6-3V5-SuOn::KAN/+ ubc9-10::NAT/+ |
| X6898-i1 | cdc7-4/cdc7-4 Mcm6-3V5-SuOn::KAN/Mcm6-IAA17-3flag::HIS3 ADH1-TIR-9myc::URA3/+ |
| X6899-i3 | cdc7-4/cdc7-4 Mcm6-3V5-ctrl::KAN/Mcm6-IAA17-3flag::HIS3 ADH1-TIR-9myc::URA3/+ |
| X6636-9c | MATa Mcm6-3V5-ctrl::KAN Mcm4-3HA::HIS3 |
| X6637-4d | MATa Mcm6-3V5-SuOn::KAN Mcm4-3HA::HIS3 |
| X6619-12d | MATa Mcm6-3V5-SuOn::KAN Mcm4-3HA::HIS3 rif1Δ::URA3 |
| X6617 | Mcm6-3V5-SuOn::KAN/+ rif1Δ::URA3/+ |
| X3186-10b | MATa rif1Δ::URA3 |
| X6617_2-3,4-2c | rif1Δ::URA3 Mcm6-3V5-SuOn::KAN |
| X6618-8b | rif1Δ::URA3 Mcm6-3V5-ctrl::KAN |
| X6779-1-5b | MATa Glc7-13myc::HIS3 Rif1-Flag::KAN |
| X6780-2-15a | MATa Glc7-13myc::HIS3 Rif1-Flag::KAN Mcm6-3V5-ctrl::KAN |
| X6779-1-7b | MATa Glc7-13myc::HIS3 Rif1-Flag::KAN Mcm6-3V5-SuOn::KAN |
| X7028-1a | Mcm2-3HA::HIS3 8his-Smt3::TRP1 |
| X7029-4c | MATa P _{ADH1} -3HA-Mcm3::NatNT2 8his-Smt3::TRP1 |
| X7030-9d | Mcm4-3HA::HIS3 8his-Smt3::TRP1 |
| X7031-2c | Mcm5-3HA::HIS3 8his-Smt3::TRP1 |
| X7032-2c | Mcm6-3HA::HIS3 8his-Smt3::TRP1 |
| X7033-1c | Mcm7-3HA::HIS3 8his-Smt3::TRP1 |
| X7069-1a | MATa P _{ADH1} -3HA-Mcm3::NatNT2 |
| X6527-5a | MATa Mcm5-3HA::HIS3 |
| X6529-12d | MATa Mcm7-3HA::HIS3 |
| X5752-9c | Mcm6-3V5-SuOn::KAN |
| X5752-9a | Mcm6-3V5-SuOn::KAN HF-Smt3::LEU2 |
| X6334-1c | MATa Mcm2-3HA::HIS3 HF-Smt3::LEU2 Mcm6-3V5-ctrl::KAN |
| X6327-3b | MATa Mcm2-3HA::HIS3 HF-Smt3::LEU2 Mcm6-3V5-SuOn::KAN |
| X6969-17a | MATa P _{ADH1} -3HA-Mcm3::NatNT2 HF-Smt3::LEU2 Mcm6-3V5-ctrl::KAN |
| X6968-8b | MATa P _{ADH1} -3HA-Mcm3::NatNT2 HF-Smt3::LEU2 Mcm6-3V5-SuOn::KAN |
| X6970-2a | MATa Mcm4-3HA::HIS3 HF-Smt3::LEU2 Mcm6-3V5-ctrl::KAN |
| X6329-19a | MATa Mcm4-3HA::HIS3 HF-Smt3::LEU2 Mcm6-3V5-SuOn::KAN |
| X6974-1a | MATa Mcm7-3HA::HIS3 HF-Smt3::LEU2 Mcm6-3V5-ctrl::KAN |
| X6973-5c | MATa Mcm7-3HA::HIS3 HF-Smt3::LEU2 Mcm6-3V5-SuOn::KAN |

| | |
|-------------|---|
| X6258-6a | <i>Pol12-TAP::HIS3 HF-Smt3::LEU2</i> |
| X6258-10b | <i>Pol12-TAP::HIS3 Mcm6-3V5-SuOn::KAN HF-Smt3::LEU2</i> |
| X6259-10b | <i>Pol32-TAP::HIS3 HF-Smt3::LEU2</i> |
| X6259-12d | <i>Pol32-TAP::HIS3 Mcm6-3V5-SuOn::KAN HF-Smt3::LEU2</i> |
| X6260-10b | <i>Rfc1-TAP::HIS3 HF-Smt3::LEU2</i> |
| X6260-10a | <i>Rfc1-TAP::HIS3 Mcm6-3V5-SuOn::KAN HF-Smt3::LEU2</i> |
| X6262-10b | <i>Rfc3-TAP::HIS3 HF-Smt3::LEU2</i> |
| X6262-7d | <i>Rfc3-TAP::HIS3 Mcm6-3V5-SuOn::KAN HF-Smt3::LEU2</i> |
| X6263-1c | <i>Pri1-TAP::HIS3 HF-Smt3::LEU2</i> |
| X6263-1d | <i>Pri1-TAP::HIS3 Mcm6-3V5-SuOn::KAN HF-Smt3::LEU2</i> |
| X6999 | <i>mcm4Δ2-174/+ Mcm6-3V5-ctrl::KAN/+</i> |
| G957 | <i>MATa mcm5-bob1</i> |
| X6100-1b | <i>MATa cdc7-4</i> |
| X6977-4a | <i>cdc7-4 rif1Δ::URA3</i> |
| X6815-4b | <i>cdc7-4 mcm5-bob1</i> |
| X6978-15b | <i>mcm5-bob1 Mcm6-3V5-SuOn::KAN</i> |
| X6528-18b | <i>MATa Mcm6-3HA::HIS3</i> |
| T1679-4-17b | <i>MATa Mcm6-SUMO-3HA::KAN</i> |
| X6966-2d | <i>MATa Mcm4-3HA::HIS3 Mcm6-3V5-ctrl::KAN rif1Δ::URA3</i> |
| X6967-3d | <i>MATa Glc7-13myc::HIS3 rif1Δ::URA3</i> |
| X6804-12d | <i>MATa Glc7-13myc::HIS3 rif1Δ::URA3 Mcm6-3V5-SuOn::KAN</i> |
| X6975-10b | <i>MATa Mcm2-3HA::HIS3 HF-Smt3::LEU2</i> |
| X6975-2b | <i>MATa rif1Δ::URA3 Mcm2-3HA::HIS3 HF-Smt3::LEU2</i> |
| X6976-1a | <i>MATa Mcm6-3HA::HIS3 HF-Smt3::LEU2</i> |
| X6976-8b | <i>MATa rif1Δ::URA3 Mcm6-3HA::HIS3 HF-Smt3::LEU2</i> |
| X6811-18d | <i>MATa Ulp2-3V5-IAA7::KAN GPD1-TIR::LEU2 Mcm4-3HA::HIS3 8his-Smt3::TRP1</i> |
| X6812-2b | <i>MATa Ulp2-3V5-IAA7::KAN GPD1-TIR::LEU2 Mcm6-3HA::HIS3 8his-Smt3::TRP1</i> |
| X6814-2b | <i>MATa Ulp1-3V5-IAA7::KAN GPD1-TIR::LEU2 Mcm6-3HA::HIS3 8his-Smt3::TRP1</i> |

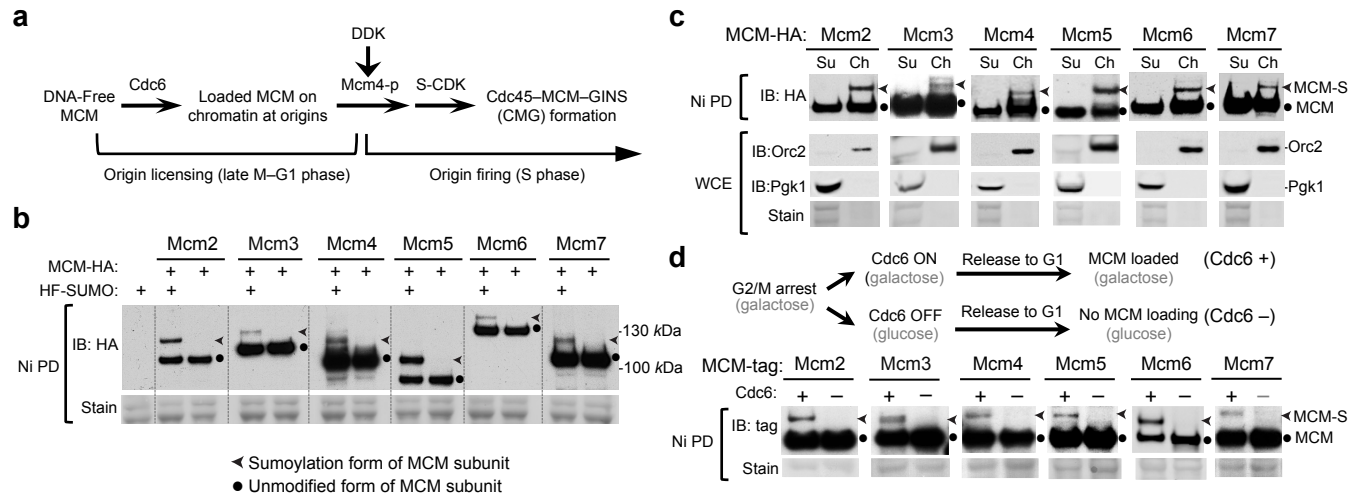


Figure 2-1. Sumoylation of six MCM subunits occurs on chromatin and depends on MCM loading at replication origins.

- a. Schematic of key events for MCM loading and activation (see text for details). Phosphorylation of Mcm4 is indicated as "Mmc4-P". CDK: S-cyclin-dependent kinase; DDK: Dbf4-dependent kinase.
- b. Mono-sumoylation of each MCM subunit occurs under normal growth conditions. HF-Smt3 denotes His6-Flag-tagged SUMO, which allows the enrichment of sumoylated proteins on Ni-NTA beads, a method indicated as "Ni PD". MCM subunits were tagged with HA. Unmodified and sumoylated bands are indicated by dots and arrowheads, respectively. Equal protein loading is shown by Ponceau S stain (stain). Similar methods and annotations are used in subsequent figure panels.
- c. Only chromatin-bound MCM subunits show sumoylation. MCM subunits were tagged with HA and examined in chromatin fractionation and Ni PD tests. Ch and Su indicate chromatin-bound and supernatant fractions. Orc2 and Pgc1 are markers for chromatin and supernatant fractions in cell extracts (WCE), respectively.
- d. Sumoylation of MCM subunits in G1 phase depends on Cdc6. Top, experimental scheme for Cdc6 depletion that prevents MCM loading. Mmc2-4, 6, and 7 were tagged with HA, while Mcm5 was tagged with strep tag II to be compatible with the Gal-Cdc6 construct. Successful Cdc6 depletion is shown in Figure 2-3a.

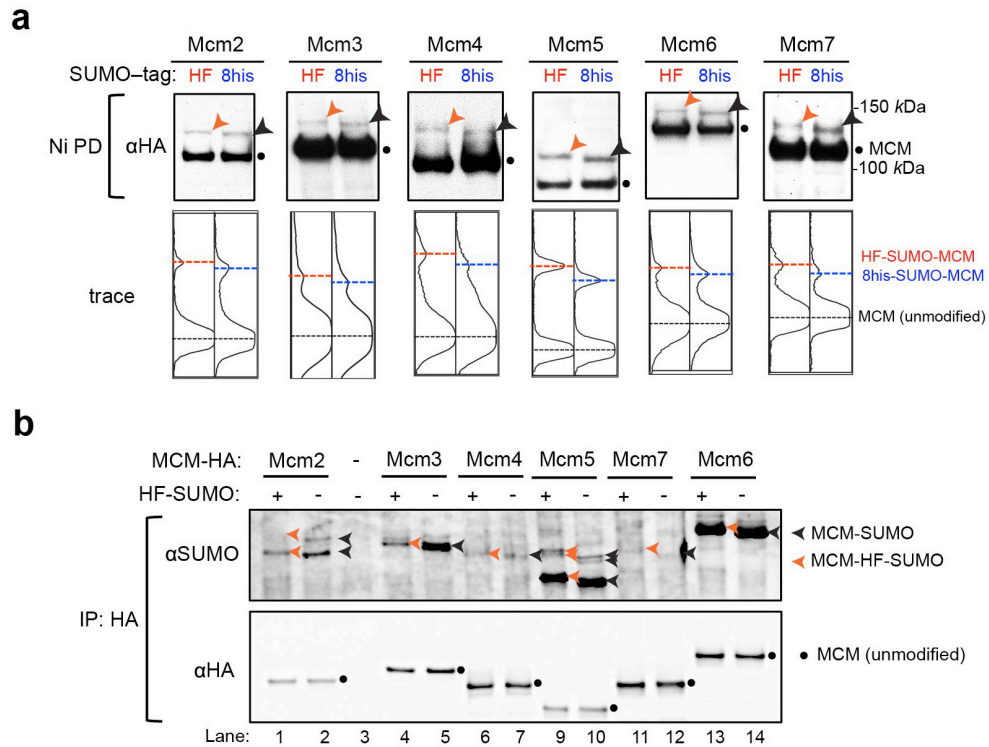


Figure 2-2

Detection of MCM subunit sumoylation under normal growth conditions

- a.** Sumoylated forms of MCM subunits show differential shifts when SUMO is attached to differently sized tags. MCM subunits were tagged with HA and SUMO was tagged with either HF (His6-Flag) or 8His at the endogenous loci. Western blots using anti-HA antibody after Ni-PD revealed the sumoylated (arrow head) and unmodified (dot) forms of MCM proteins. The relative shift of the sumoylated forms vs. the unmodified forms was bigger when SUMO was tagged with the larger tag (HF) than with the smaller tag (8His). The differences were better seen by the traces of the bands generated by the image quantification function from Image J (bottom).
- b.** HA-tagged MCM2-7 subunits were immunoprecipitated and examined by western blots. Cells contained either HF-SUMO (+) or untagged SUMO (-). Unmodified MCM subunits (dots) were detected by anti-HA blots, and sumoylated forms by anti-SUMO antibody (arrow heads). Sumoylated forms containing HF-SUMO (orange) migrated slightly slower than the ones containing untagged SUMO (black). Untagged MCM (lane 3) showed that bands in other lanes were MCM forms.

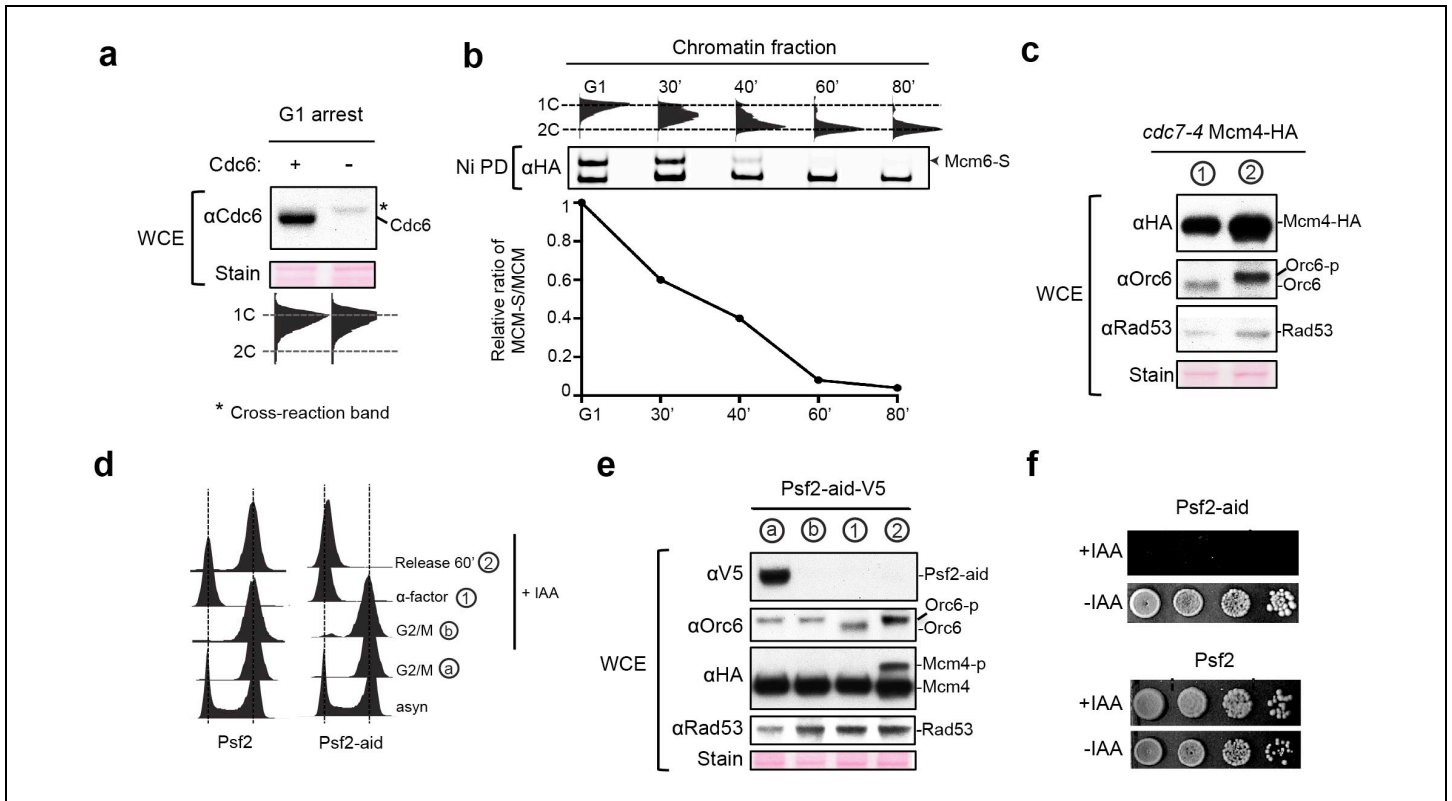


Figure 2-3

Examination of MCM subunits in the absence of Cdc6, DDK, and GINS.

- a.** Western blotting analysis of samples from Figure 1d for Cdc6 protein level.
- b.** Sumoylation levels of chromatin-bound Mcm6 peak in G1 and decline during S phase. Chromatin-bound Mcm6 was examined as in Figure 2-4a from cells arrested in G1 and at indicated time points after release into S phase. FACS profile is shown at the top, immunoblot detection of Mcm6 is in the middle, and quantification of the relative ratio of sumoylated to unmodified Mcm6 is at the bottom.
- c.** Western blotting analysis of samples from Figure 3a for phosphorylation of Mcm4, Orc6, and Rad53.
- d-e.** Flow cytometry and western blotting analysis of samples from Figure 2-5b. Experimental procedure and FACS analysis are depicted in **d**. Asynchronous cells (asyn) from both Psf2-aid and the control cells (no tagging) were arrested in G2/M by nocodazole for 3 h. IAA was then added to the media for 1 h to degrade Psf2-aid. Subsequently, cells were released into media containing IAA and alpha-factor to arrest cells in G1 phase. Once arrest was achieved, cells were released into media containing IAA. FACS analyses showed that Psf2 degradation did not affect cells entering G1 phase, but blocked G1 cells from replication when alpha-factor was washed out. The control cells showed bulk replication when cells were released from G1. In **e**, Western blots of cell extracts showed expected patterns of CDK-mediated Orc6 phosphorylation and DDK-mediated Mcm4 phosphorylation, and no checkpoint kinase Rad53 phosphorylation in Psf2-aid cells. Efficient degradation of Psf2-aid that was tagged with a V5 tag was also evident.
- f.** Psf2-aid fails to support cell viability in the presence of IAA, whereas the control fully supports cell viability. Media contains 1 mM IAA.

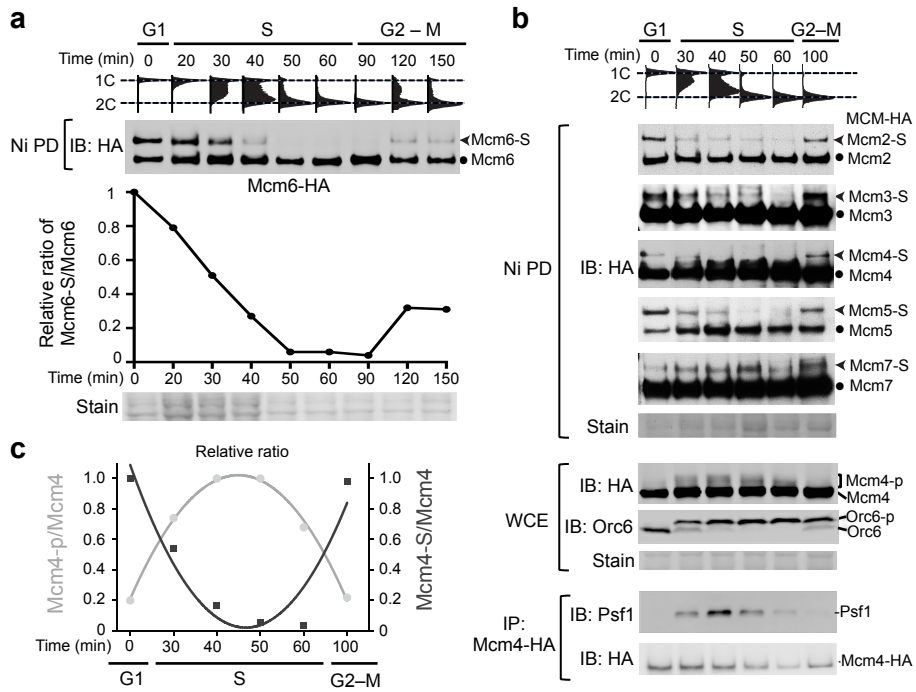


Figure 2-4. Sumoylation levels of MCM subunits oscillate during the cell cycle.

- a. Mcm6 sumoylation level peaks in G1 phase, declines during S phase, and reappears in late M phase. Flow cytometry (top) and immunoblotting (middle) show cell cycle progression and Mcm6 sumoylation status from cells arrested in G1 and indicated time points after release from G1. The graph depicts the relative ratio of sumoylated/unmodified Mcm6 on the western blot with the ratio in G1 cells set to 1. The ratio presented here and in other figures is not the absolute sumoylation level, as sumoylated forms were enriched; rather it is used to index changes in sumoylation levels. Staining at the bottom shows loading.
- b. Dynamic MCM sumoylation and phosphorylation during the cell cycle. As in (a), FACS profiles and immunoblotting after Ni PD show sumoylation status of HA-tagged MCM subunits at indicated time points. Middle: examination of phosphorylation levels of Mcm4 and Orc6. Bottom: examination of CMG levels after immunoprecipitation of Mcm4 and probing for Psf1, a subunit of GINS.
- c. The relative ratio of sumoylated or phosphorylated Mcm4 to total Mcm4 level. The ratio was calculated based on results in (b), the ratio in G1 cells was set to 1.

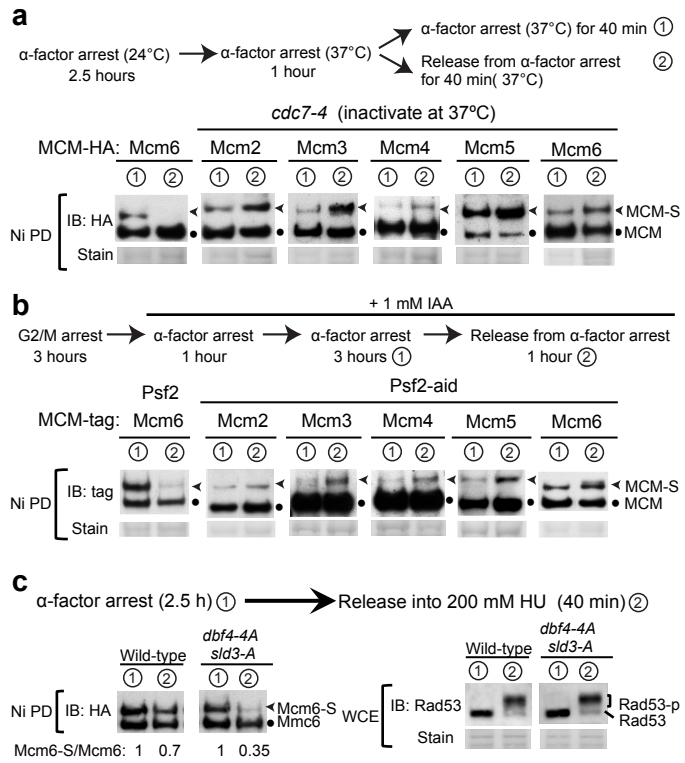


Figure 2-5. Mcm2-6 sumoylation loss at the G1-S transition requires DDK, GINS, and replication initiation.

- a. Mcm2-6 sumoylation in G1 phase does not require DDK, but its decrease in S phase depends on DDK. Top: experimental schemes for Cdc7 inactivation (see Methods). The sumoylation status of each HA-tagged MCM at indicated time points is shown as in Fig. 2-1b.
- b. Sumoylation of Mcm2–6 in G1 phase does not require GINS, but its decrease in S phase depends on the GINS subunit Psf2. Top: experimental schemes for Psf2 depletion (see Methods). Mcm5 was tagged with strep tag II to be compatible with the Psf2–aid construct, and other MCM subunits are tagged with HA.
- c. Mcm6 sumoylation loss coincides with firing of both early and late origins. Top: experimental schemes for G1 arrest and release. Immunoblots show Mcm6 sumoylation status at indicated time points. Note that *dbf4-4A sld3-A* cells allow late origin firing under this condition. Rad53 phosphorylation (bottom) shows the effectiveness of HU treatment.

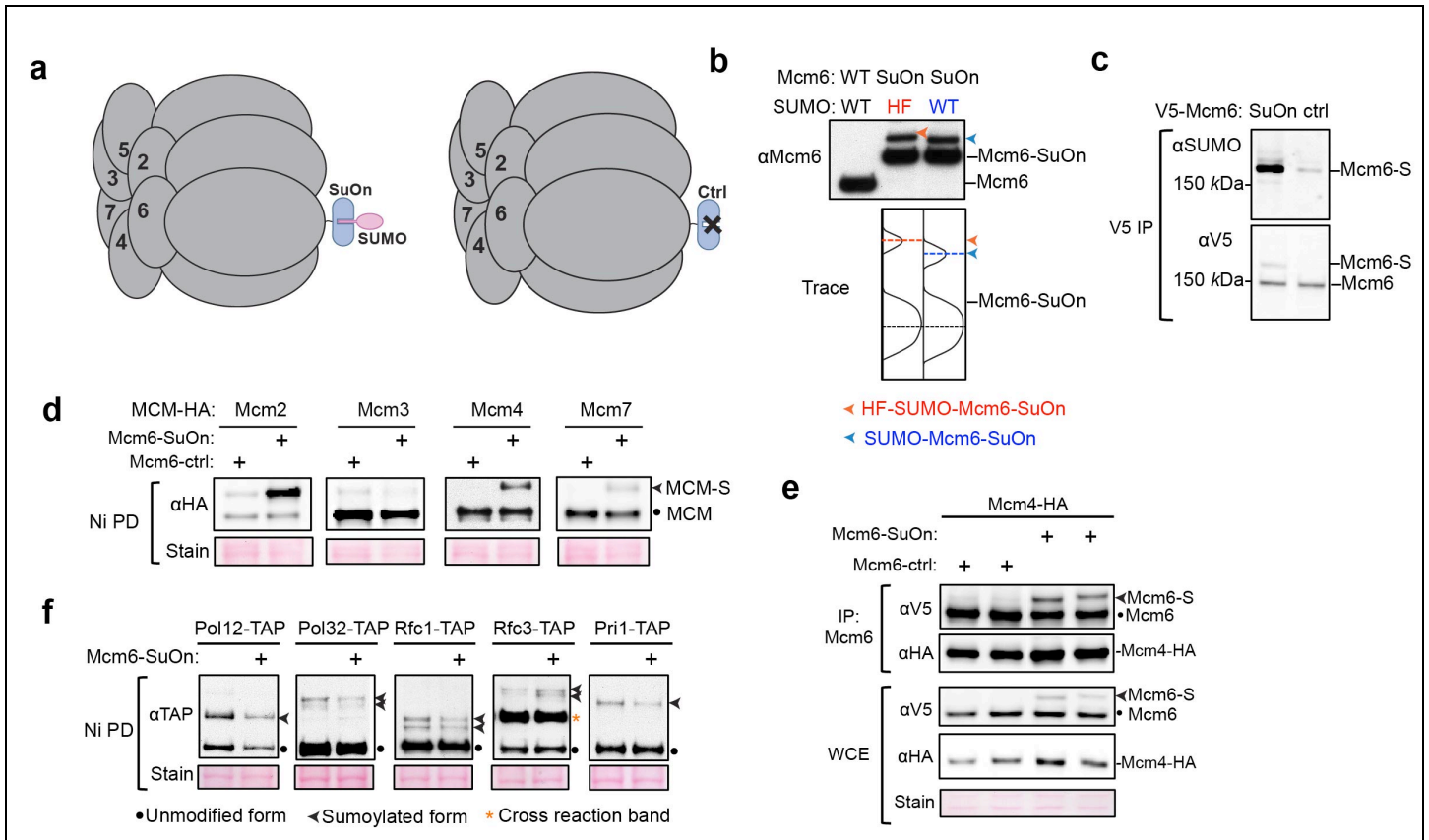


Figure 2-6

Examination of Mcm6-SuOn effects on sumoylation and MCM complex levels

- Diagram depicting Mcm6 fused with SuOn or ctrl tag. The SuOn tag is part of the desumoylation domain with catalytic site mutated and exhibits strong SUMO binding^{34,35}. The ctrl tag is the same as the SuOn, except for a single mutation disrupting SUMO binding^{34,35}. The MCM complex, tags, and SUMO are drawn in proportion to the sizes of the proteins.
- Examination of the modified form of the Mcm6-SuOn protein. Cell extracts from the indicated strains were probed on western blots for Mcm6. The low migrating bands (arrows) containing Mcm6-SuOn were sumoylated forms as HF-SUMO caused a upshift compared with untagged SUMO. The differential shift in the two situations is also depicted by the trace of the bands in Image J (bottom).
- Examination of sumoylation of Mcm6-SuOn and Mcm6-ctrl proteins. Both proteins (tagged with V5) were immunoprecipitated and probed with anti-V5 and anti-SUMO antibodies on western blots. Anti-V5 detected both unmodified and sumoylated forms, with the latter being more abundant in Mcm6-SuOn cells. Anti-SUMO antibody detection verified that the upper band was indeed the sumoylated form.
- Mcm6-SuOn increases the sumoylation of Mcm2, 4, and 7, but not Mcm3. Cells with the indicated constructs were examined by Ni-NTA method. Compared with Mcm6-ctrl, Mcm6-SuOn cells had more sumoylated forms of Mcm2, 4, and 7, and less sumoylated Mcm3.
- Mcm6-SuOn does not affect MCM complex formation. Top: Mcm6 was immunoprecipitated and Mcm4-HA was detected by immunoblotting. Note that similar levels of Mcm4 were recovered from both Mcm6-SuOn and Mcm6-ctrl strains. Bottom: Total protein extracts were probed to show that Mcm6 and Mcm4 protein levels were similar in Mcm6-SuOn and Mcm6-ctrl cells.
- Mcm6-SuOn does not significantly affect the sumoylation levels of other replication proteins. Samples were processed as in Fig. 2-1b; antibody recognizing the TAP tag was used for western blotting.

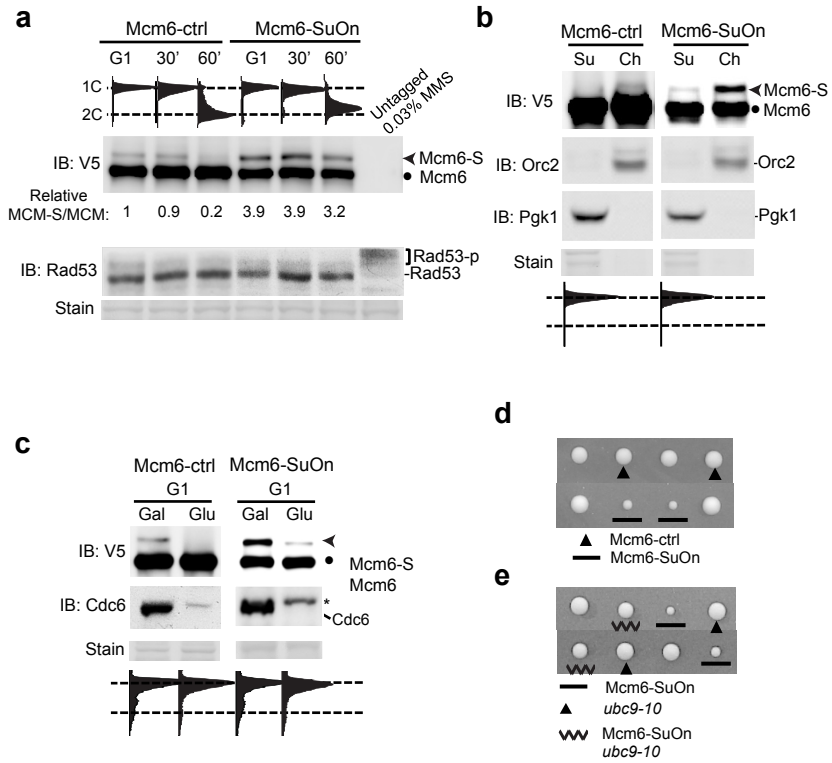


Figure 2-7. Increasing sumoylation by Mcm6-SuOn slows growth and this defect is suppressed by a *ubc9* mutant.

- a. Mcm6-SuOn exhibits elevated sumoylation in G1 and S phases. Immunoblot at top shows Mcm6-ctrl and Mcm6-SuOn proteins (tagged with V5) from whole cell lysates. Equal loading is indicated by Ponceau stain, and lack of checkpoint activation is shown by the absence of Rad53 phosphorylation. MMS-treated sample without tagging shows no cross-reaction bands on α -V5 blot (top) and robust Rad53 phosphorylation (bottom).
- b. Sumoylation of Mcm6-SuOn occurs in the chromatin-bound fraction in G1 cells.
- c. Sumoylation of Mcm6-SuOn in G1 requires Cdc6. Cell growth is described in Fig. 2-1d and Mcm6 sumoylation is detected as in a. Cdc6 depletion is detected by immunoblotting. * indicates a cross-reaction band.
- d. Mcm6-SuOn, but not Mcm6-ctrl, results in slow growth. Representative tetrads from Mcm6-SuOn⁺ or Mcm6-ctrl/⁺ diploid strains are shown. Spores clones were grown at 30°C for 3-4 days and genotypes are indicated.
- e. Slow growth of Mcm6-SuOn cells is suppressed by a SUMO E2 Ubc9 mutation. Representative tetrads from dissection of Mcm6-SuOn/⁺ *ubc9-10*/⁺ diploid strains are shown as in (d).

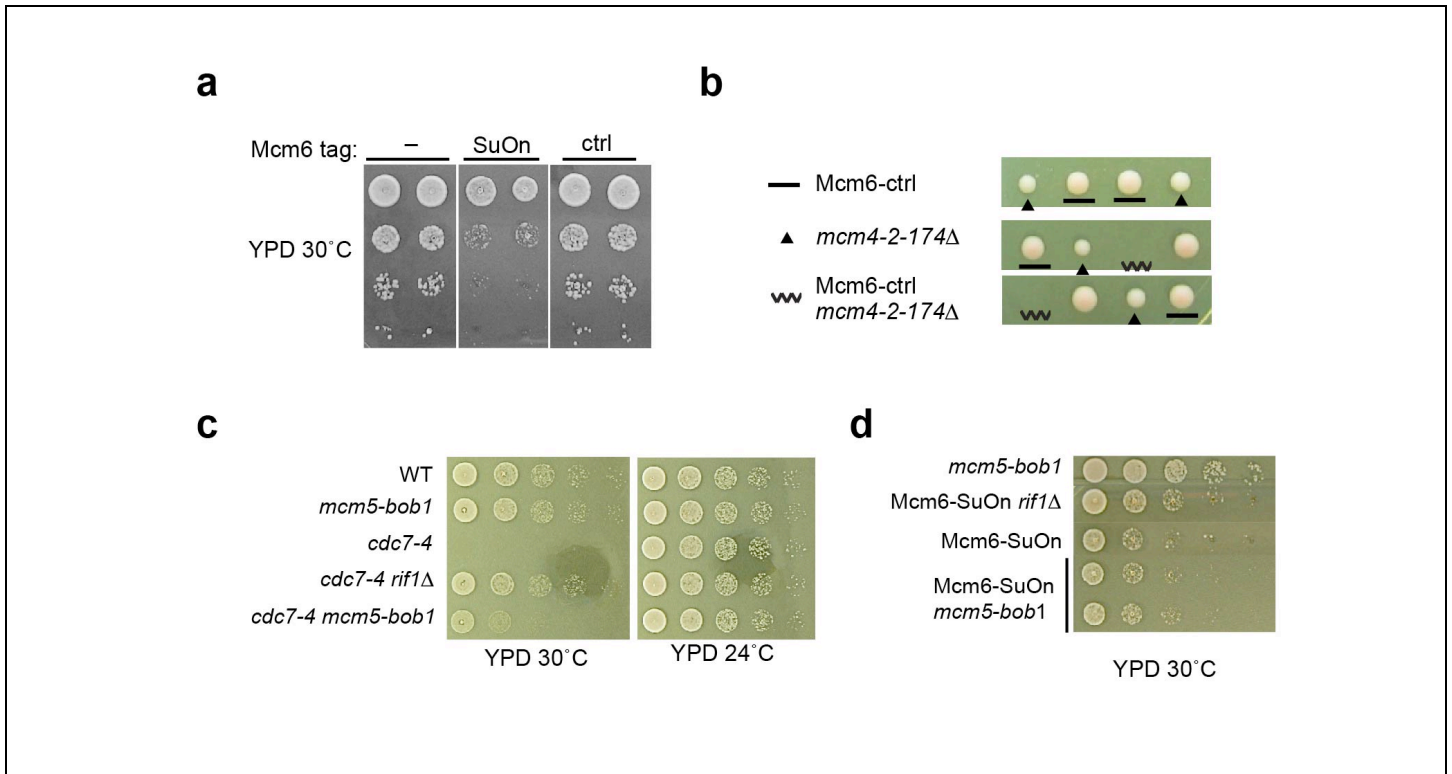


Figure 2-8

Genetic examination of Mcm6-SuOn

- a.** Mcm6-SuOn, but not Mcm6-ctrl, exhibits growth defects. 10-fold serial dilutions of cells were spotted on YPD plates and grown at 30°C for 36 hours.
- b.** *mcm4-2-174Δ* is synthetic lethal with Mcm6-ctrl. Spore clones of the double mutants failed to grow on dissection plates, whereas those of other genotypes grew well.
- c.** *mcm5-bob1* showed weaker suppression of *cdc7-4* growth defects than *rif1Δ* at 30°C.
- d.** Unlike *rif1Δ*, *mcm5-bob1* does not suppress the growth defects of Mcm6-SuOn.

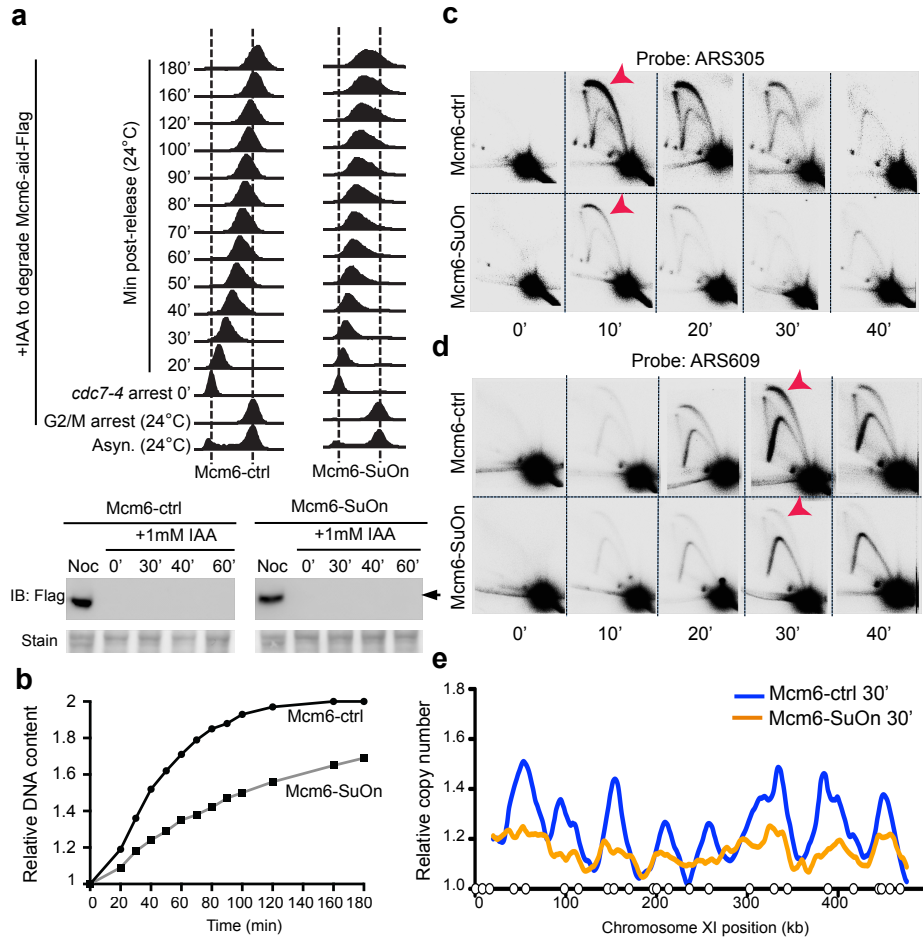


Figure 2-9. Mcm6-SuOn impairs replication initiation.

- a. Mcm6-SuOn cells exhibit slower replication by FACS analyses. Strains contained *cdc7-4* to arrest cells before replication initiates. Experimental scheme and FACS profiles show that cells were arrested in G2-M followed by IAA addition to degrade Mcm6-aid, then temperature shift to 37°C to inactivate *cdc7-4* and achieve arrest before replication initiation, and cooling to 24°C to allow cells progress into S phase. Mcm6-aid degradation is shown (bottom) and arrow marks the Mcm6-aid band.
- b. Quantification of DNA contents from (a) was plotted.
- c. Mcm6-SuOn shows defective firing at the ARS305 locus. 2D gel results show different origin firing between Mcm6-ctrl and Mcm6-SuOn strains. Cells were from experiment in (a). Bubble DNA structures representing origin firing events are labeled by red arrows.
- d. Mcm6-SuOn shows defective firing at the ARS609 locus. As in (c), except ARS609-specific probe was used.
- e. Copy number changes of a section of chromosome XI are shown based on genome sequencing of the 30 min post-release samples in (a). Open circles represent the confirmed replication origins according to OriBD.

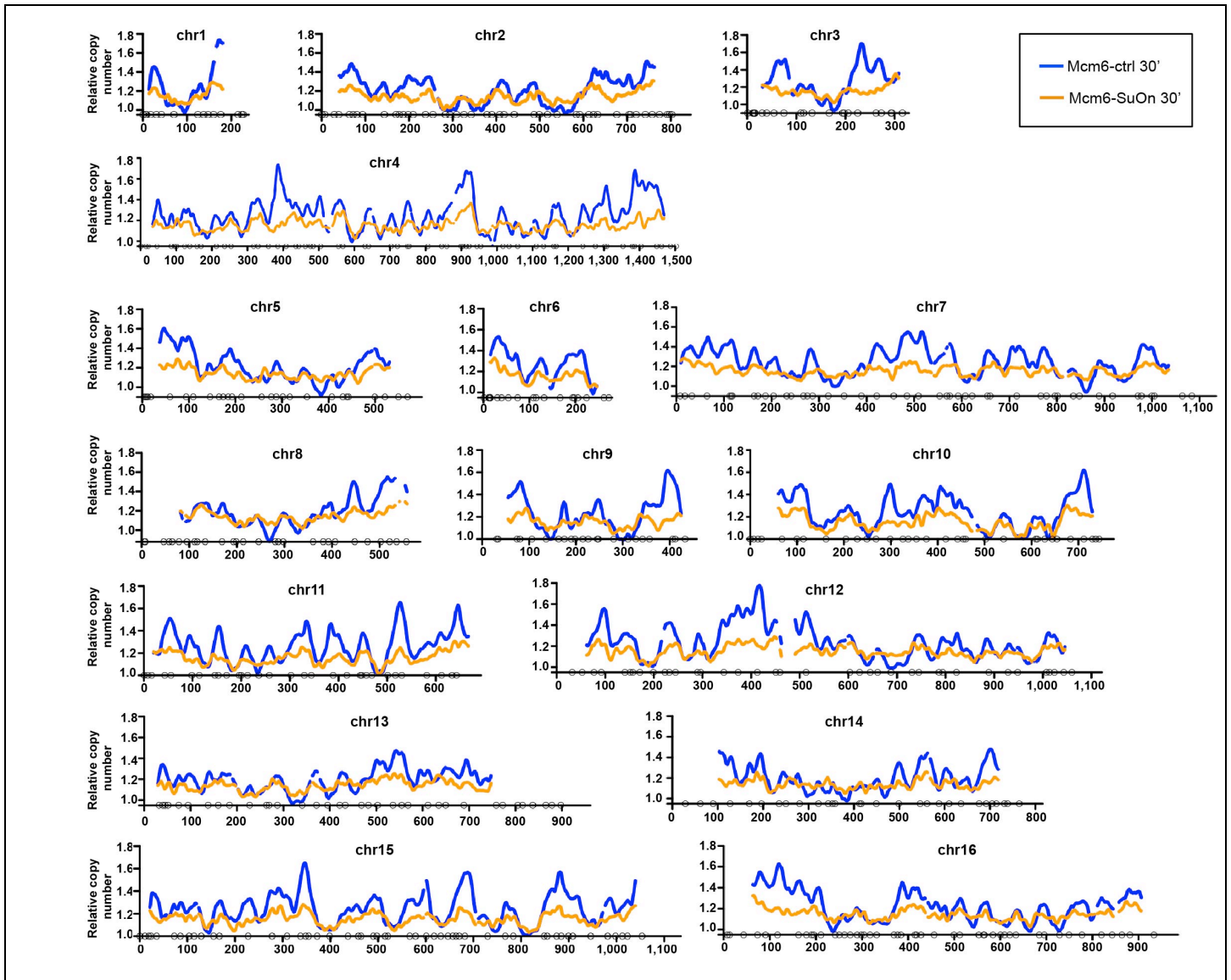


Figure 2-10

Genome-wide profiles of copy number changes in Mcm6-SuOn and Mcm6-ctrl cells.

Results for all 16 chromosomes from samples in Figure 2-9e are shown. Cells collected from 0 min and 30 min post *cdc7-4* release were subjected to whole-genome sequencing, and relative copy number changes were plotted. Open circles on the x-axis represent confirmed replication origins.

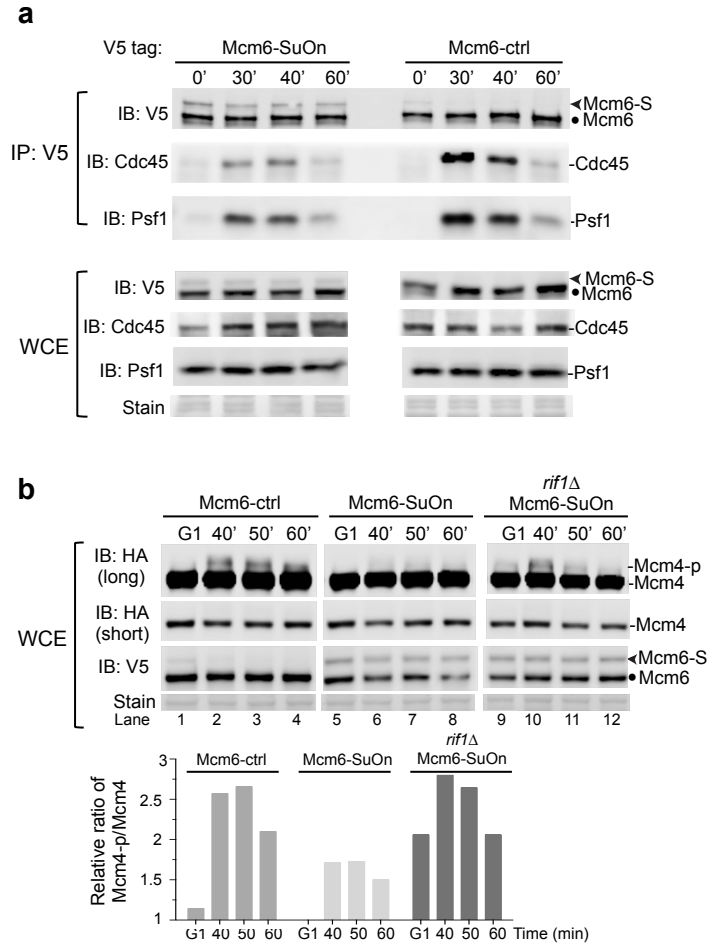


Figure 2-11. Mcm6-SuOn cells exhibit low levels of CMG and phosphorylation of Mcm4 that can be suppressed by *rif1* Δ

- a. Mcm6-SuOn cells have reduced CMG levels. Immunoblots at top show immunoprecipitated Mcm6 and associated Cdc45 and Psf1. Immunoblots at bottom show Mcm6, Cdc45, and Psf1 protein levels in the input. Indicated time points are the same as experiments depicted in Fig. 2-5a.
- b. The reduced Mcm4 phosphorylation in Mcm6-SuOn cells is restored by *rif1* Δ . As in Fig. 2-4b, immunoblots (top two) shows Mcm4 phosphorylation with long exposure for detecting Mcm4 phosphorylation and short exposures for detecting unmodified Mcm4 protein levels. Immunoblot at bottom shows Mcm6 protein levels and sumoylation status. Relative ratio of phosphorylated Mcm4 versus unmodified Mcm4 shown is plotted in the graph.

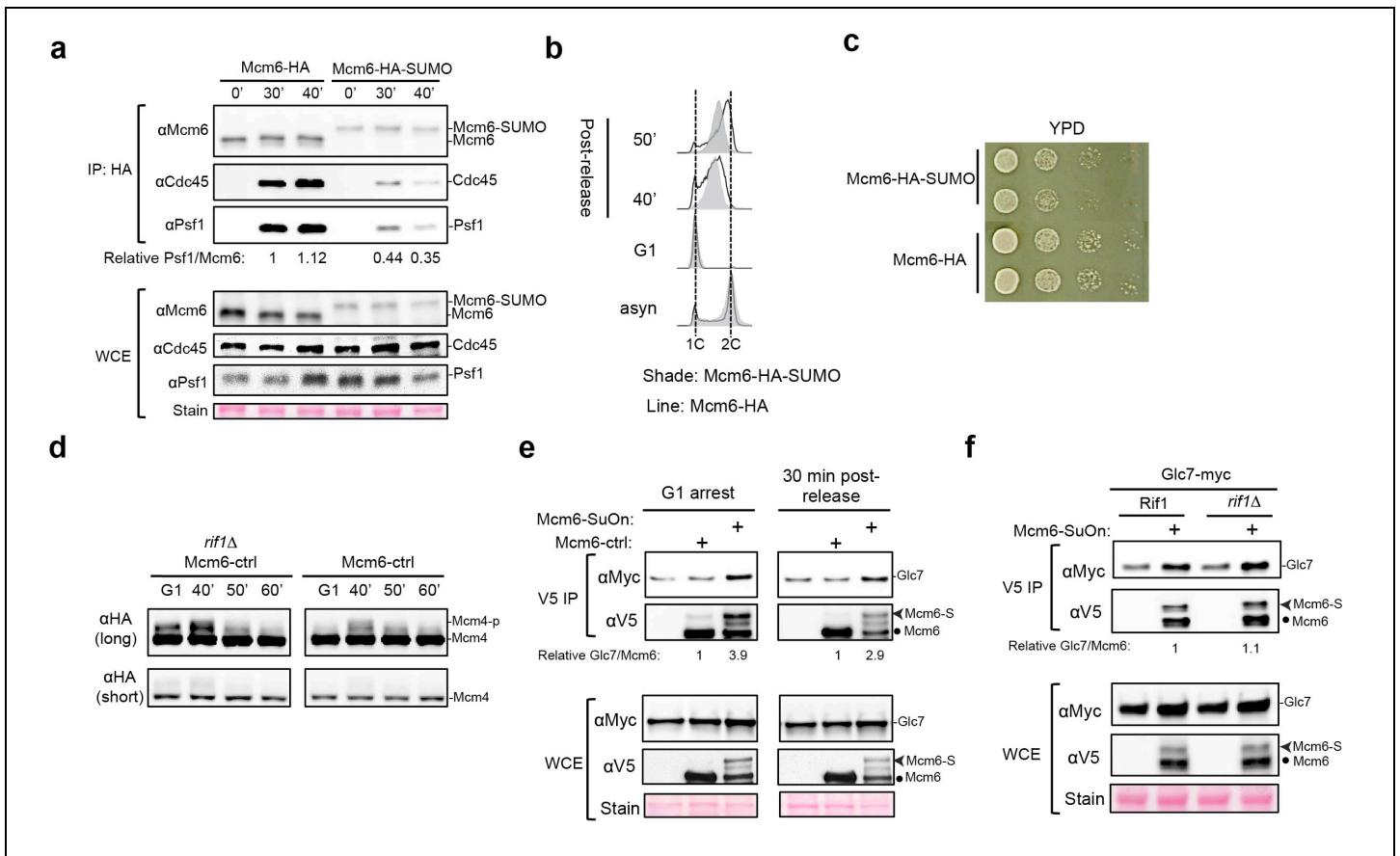


Figure 2-12

Examination of Mcm6-SUMO fusion and Glc7-Mcm6 association.

- Lower levels of Cdc45 and Psf1 are associated with Mcm6-SUMO fusion in G1 and S phase cells. Cells were arrested in G1 using alpha factor (0') and released into S phase. Co-immunoprecipitation of Cdc45 and Psf1 with Mcm6-HA or Mcm6-HA-SUMO was examined. Relative ratios of Psf1/Mcm6 in the IP fraction are indicated and a two- to three- fold reduction is seen for Mcm6-HA-SUMO strain compared to the control Mcm6-HA strain.
- Mcm6-SUMO fusion yields a slow replication profile. Both the Mcm6-HA-SUMO fusion and Mcm6-HA control strains were arrested in G1 phase using alpha factor and released into S phase. Samples at indicated time points were examined by FACS.
- Cells containing Mcm6-SUMO fusion grow slowly compared to control cells.
- Examination of Mcm4 phosphorylation in Mcm6-ctrl strains (related to Figure 2-11b). Mcm4 phosphorylation in Mcm6-ctrl was similar to what has been reported for wild-type cells (e.g. Fig. 2-4b), and *rif1Δ* increased this modification as expected.
- Increased amounts of Glc7 are associated with Mcm6-SuOn than Mcm6-ctrl in both G1 and S phase samples. Similar to Figure 2-13b, except both G1-arrested and S phase (30 min after G1 release) cells were examined.
- Increased Glc7-Mcm6 association in *rif1Δ* cells. G1-arrested cells were examined for Glc7 association with Mcm6-SuOn as in e.

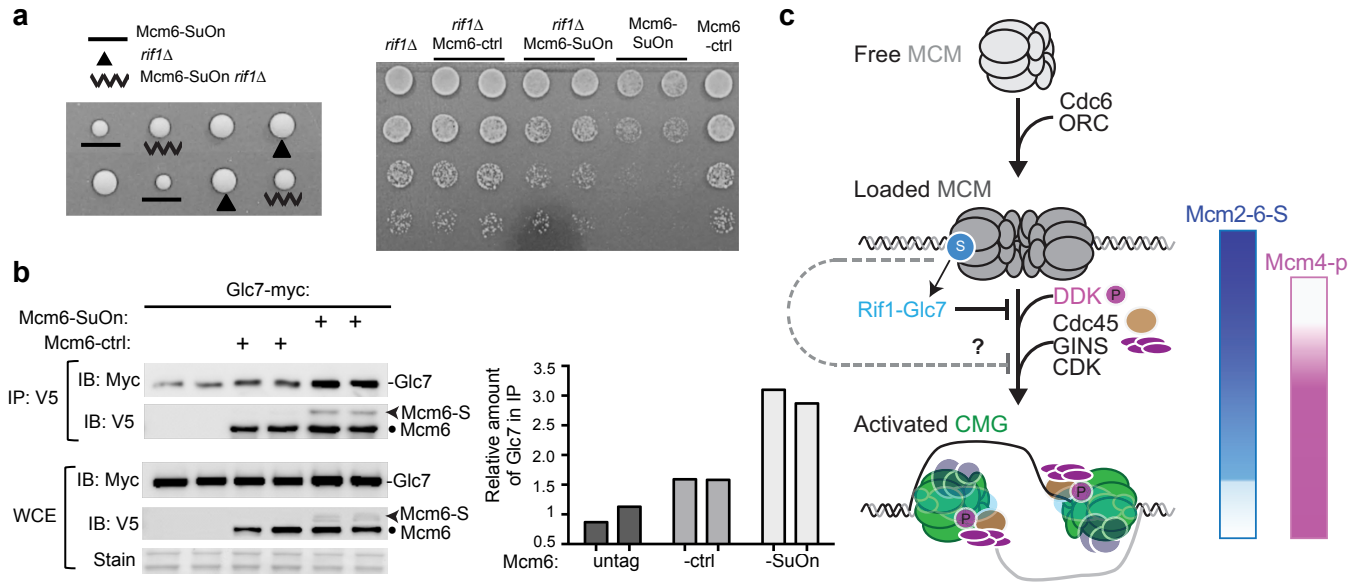


Figure 2-13. *rif1* Δ suppresses Mcm6-SuOn growth defects and Mcm6-SuOn leads to enhanced association between Mcm6 and the Glc7 phosphatase

- a. Rif1 removal partially rescues the growth defects of Mcm6-SuOn. Left, representative tetrads from dissection of the Mcm6-SuOn/+ *rif1* Δ /+ diploid strain. Right, 8-fold serial dilutions of cells spotted on YPD plates.
- b. Increased levels of Glc7 are associated with Mcm6-SuOn, compared to Mcm6-ctrl. Using G1-arrested cells, Mcm6 was immunoprecipitated and the associated Glc7 levels were examined. Quantification of the relative amount of Glc7 in the immunoprecipitated fraction is normalized to the amount of Mcm6 in the immunoprecipitated and plotted from two trials.
- c. A model depicts the spatial and temporal pattern of the MCM sumoylation cycle and a role of MCM sumoylation in negatively regulating replication initiation. For simplicity, only the replication factors used in this study are shown. After Cdc6-mediated MCM loading at replication origins, a fraction of Mcm2–7 subunits is sumoylated. This occurs prior to DDK-mediated Mcm4 phosphorylation and CMG formation. One function of MCM sumoylation is aid Glc7 phosphatase recruitment to counteract Mcm4 phosphorylation in G1, preventing premature CMG formation. Roles for MCM sumoylation at an event after DDK activation are possible (“?”). As replication is initiated in waves from early and late origins, Mcm2–6 sumoylation decreases. The loss of Mcm2–6 sumoylation occurs concomitantly with the appearance of DDK-mediated Mcm4-phosphorylation, both promoting replication initiation.

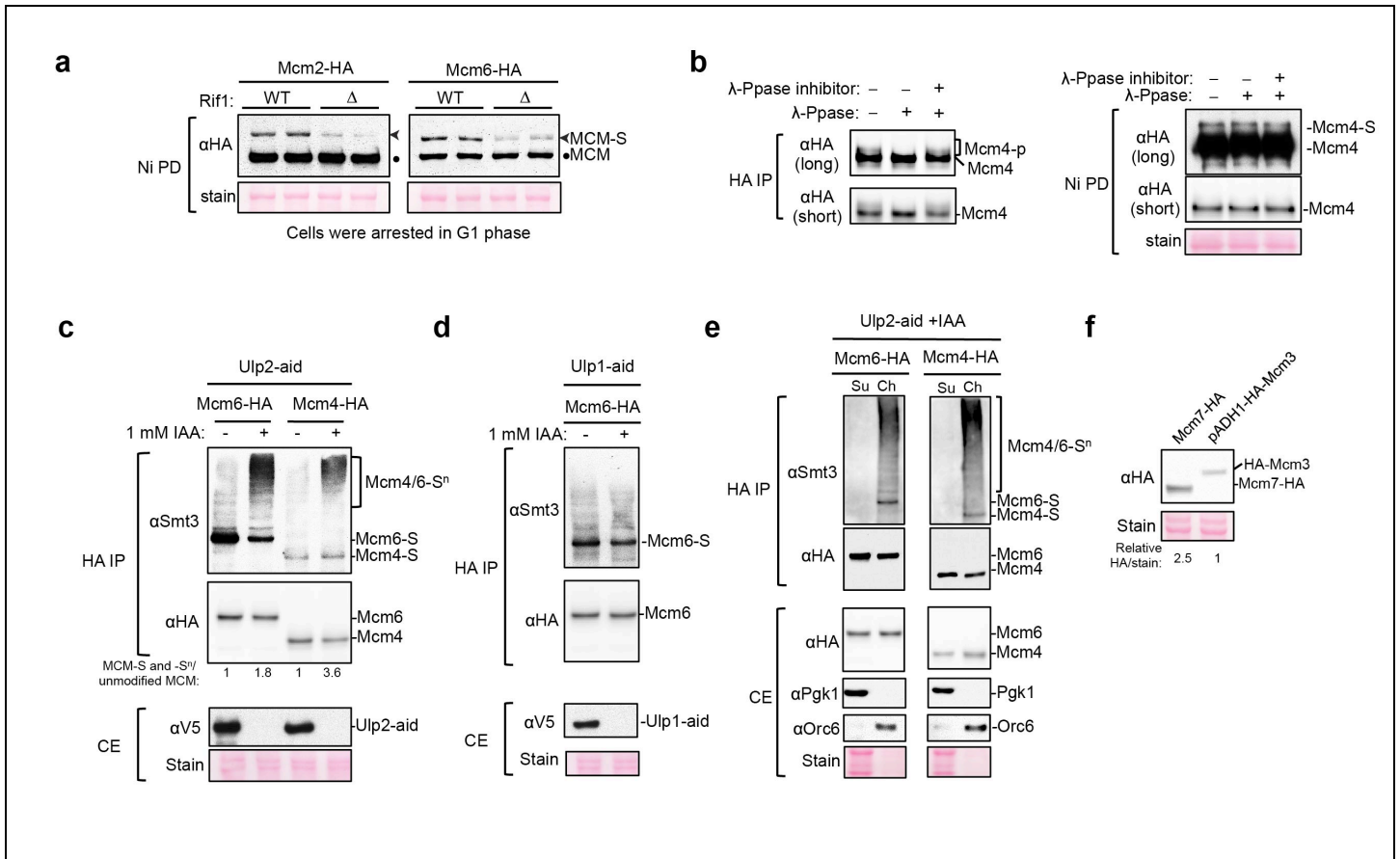


Figure 2-14

Examination of Mcm4 sumoylated form, MCM desumoylation, and verification of Mcm3 protein levels.

- a.** *rif1*Δ decreases sumoylation of Mcm2 and Mcm6 in G1 cells. Experiments were done as in Figure 2-4a with G1 cells examined.
- b.** Lambda phosphatase treatment does not affect the mobility of the sumoylated form of Mcm4 on western blots. The control treatment showed that phosphatase treatment reduced the mobility of phosphorylated Mcm4, which was not sumoylated.
- c.** Ulp2 loss leads to increased levels of sumoylated Mcm4 and 6. Sumoylation changes in Mcm4 and 6 were examined by HA-IP in the presence or absence of Ulp2. Ulp2 depletion was achieved by the use Ulp2-aid degron tagged with V5 upon the addition of 1 mM IAA for 1 hr (+IAA), and verified by western blotting (bottom). For Mcm4 and 6, Ulp2 depletion increased the levels of poly-sumoylated forms of the proteins, such that the total sumoylated Mcm4 or 6 increased 2-4 fold. Increase of poly-sumoylated form of the proteins upon Ulp2 depletion is consistent with the previous finding of the enzyme's preferences in desumoylating poly-sumoylated proteins.
- d.** Sumoylation of Mcm6 does not change upon Ulp1 depletion. Experiments were similar as in c, except Ulp1-aid construct was used. Mcm6 sumoylation levels were maintained upon efficient Ulp1 depletion.
- e.** Mcm4 and 6 sumoylation is detected in the chromatin fraction when Ulp2 is depleted. As in panel (c), except chromatin-bound and soluble fractions were examined.
- f.** Examination of the protein levels of Mcm3 tagged with HA. N-terminal HA-tagged Mcm3 was used in the study due to toxicity of C-terminal tagging. This construct was expressed at the endogenous *MCM3* locus from the *ADH1* promoter. It is known that endogenous Mcm3 protein levels are about half that of Mcm7. This ratio was maintained in our strains wherein Mcm7-HA was driven by its own promoter and Mcm3-HA from the *ADH1* promoter.

Chapter 3

Function and modification of Pol2 N-terminal unique domain

Introduction

DNA polymerase Pol ϵ plays two critical roles during genome replication. In addition to catalyzing leading strand DNA synthesis, Pol ϵ also has a central role in replisome assembly (Nick McElhinny et al. 2008; Muramatsu et al. 2010; Yeeles et al. 2015). Replisome assembly entails an intricate series of protein recruitment to replication origins (Kelly and Brown 2000; Bell and Dutta 2002; Sclafani and Holzen 2007; Fragkos et al. 2015). First, the DNA helicase MCM is loaded onto the origins in an inactive form. Subsequently, the Cdc45-Sld3 complex is recruited in a DDK-dependent manner, as DDK-mediated phosphorylation of MCM fosters interaction with Sld3 (Deegan et al. 2016). Next, Pol ϵ and several other proteins form the pre-LC which is then recruited to loaded MCM (Muramatsu et al. 2010) (Figure 3-1). Besides Pol ϵ , the pre-LC contains the GINS complex (Sld5, Psf1-3) and two scaffold proteins, namely Dpb11 and Sld2. CDK-mediated phosphorylation of Sld2 (Sld2-p) and Sld3 (Sld3-p) allows their simultaneous binding to Dpb11, bringing the entire pre-LC to loaded MCM (Tanaka et al. 2007; Zegerman and Diffley 2007). At this step, CMG forms, which can unwind duplex DNA. After recruitment of ~20 more proteins, including DNA polymerases Pol α and Pol δ , as well as several structural proteins, replisome assembly is completed (Gambus et al. 2006; Morohashi et al. 2009; Fragkos et al. 2015).

The critical role of Pol ϵ in replisome assembly is executed by its largest subunit Pol2, which also catalyzes DNA polymerization, and a structural subunit Dpb2 that binds to the C-terminal half of Pol2 (Dua et al. 2000). Dpb2 directly binds to the GINS subunit

Psf1, and this interaction is critical for both pre-LC and replisome formation (Sengupta et al. 2013). Pol2's role in pre-LC formation is less well defined. In addition to binding to Dpb2, Pol2 also binds to Dpb11 and Sld2, though which parts of Pol2 mediate these interactions are unclear (Muramatsu et al. 2010). Despite the fact that the N-terminal half of Pol2 contains the polymerase domain, only its C-terminal half is thought to account for Pol2's essentiality. This is based on the finding that removal of the C-terminal half of Pol2 is lethal while removal of its N-terminal half only causes slow growth (Dua et al. 1999; Kesti et al. 1999; Dua et al. 2000). This evidence shaped the current model for Pol2 function, in which the Pol2 N-terminal half only functions in DNA polymerization and its C-terminal half carries out the essential function in pre-LC formation through binding to Dpb2.

It has been noted that while the N-terminal half of Pol2 is largely similar to other replicative DNA polymerases, such as Pol α and Pol δ , it contains a unique 68 amino acid region not found in other polymerases but which is highly conserved among Pol2 homologs (Shcherbakova et al. 2003; Hogg et al. 2014) (Figure 3-2a). This N-terminal unique domain (referred to as the NUD hereafter) is located outside of the catalytic center and is fully exposed to solvent in the three dimensional structure, but has not been studied previously (Hogg et al. 2014). In this study, I examined the function of this Pol2 NUD. Guided by high frequency NUD mutations found in cancer patients, I generated several mutations in conserved residues of the NUD (Cerami et al. 2012; Gao et al. 2013). Surprisingly, in contrast to deleting the whole N-terminal half of Pol2, I found that mutating five residues at the same time caused lethality, while mutating only three of these five caused temperature sensitivity. Examination of a temperature-sensitive NUD allele showed that consistent with its growth impairment, it is defective in replication initiation and CMG formation. Mechanistically, these NUD mutations diminish Pol2-Dpb11 interaction and pre-LC formation without affecting Pol2-Dpb2 binding or protein

levels. Finally, I found that Pol2 NUD is sumoylated during S phase, and mutating the sumoylation site impairs replisome assembly. These data reveal a previously unrecognized role of the Pol2 N-terminal half in replisome assembly and suggest that the highly conserved NUD is critical for supporting pre-LC formation during replication initiation. They also suggest that NUD sumoylation has a positive influence on the role of this domain in promoting pre-LC formation.

Results

Pol2-NUD and cancer mutations in this domain

To gain a functional understanding of Pol2 NUD, I first examined the structure of the NUD. In particular, I superimposed the crystal structure of Pol2 N-terminus and Pol3, which is the catalytic subunit of Pol δ . As shown in Figure 3-2b, the NUD is localized outside of the three canonical domains essential for polymerase activity, the finger, thumb, and palm domains. The NUD resides beneath the palm domain and is fully exposed to solvent. In addition, the NUD is 20 Å away from the catalytic center, where the DNA polymerization reaction occurs. These structural features suggest that Pol2-NUD is likely not involved in DNA polymerization, but rather has the potential to support protein-protein interactions.

The NUD assumes a unique fold with two beta-sheets (b1 and b2), and two major alpha-helices α 1 and α 3, separated by a small 2-turn alpha-helix α 2 (Figure 3-2b, right). Both the sequence and the fold of the NUD are highly conserved from yeast to human. Interestingly, mutations in different parts of the NUD have been identified in various human cancers, including melanoma and stomach cancer (Figure 3-2b, 2c). Among these mutations, five occurred at moderate to high frequency and on conserved

residues (Cerami et al. 2012; Gao et al. 2013). These include R553C, R579C, A581P, E597K, and L607F (Figure 3-2b, 2c). The corresponding mutations in yeast are R567C, K593C, S595P, E611K, and L621F (Figure 3-2b, 2c). These naturally occurring NUD mutations at conserved residues provide a hint that could allow us to understand the function of the NUD in DNA replication initiation by studying their mutant phenotypes in yeast.

Pol2-NUD is essential for viability

The NUD residues corresponding to those found in cancer patients were mapped on yeast Pol2. Among these, R567C is localized in a loop region, while K593C, S595P, E611K, and L621F are localized in helices $\alpha 1$ and $\alpha 3$ (Figure 3-2b). In order to maximally perturb the NUD function, I first mutated all five sites or only the four located in helical regions (without R567C). The effect of the mutations on growth was examined using a plasmid shuffle assay (Figure 3-2d). In this assay, a centromere-based plasmid with a single replication origin and HIS3 auxotrophic marker was used to carry the Pol2 NUD alleles driven by its endogenous promoter. These Pol2-NUD-HIS3 plasmids were transformed into a Pol2 deletion strain harboring Pol2-WT on a plasmid with URA3 auxotrophic marker. 5-fluoroorotic acid (5-FOA) counter selection was used to eliminate cells harboring URA3-containing Pol2-WT plasmid, leaving Pol2-NUD-HIS3 plasmids the only sources of Pol2 protein. As shown in Figure 3-2d, both Pol2-NUD mutants failed to support cell growth on 5-FOA plates, indicating that Pol2-NUD is essential for cell viability. Due to the inviability of these two mutants, it is unclear if the lethality is caused by defects in replication itself or other processes related to replication, such as checkpoint.

The Pol2-NUD mutant *pol2-REL* is defective in replication

In order to examine in detail whether and how NUD mutations affect replication, I generated additional NUD mutant alleles. I recovered a viable allele of the NUD, which contained three out of the five conserved mutations (R567C, E611K, and L621F; referred to as *pol2-REL* hereafter) and showed temperature sensitivity (Ts). As shown in Figure 3-3a, *pol2-REL* had a slight growth defect at 24°C compared to Pol2-WT cells and was inviable at 37°C. The growth defect was not due to general protein instability, since the Pol2 protein level was similar to WT at both temperatures (Figure 3-3b). The tight Ts phenotype of *pol2-REL* provides a useful tool to further examine the effects of NUD in replication.

I first examined the replication profiles of *pol2-REL* and Pol2-WT cells by FACS (Figure 3-3c). In a G1 release experiment, cells were released from alpha factor induced G1-arrest into S phase at both permissive (24°C) and non-permissive temperatures (37°C) and DNA content was monitored. As shown in Figure 3-3c, *pol2-REL* had a slower replication profile than Pol2-WT at the permissive temperature 24°C, consistent with a slight growth defect at this temperature (Figure 3-3a). At 37°C, the defect of *pol2-REL* was more pronounced: while Pol2-WT cells finished bulk replication ~40min after release from G1-arrest, DNA content in *pol2-REL* cells barely increased even after 60 min (Figure 3-3c, right). These results indicate that Pol2-NUD is essential for DNA replication.

***pol2-REL* impairs CMG formation and replisome assembly**

I moved on to examine whether the *pol2-REL* defect in DNA replication is due to impaired replication initiation. Because CMG formation is a key event during replication

initiation, I examined CMG levels by measuring the amount of Cdc45 or GINS (monitored by the subunit Psf1) co-immunoprecipitated with Mcm2. I examined *pol2-REL* and Pol2-WT in G1 release experiments at both permissive and non-permissive temperatures, as described above (Figure 3-3c). I found that *pol2-REL* had a delay in CMG formation at the permissive temperature (24°C) (Figure 3-4a, 4b). In wild type cells, the level of Psf1 co-purified with Mcm2 peaked at 40 min post G1 release, while those in *pol2-REL* peaked at 50 min. The delay in CMG formation in *pol2-REL* cells correlates with their slower replication profile and growth (Figure 3-3a, 24°C). These defects were more pronounced at the non-permissive temperature (37°C). Co-purified Psf1 was barely detectable in *pol2-REL* cells, and DNA content barely increased after G1 release (Figure 3-4d, 4e). These defects observed for *pol2-REL* were specific for CMG formation, since the formation of Pol ϵ was not affected in *pol2-REL*, as indicated by the wildtype level of Pol2-Dpb2 interaction (Figure 3-4a, 4d). These results indicate that Pol2-NUD is essential for CMG formation during replication initiation.

Pol ϵ associates with CMG to form the so-called CMGE (CMG-Pol ϵ) complex to synthesize DNA on the leading strand, and CMGE is part of the replisome (Langston et al. 2014; Sun et al. 2015). I reasoned that a reduction of CMG in *pol2-REL* should also result in diminished CMGE formation. This was indeed the case. At permissive temperature (24°C), while an increase of Pol2 association with Mcm2 was observed in S phase compared to G1 phase in WT cells, the increase was less pronounced in *pol2-REL* cells (Figure 3-4a, 4c). More dramatic defects for Pol2-MCM interaction were observed in *pol2-REL* cells at the non-permissive temperature (37°C), such that barely any detectable increase of Pol2 associated with Mcm2 during S phase could be seen (Figure 3-4d, 4f). The reduced CMGE formation as reflected by diminished Pol2-MCM

interaction during S phase in *pol2-REL* cells is consistent with defective CMG formation in this mutant.

pol2-REL is defective in pre-LC formation

I next asked how *pol2-REL* affects CMG formation. As described in the introduction, CMG formation requires the pre-LC, in which Pol2 supports multiple interactions with Dpb2, Dpb11, and Sld2 (Muramatsu et al. 2010) (Figure 3-5a). Thus to examine if the CMG defect stems from impaired pre-LC formation, I tested whether *pol2-REL* affects its interactions with Dpb11 and Dpb2. Sld2 was not tested due to lack of antibodies, but it will be tested in the future using a tagged version of Sld2.

I subjected Pol2-WT and *pol2-REL* cells to a G1 release experiment at permissive temperature (24°C), and examined co-immunoprecipitation of Pol2-Dpb2 and Pol2-Dpb11. Following an established protocol (Muramatsu et al. 2010), samples were taken at 60 min after release, when the pre-LC is best detected. As shown in Figure 3-5b, the co-purified Dpb11 with Pol2 was barely detectable in *pol2-REL* as compared to Pol2-WT. In contrast, the interaction between Dpb2 and Pol2 was not affected (Figure 3-5b). These findings show that *pol2-REL* interferes with pre-LC formation by affecting Pol2-Dpb11 association, and suggest that at a molecular level, the NUD may be involved in Dpb11 binding.

The Pol2-Dpb11 interaction has not been well characterized, and it is unclear which region of Pol2 is involved in the interaction. I reasoned that if the NUD mediates the interaction between Dpb11 and Pol2, then the N-terminus of Pol2 should interact with Dpb11. This is indeed the case, as the N-terminus but not the C-terminus of Pol2 showed interaction with Dpb11 by yeast two-hybrid assay (Y2H) (Figure 3-5c). Our findings that *pol2-REL* specifically diminished Pol2-Dpb11 interaction in pre-LC

formation and that the N-terminal half of Pol2 interacted with Dpb11 provide molecular evidence for a model where the NUD supports Dpb11 association and thus pre-LC formation. Our findings challenge the previous model that Pol2 N-terminus only supports DNA polymerization, and suggest that both the N-terminal and C-terminal halves of Pol2 are important for pre-LC formation, likely by contributing to Dpb11 and Dpb2 interaction, respectively.

Pol2 is sumoylated during DNA replication

Replication initiation is heavily regulated to enforce the temporal and spatial order of events leading to replisome formation. PTMs are an essential regulatory means for replication initiation. I have shown in Chapter 2 that MCM sumoylation occurs in G1 and keeps the loaded MCM inactive. A previous study from our lab showed that Pol2 was also sumoylated (Cremona et al. 2012). Pol2 sumoylation is detected by immunoprecipitating Pol2 under denaturing conditions and probing with SUMO specific antibody by western blotting (Cremona et al. 2012). I found that Pol2 sumoylation showed a different pattern than MCM sumoylation. Pol2 sumoylation occurred during S phase, but not G1 phase, and was low in G2-M phase (Figure 3-6a). Cells arrested in S phase by HU treatment showed approximately 3 fold higher Pol2 sumoylation level than asynchronous populations of cells (Figure 3-6e), indicating that Pol2 sumoylation correlates with replication. The different patterns of Pol2 and MCM sumoylation indicate that they are sumoylated at different steps during replication and thus may have different functions.

Pol2 sumoylation occurs on a single lysine on the NUD

To examine the function of Pol2 sumoylation, I first mapped its sumoylation sites using a candidate site approach. It is known that half of all sumoylation sites conform to consensus [Ψ KX(D/E)] or reverse consensus sequences [(D/E)XK Ψ] (Lamoliatte et al. 2014). Pol2 contains eight such sites (M1-M8), two of which are located in the NUD (M2 and M3) (Figure 3-6b). I made combinations of mutations at these sites and examined their sumoylation under treatment with the replication stress agent methyl methanesulfonate (MMS), since Pol2 sumoylation level is higher in this condition than untreated condition (Cremona et al. 2012).

Mutating the lysines at sites M1-M8 to arginines in different combinations revealed that mutations of M2 and M3 in the NUD were associated with loss of Pol2 sumoylation (Figure 3-6c). Further analysis by generating single mutations of M2 (K571R) and M3 (K575R) showed that *pol2-K571R*, but not *pol2-K575R*, greatly diminished Pol2 sumoylation under MMS treatment (Figure 3-6d). Sumoylation of *pol2-K571R* was almost undetectable in both normal growth and HU treated conditions (Figure 3-6e). These results indicate that K571 in the NUD is the sumoylation site of Pol2 under several conditions, including normal growth and replication stress. In addition, an earlier finding of our lab has shown that Pol2 sumoylation under MMS treatment is largely dependent on the SUMO E3 ligase Mms21, a subunit of the octameric Smc5/6 complex (Hang et al. 2015).

pol2-sd exacerbates the growth defects of pol2-REL

Considering my findings suggest that Pol2-NUD contributes to replication initiation by promoting pre-LC formation, I tested if the Pol2 sumoylation deficient K571R mutant

(*pol2-sd*) has defects in these processes. As described in the introduction, replication initiation is regulated by multiple mechanisms to ensure precise origin firing. Thus, lack of Pol2 sumoylation alone is unlikely to drastically affect replication initiation. Indeed, I found that *pol2-sd* supported WT levels of growth and resistance to genotoxins (Figure 3-6f). The multi-layered regulation of replication initiation also suggests that if there is a contribution by Pol2 sumoylation, *pol2-sd* may generate a phenotype when other parts of the regulation are weakened.

Based on the logic described above, I used genetic approaches to probe the effect of *pol2-sd* on replication. As Pol2 sumoylation occurs on the NUD, I examined whether *pol2-sd* could exacerbate or suppress the defects of *pol2-REL*. I found that the *pol2-REL-sd* mutant grew worse than *pol2-REL* at the semi-permissive temperature 34°C (Figure 3-7a). Consistent with the growth defects at 34°C, *pol2-REL-sd* showed a slower replication profile by FACS compared to *pol2-REL* (Figure 3-7b, 7c). These results indicate that Pol2 sumoylation becomes important in DNA replication when the NUD function is perturbed.

pol2-sd exacerbates the replisome assembly defect in pol2-REL

As my data suggest that Pol2 NUD contributes to replication initiation, I assessed CMGE and CMG formation in *pol2-REL-sd*, *pol2-REL*, and Pol2-WT cells. Since the phenotype of *pol2-REL-sd* is more pronounced at the semi-permissive temperature 34°C, this condition was used for the tests in G1 release experiments. First, I found that Pol2-MCM association was diminished in *pol2-REL-sd* compared to *pol2-REL*, indicating defective CMGE formation and replisome assembly (Figure 3-7d, 7e). This defect is specific since Pol2-Dpb2 interaction was not affected (Figure 3-7d). In addition, Psf1 co-purified with Mcm2 was readily detected in Pol2-WT cells at 34°C, but was barely detectable above

background in *pol2-REL-sd* and *pol2-REL* cells (Figure 3-7d). Accurate quantification in this case is not feasible and thus the levels were not compared between *pol2-REL-sd* and *pol2-REL*. Testing CMG formation by probing Cdc45 will clarify if CMG formation is more defective in *pol2-REL-sd* than *pol2-REL*. These results indicate that Pol2 sumoylation likely affects replisome assembly when NUD function is perturbed and that this role pertains to the Pol2-MCM association or another step required for this interaction.

Discussion

Pol2 NUD is essential?

Our findings that four to five tested point mutations in the NUD cause lethality suggest that the NUD is essential (Figure 3-2d). However, we cannot rule out that the observed cell lethality is caused by reduced protein levels. We plan to examine these two mutants in diploid cells containing HA tagged mutant Pol2 and TAF tagged wild-type Pol2 so that we can compare the protein levels by western blotting using anti-Pol2 antibodies.

The paradox of the essential NUD within the dispensable Pol2 N-terminus

If we were able to confirm that the above mutant proteins were expressed at normal levels yet caused lethality, then we could conclude that the NUD is essential. This conclusion may be surprising at the first glance, since deleting the entire Pol2 N-terminus (*pol2-ΔN*) results in slow growing cells (Dua et al. 1999; Kesti et al. 1999). It is known that in other cases, point mutations have more severe phenotypes than truncations. For example, the catalytically dead Pol2 mutant, *pol2-D875A, D877A*, which harbors two mutations in the N-terminal catalytic center, is lethal (Dua et al. 1999). In the case, it was thought that the mutant protein can bind to leading strand DNA substrate,

blocking the access of alternative polymerases such as Pol δ , while deletion mutation allows for access by Pol δ , thus supporting DNA replication and cell growth.

Since the NUD is 20 Å away from Pol2's active site (Figure 3-2b), it is not likely that the lethality of NUD mutant results from the same reason as for *pol2-D875A*, *D877A*. Furthermore, my data suggest that the NUD mutant has reduced Dpb11 binding and defective pre-LC formation during replication initiation (Figure 3-5b). A direct test of the polymerase and DNA binding activities of lethal Pol2-NUD mutants using purified proteins will further clarify if they behave differently than *pol2-D875A*, *D877A*.

If NUD is essential for the formation of pre-LC, why is *pol2- Δ N* viable? There can be two possible explanations. First, the N-terminal half of Pol2 could have an inhibitory effect on pre-LC formation. In this scenario, interaction of the NUD with Dpb11 would be required to alleviate this inhibition to promote pre-LC formation. Thus, deleting the entire N-terminal half would bypass the role of the NUD, thus rendering cells viable. This hypothesis predicts that Pol2 C-terminal half is sufficient to support pre-LC formation, which could be tested using purified proteins. The second possibility is that NUD mutations used here could be gain-of-function alleles disrupting the pre-LC formation, while the NUD itself does not participate in pre-LC formation. I disfavor this possibility since Pol2-N terminal half, which contains the NUD, binds Dpb11 (Figure 3-5c). Further examination of the interaction between the NUD and Dpb11 using purified proteins will clarify the requirement of the NUD in the pre-LC formation.

The effect of *pol2-REL* on Dpb11 binding

Using a protocol to extract pre-LC complex, I found that Dpb11 binding to Pol2 was about eight-fold less in *pol2-REL* compared to Pol2-WT cells, at permissive temperature

24°C (Figure 3-5b) where *pol2-REL* cells only showed a slight growth defect (Figure 3-3a). We are currently testing to exclude the possibility that this reduction is due to reduced protein levels. If this possibility can be ruled out, our data would suggest that the Pol2 NUD is involved in Dpb11 interaction. An encouraging result came from our preliminary Y2H test wherein I found that the N-terminal half of Pol2 was associated with Dpb11 (Figure 3-5b). We will follow up this result by several *in vitro* tests, such as examining whether purified NUD and Dpb11 directly bind. We note that Pol2 full-length Y2H construct did not interact with Dpb11. A close examination reveals that this construct did not interact with Dpb2, a known binding partner of Pol2. It is this likely that this particular Pol2 Y2H construct is not expressed well. This notion will be examined directly by western blotting.

It may be strange at the first glance that at 24 °C, *pol2-REL* cells grew only slightly slower but the Dpb11 levels in pre-LC were greatly reduced. These results suggest that low levels of pre-LC are sufficient for cell growth. This notion is supported by the fact that only one MCM double-hexamer and two pre-LCs are required for firing each origin. In addition, parts of the pre-LC (Dpb11, Sld2, and Sld3) can be recycled and used at multiple origins throughout S phase, thus a small amount of pre-LC may be sufficient to support multiple rounds of origin firing (Mantiero et al. 2011).

It is worth noting that Pol2-WT and *pol2-REL* progress through S phase at different speeds (Figure 3-3c). The cells used in Figure 3-5b are from 60 min after release and have different DNA content when harvested (Figure 3-3c, 60min, 24°C), so I can not rule out the possibility that the defective Pol2-Dpb11 binding in *pol2-REL* is due to the fact that they progress through S phase more slowly. To this end, two strategies could be used to address this question. First, HU treatment could arrest cells in S phase

and eliminate the cell cycle difference between Pol2-WT and *pol2-REL*. Second, diploid Pol2-WT/*pol2-REL-tag* and Pol2-WT/Pol2-WT-tag cells may progress through S phase at similar rates and could potentially be used to test if Dpb11 binding is defective with *pol2-REL*.

Pol2 NUD mutations in cancer

In my study, the naturally occurring mutations found in cancer patients informed us of useful NUD mutations to deduce the functions of this domain. In order to maximally perturb the NUD function, I combined three to five mutations in haploid budding yeast cells, and provided evidence that the NUD is critical in replication initiation. There is still a major gap to use my findings to deduce the effects of those mutations in cancer patients. While a clear understanding of how NUD mutations contribute to cancer is out the scope of this thesis study, I can provide some thoughts on how my study can inform the understanding of these mutations in cancer cells.

First, to better understand how NUD mutations affect cancer, single NUD mutations need to be generated and examined in diploid cells. This can be first conducted in yeast to determine how each mutation influences replication and genome stability. Such information will subsequently facilitate the interrogation of the equivalent mutants in human cells. Further more, impaired replication initiation can also lead to increased mutation rates. In principle, insufficient replication initiation can lead to large replicons, which are known to be associated with increased mutation rates (Deem et al. 2011; Sakofsky et al. 2014). In addition, cancer cells are known to suffer from replicative stress (Lecona and Fernandez-Capetillo 2014; Gaillard et al. 2015; Macheret and Halazonetis 2015), which may exacerbate the replication initiation defects of the NUD mutants. Indeed, cancer cells with NUD mutations contain 351-2,233 mutations/cell,

which are lower than the rate of 1,200-15,000 mutations/cell associated with Pol2 exonuclease mutations (Cerami et al. 2012; Gao et al. 2013) but higher than average rate of 33-163 mutations/cell in common solid tumors (Vogelstein et al. 2013). Besides increased mutation rates, it is likely that initiation defects can also lead to increased frequencies of DNA rearrangements. We plan to test these ideas in yeast by examining NUD single mutants in several aspects of replication, including 1) replication initiation, 2) the generation of large replicons, 3) increasing mutation rates, and 4) chromosomal translocations.

Second, because defective polymerization and exonuclease activities can also lead to high mutation rates, my work does not rule out potential roles of the NUD in DNA polymerization and exonuclease activities. Our future work will address these possibilities in yeast cells by examination of the polymerase and exonuclease activities using purified proteins. These results will help clarify how the POLE NUD affects these processes in humans.

Pol2 sumoylation on the NUD contributes to replisome assembly

Every step during replication initiation is subjected to regulation. My study suggest for a potential mode of regulation of the NUD function. Pol2 is sumoylated at a single site within the NUD during S phase but not G1 phase, (Figure 3-6). Although *pol2-sd* alone did not show any growth defects, it exacerbated the growth and replisome assembly defects of the NUD mutant *pol2-REL* (Figure 3-7). These data indicate that sumoylation of Pol2 may contribute to NUD function in replisome assembly, in particular CMGE formation. I will test if *pol2-sd* alone affects pre-LC, CMG, and CMGE formation.

One caveat of using the K571R mutation in *pol2-sd* is that this mutation may have two effects. The first is loss of Pol2 sumoylation, and second is perturbation of sumoylation independent functions of K571. In order to further test if loss of Pol2 sumoylation leads the defects in *pol2-REL*, fusion of SUMO to *pol2-sd-REL* will be used to test if it rescues the growth and replisome assembly defects of *pol2-REL-sd*.

Molecular mechanisms of the function of Pol2 sumoylation

Our findings suggest that Pol2 sumoylation affects replisome assembly, at least in the background of perturbed NUD function. However, the molecular mechanism of how Pol2 sumoylation affects replisome assembly is still unknown. There are several hypotheses for the role Pol2 sumoylation, for example, in promoting formation of the pre-LC, CMG, and/or the replisome (Figure 3-8). Pol2 sumoylation needs to be characterized in more detail to clarify its mechanistic contribution.

Using my study of MCM as a model, in order to elucidate the function of Pol2 sumoylation, I need to examine precisely when and where Pol2 is sumoylated. I have shown that Pol2 is sumoylated during S phase, which contains several events, including pre-LC formation, CMG formation, replisome assembly, and DNA synthesis. These events occur throughout S phase and cannot be separated during a natural S phase. To this end, genetic manipulations could be used to arrest cells at specific stages in order to study the requirements for Pol2 sumoylation. For example, inactivation of Cdc7 would allow pre-LC formation but not CMG formation. Pol α depletion would allow the formation of both pre-LC and CMG complexes but not DNA polymerization. The precise timing of sumoylation could be determined using these alleles. Additionally, like MCM, Pol2 distributes in cytoplasmic and chromatin pools. The replisome is chromatin bound, while

the pre-LC is cytoplasmic. Determination of which pool of Pol2 is sumoylated would also help identify the function of Pol2 sumoylation.

Replication initiation relies heavily on protein-protein interactions to achieve precise and timely activation of origins. Mediating protein-protein interactions has emerged as one of the key mechanisms for the function of sumoylation. It is possible that Pol2 sumoylation promotes pre-LC formation, CMG formation or replisome assembly through enhancement of protein interactions (Figure 3-8). I am currently testing the components in the pre-LC and replisome for their interactions with SUMO, as this will greatly expand our understanding of effects of SUMO in replication initiation.

Multiple functions of sumoylation in replication initiation

My data suggest that Pol2 sumoylation has a positive role in replication initiation. Meanwhile, my findings in chapter 2 show that MCM sumoylation plays a negative role in replication initiation. These two functions of sumoylation in replication initiation may appear to be contradictory at first glance. However, sumoylation may play highly coordinated roles in different steps of replication initiation. Replication initiation contains two steps, namely origin licensing and origin firing. MCM and Pol2 sumoylation occur at different steps of replication initiation. The former occurs during the licensing step in G1 phase, functioning to prevent premature origin firing by counteracting DDK-mediated MCM phosphorylation. In contrast, Pol2 sumoylation occurs in S phase, after the licensing step and likely during origin firing. In addition, my data suggest that Pol2 sumoylation promotes replisome assembly. I propose that MCM and Pol2 sumoylation occur sequentially to ensure efficient replication initiation and minimize re-replication events.

An earlier report from our lab revealed that in addition to MCM and Pol2, a dozen other proteins involved in replication are also SUMO substrates (Cremona et al. 2012). These proteins are involved in nearly all aspects of replication, from replication initiation to elongation. This indicates that sumoylation may have multiple roles in replication, and the understanding of these roles awaits mechanistic studies of these additional targets. Eventually, I will have a cohesive picture of how sumoylation of individual substrates regulates distinct steps in DNA replication. It is worth noting that a large fraction of replication proteins are also involved in DNA repair. Considering that many DNA lesions stem from errors in the DNA replication process, the dual functions of these proteins in both DNA replication and repair is not surprising. How sumoylation of these proteins affect DNA repair is also a topic to be investigated in the future.

In summary, my findings reveal for the first time that the N-terminus of Pol2 has a DNA polymerization independent role. The N-terminus of Pol2 shares an essential function in DNA replication initiation with Pol2 C-terminus. I showed that the 68aa NUD of Pol2 is essential. This domain promotes the formation of pre-LC and subsequent CMG and CMGE complexes during replication. Mechanistically, the NUD likely promotes the recruitment of Dpb11, thus contributing to pre-LC formation during replication initiation. My findings add to known mechanisms of pre-LC formation. In addition, my results reveal that the sumoylation of Pol2 on the NUD promotes replisome assembly, which expands the range of regulation of replication initiation. Given that the NUD and the sumoylation of Pol ϵ are conserved, my work may also stimulate the elucidation of functions of the NUD and Pol ϵ sumoylation in higher organisms.

Methods and materials

Yeast strains and techniques

Standard procedures were used in cell growth and medium preparation. Strains were isogenic to W1588-4C, a *RAD5* derivative of W303 (*MATa ade2-1 can1-100 ura3-1 his3-11,15 leu2-3,112 trp1-1 rad5-535*)(Zhao and Blobel 2005b). Strains and their usage in specific figure panels are listed in table 2. Proteins were tagged at their endogenous loci and expressed from their own promoters by standard methods, and correct tagging was verified by sequencing. Yeast spotting assays were performed with standard procedures.

Plasmid shuffle assay

Plasmid shuffle assay in Figure 3-2d was performed as previously described(Sheu and Stillman 2010). pRS413 based plasmids expressing Pol2 mutant proteins were transformed into *pol2Δ* strain supplemented with a pRS416-Pol2 plasmid, and cells containing both pRS413 and pRS416 plasmids were selected on –His-Ura drop out plates. Single colonies were then picked and grown in –His-Ura drop-out media to mid logarithmic phase and 10-fold dilutions of cells were spotted onto the –His-Ura drop out or 5-FOA plates. Pictures were taken after 48-72 h.

Synchronization and flow cytometry procedures.

For experiments in Figures 3-3c, 3-6a and 3-7b, cells were grown to early logarithmic phase (1×10^7 cells/ml) and then treated for 2.5 h with 5 μ g/ml alpha factor at 24°C. The temperature was raised to 34°C or 37°C or remain at 24°C as indicated for 1 hour and then cells were released into S phase by addition of pronase at a final concentration of

100 µg/ml at indicated temperatures. Cells were collected at indicated time points and flow cytometry analysis was performed as described (Cremona et al. 2012).

Protein extraction and immunoprecipitation (IP) to detect CMGE formation and Pol- ε formation.

For Mcm2-TAP IP in Figures 3-4 and 3-7d, 7.5×10^8 cells were washed once with 5 ml of ice-cold water, suspended in 0.5 ml of Lysis buffer (100 mM HEPES/KOH, pH 7.9, 100 mM KOAC, 2 mM MgOAC, 1 mM ATP, 1% Triton X-100, 2 mM NaF, 0.1 mM Na₃VO₄, 20 mM β-glycerophosphate, 1 mM PMSF, 10 mM benzamidine HCl, 10 µg/ml leupeptin, and 1 µg/ml pepstatin, 1x protease inhibitors (EDTA free, Roche) and 20 mM NEM). Cells were disrupted by bead-beating (FastPrep 24, MP biomedical). 250U of Benzonase was added to cell lysates, which were incubated for 1 h at 4 °C. After centrifugation for 20 min at 15,000 r.p.m. at 4 °C, the supernatant was collected and incubated with prewashed IgG sepharose (17-0969-01,GE) for 2 h at 4 °C. Two changes were made in Pol2-3HA IP, 1) 2 mM NaF, 0.1 mM Na₃VO₄, 20 mM β-glycerophosphate were omitted from the Lysis buffer and 2) the lysates were incubated with prewashed anti-HA conjugated agarose (26182, Fisher).

Detection of the Pre-LC formation by cross-linking method

Detection of the Pre-LC complex formation in Figure 3-5b was performed as previously described (Muramatsu et al. 2010). In Brief, 7.5×10^8 cells were treated with formaldehyde at a final concentration of 1% for 20 min at 24°C. 2.5 M glycine was added to a final concentration of 120 mM and incubated for 5 min at 24°C to neutralize formaldehyde. Cells were then washed twice with 20 ml of ice-cold TBS buffer (20 mM Tris-HCl [pH 7.5], 150 mM NaCl), suspended in 0.4 ml of Lysis buffer (50 mM HEPES-

KOH [pH 7.5], 140 mM NaCl, 1% TritonX-100, 0.1% sodium deoxycholate, 1x protease inhibitors (EDTAfree, Roche), 1% protease inhibitor, 2mM MgCl₂) and disrupted by bead-beating (FastPrep 24, MP biomedical). The cell lysates were then sonicated to reduce the DNA size to less than 500 bp. 250U of Benzonase was added to cell lysates, which were incubated for 40 min at 4 °C. The extracts were spun at 15,000rpm for 20min at 4°C. The supernatant was mixed with prewashed anti-HA conjugated agarose beads (26182, Fisher) and incubated at 4°C for 2 hr. The beads were washed with 1 ml of Lysis buffer, 1 ml of Lysis buffer containing 0.5 M NaCl, 1 ml of Wash buffer (10 mM Tris-HCl [pH 8.0], 250 mM LiCl, 0.5% NP-40, 0.5% deoxycholate, 1 mM EDTA), 1ml of Lysis buffer and suspended in 36 µl of Elution buffer (50 mM Tris-HCl [pH 8.0], 10 mM EDTA, 1% SDS). The suspension was incubated at 65°C for 10 min and laemmli buffer was added to the supernatant to a final concentration of 1x and incubated at 95°C for 30 min before SDS-PAGE and western blotting.

Detection of Pol2 sumoylation.

Detection of Pol2 sumoylation in Figure 3-6 was performed as previously described(Zhao and Blobel 2005b). In brief, 5 x 10⁸ cells were harvested and disrupted by bead-beating (FastPrep 24, MP biomedical) under denaturing conditions. Whole cell lysates were cleared by centrifugation and supernatant was incubated with IgG, anti-myc antibody or anti-HA antibody conjugated beads for 2 h at 4°C. The beads were then washed and the eluents were subjected to SDS-PAGE and western blotting with antibodies against SUMO(Zhao and Blobel 2005b) to detect sumoylated Pol2 band. Unmodified Pol2 was detected by PAP, anti-myc or anti-HA antibodies, depending on the tags on Pol2.

Immunoblotting analysis and antibodies.

Protein samples were resolved on 3-8% or 4–20% gradient gels (Life Technologies and Bio-Rad) and transferred to a 0.2- μ m nitrocellulose membrane (G5678144, GE). Antibodies used were anti-HA (3F10, Sigma), anti-myc (9E10, Bio X cell), PAP (P1291, Sigma), anti-Pgk1 (22C5D8, Invitrogen), anti-Psf1 (gift from K. Labib), anti-Cdc45 and anti-Dpb11 (gifts from B. Stillman), anti-Dpb2 (gift from H. Araki) and anti-SUMO. Validation of these antibodies is provided either on the manufacturers' websites or in the cited references. For quantification purposes, membranes were scanned with a Fujifilm LAS-3000 luminescent image analyzer, which has a linear dynamic range of 10^4 . Quantification of blots and generation of figures was performed with ImageGauge and Photoshop.

Yeast two hybrid assay (Y2H)

Y2H was performed as previously described (Chung and Zhao 2015). In brief, AD and BD plasmid constructs were transformed into reporter strains and cells were grown on -Trp-Leu dropout plates at 30°C for 48 hours. Positive interactions were assessed by growth after spotting cells onto -Trp-Leu-His, Trp-Leu-His + 3 mM 3-amino-1,2,4-triazole (3AT), or Trp-Leu-Ade plates.

Table 2: Strains and plasmids used in this study

All strains are isogenic to W1588-4C (a RAD5 derivative of W303: MATa ade2-1 can1-100 his3-11,15 leu2-3,112 trp1-1 ura3-1). One strain is listed for each genotype, and two were used in experiments.

| Strain | Genotype |
|----------------|---|
| T1926-1 | <i>pol2Δ::KAN pRS416-Pol2-3HA::KAN pRS413-Pol2-3HA::KAN</i> |
| T1933-1 | <i>pol2Δ::KAN pRS416-Pol2-3HA::KAN pRS413-pol2-K593C, S595P, E611K, L621F-3HA::KAN</i> |
| T1929-1 | <i>pol2Δ::KAN pRS416-Pol2-3HA::KAN pRS413-pol2-R567C, K593C, S595P, E611K, L621F-3HA::KAN</i> |
| X7021-4a | <i>MATa Pol2-3HA::KAN</i> |
| X7022-7a | <i>MATa pol2-R567C, E611K, L621F-3HA::KAN (pol2-REL)</i> |
| X7023-18b | <i>MATa pol2-R567C, K571R, E611K, L621F-3HA::KAN (pol2-REL-sd)</i> |
| X7021-13c | <i>MATa Pol2-3HA::KAN Mcm2-TAP::HIS3</i> |
| X7022-11c | <i>MATa pol2-R567C, E611K, L621F-3HA::KAN Mcm2-TAP::HIS3</i> |
| X7023-4a | <i>MATa pol2-R567C, K571R, E611K, L621F-3HA::KAN Mcm2-TAP::HIS3</i> |
| X3613-2a | <i>Mat alpha Pol2-TAF::KAN</i> |
| T887 | <i>MAT alpha pol2-K1553R, K1581R, K1681R, K2171R-TAF::KAN (pol2-M4-M7)</i> |
| T885 | <i>MAT alpha pol2-K427R, K571R, K575R, K660R, K2171R-TAF::KAN (pol2-M1,M2,M3,M7)</i> |
| T892 | <i>pol2-K571R, K575R, K660R, K1553R, K1581R, K1681R, K2171R-TAF::KAN3 (pol2-M2-M7)</i> |
| T695-12 | <i>pol2-K427R, K660R, K2171R-TAF::KAN (pol2-M1,M3,M7)</i> |
| T1126-A3C3-16a | <i>pol2-K571R-3HA::KAN</i> |
| T1004 | <i>pol2-K575R-3HA::KAN</i> |

| Plasmid | Genotype |
|---------------|---|
| <i>pXZ860</i> | <i>pRS416-Pol2-3HA::KAN</i> |
| <i>pXZ861</i> | <i>pRS413-Pol2-3HA::KAN</i> |
| <i>pXZ868</i> | <i>pRS413-pol2-K593C, S595P, E611K, L621F-3HA::KAN</i> |
| <i>pXZ864</i> | <i>pRS413-pol2-R567C, K593C, S595P, E611K, L621F-3HA::KAN</i> |
| <i>pXZ532</i> | <i>pOAD-pol2-N (1-1264)</i> |
| <i>pXZ533</i> | <i>pOAD-pol2-C (1265-2222)</i> |
| <i>pXZ534</i> | <i>pOAD-pol2</i> |
| <i>pXZ535</i> | <i>pOAD-Dpb2</i> |
| <i>pXZ536</i> | <i>pOAD-Dpb3</i> |
| <i>pXZ537</i> | <i>pOAD-Dpb4</i> |
| <i>pXZ538</i> | <i>pOAD-Mrc1</i> |
| <i>pXZ539</i> | <i>pOAD-Dpb11</i> |
| <i>pXZ515</i> | <i>pOBD-Pol2-N (1-1264)</i> |

| | |
|---------------|--------------------------------|
| <i>pXZ516</i> | <i>pOBD-Pol2-C (1265-2222)</i> |
| <i>pXZ517</i> | <i>pOBD-Pol2</i> |
| <i>pXZ518</i> | <i>pOBD-Dpb2</i> |
| <i>pXZ519</i> | <i>pOBD-Dpb3</i> |
| <i>pXZ520</i> | <i>pOBD-Dpb4</i> |
| <i>pXZ522</i> | <i>pOBD-Dpb11</i> |

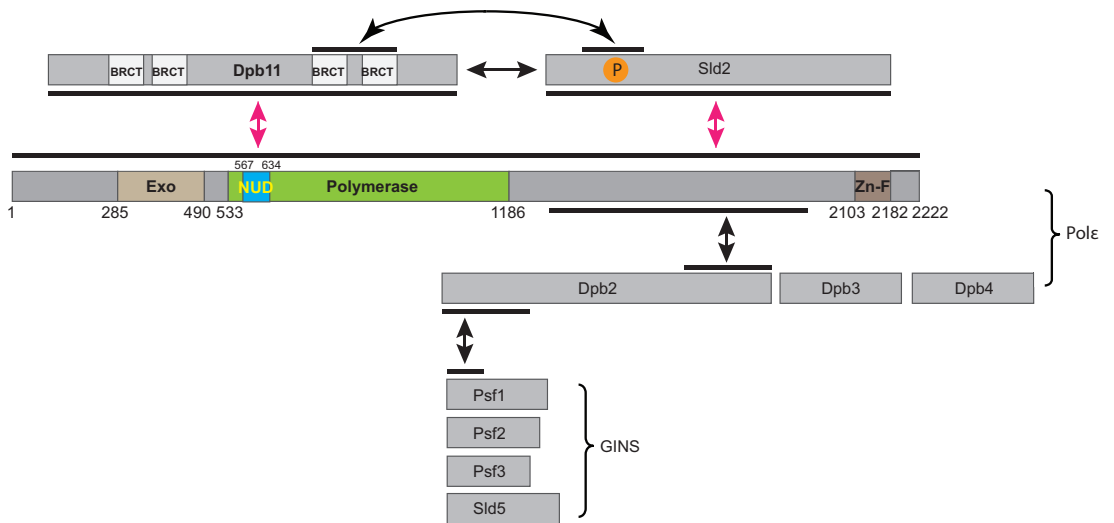


Figure 3-1. Pol2 is the hub for the interaction network for the pre-LC.

Black arrows: reported interactions with known binding regions. Red arrows: binding regions unclear. BRCT: BRCA1 C Terminus; P: CDK mediated phosphorylation at Sld2 T84; Exo: exonuclease domain; NUD: N-terminal unique domain; Zn-F: Zn finger domain.

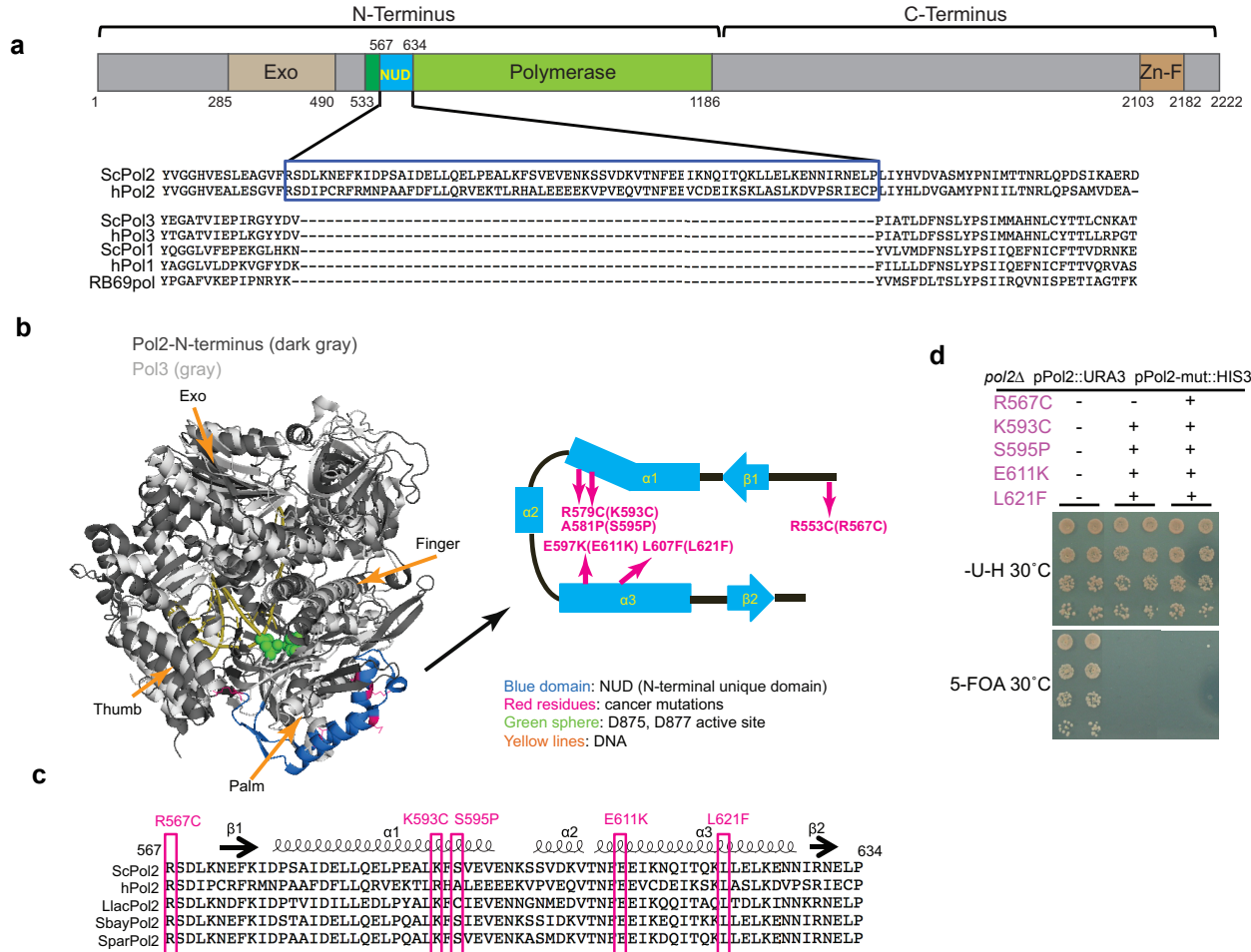


Figure 3-2. The N-terminal unique domain (NUD) of Pol2 is essential for cell growth.

- a. The NUD is not found in other B family polymerases. Pol1, Pol3 and bacteriophage RB69 polymerases are aligned. *sc*: *Saccharomyces cerevisiae*; *h*: human.
- b. Right: *Saccharomyces cerevisiae* Pol2 N-terminus (dark gray, pdb code: 4M8O) and Pol3 N-terminus (light gray, pdb code:3IAY) are superimposed. The NUD is labeled in blue. Exonuclease (Exo), thumb, palm and finger domains are indicated. DNA is highlighted in yellow. The catalytic center (D875 and D877) is marked by green spheres. Five conserved cancer mutation residues in NUD are labeled in red. Left: The close up topology cartoon of the NUD is shown. The residues indicated by arrows are five conserved human cancer mutations. The residues in parentheses are the corresponding cancer mutation residues in budding yeast.
- c. Alignment of NUD of Pol2 from different species, the numbering corresponds to *Saccharomyces cerevisiae*. The five conserved cancer mutations are shown in red.
- d. Plasmid shuffling assay shows that NUD mutant plasmids does not support cell growth. 5-FOA: 5-fluoroorotic acid. –U-H plate: Uracil and histidine double dropout plate.

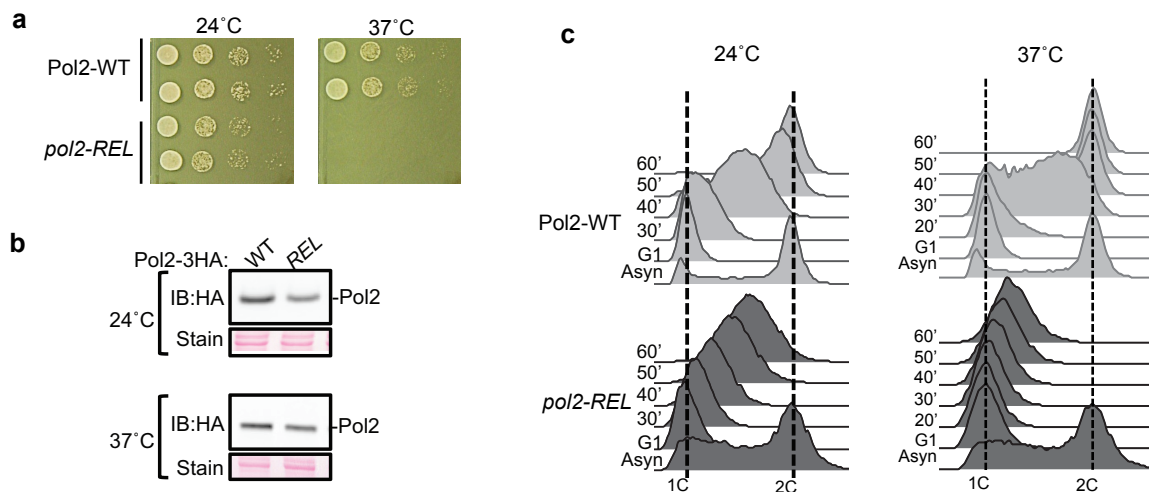


Figure 3-3. Mutations in the Pol2 NUD cause temperature sensitivity and slow S phase progression

- a. *pol2-REL* contains three conserved cancer mutations (R567C, E611K, L621F). *pol2-REL* grew slower at 24°C and were not viable at 37°C. 10-fold serial dilutions of cells were spotted on plates and grown at indicated temperatures for 36-48 hours before pictures were taken.
- b. Pol2 protein levels of Pol2-WT and *pol2-REL* strains at 24°C and 37°C were compared by western blotting using anti-HA antibody. Stain was shown for protein loading comparison. Asynchronous cells were grown at 24°C to mid log phase and then temperature was shifted to 37°C for an hour before harvesting.
- c. Flow cytometry analyses of the replication profiles of Pol2-WT and *pol2-REL* at 24°C and 37°C. Cells were synchronized at G1 phase by alpha factor, and released into S phase. Samples were taken at indicated time points. Note that a 20 min time point was taken at 37°C, due to faster progression of cell cycle. Asyn: asynchronous culture; 1C and 2C indicate genome size.

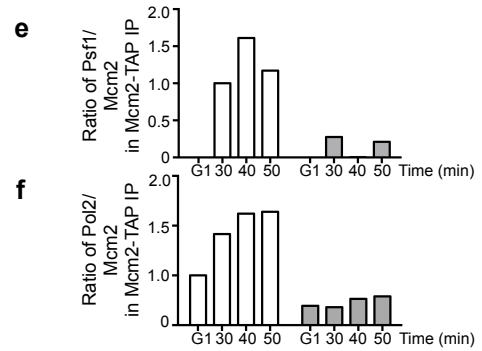
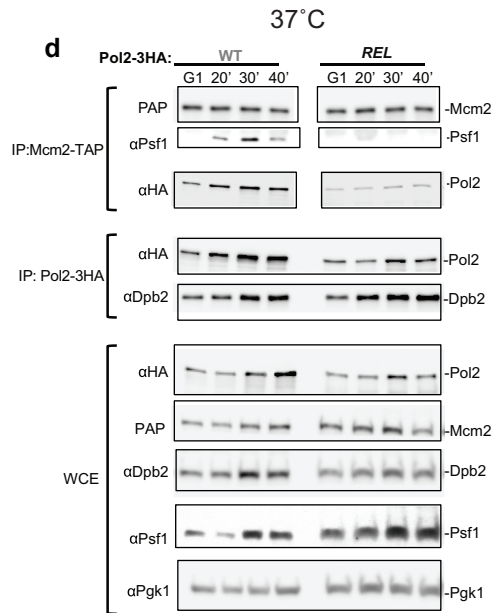
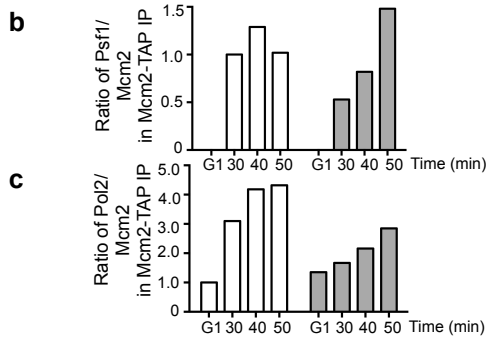
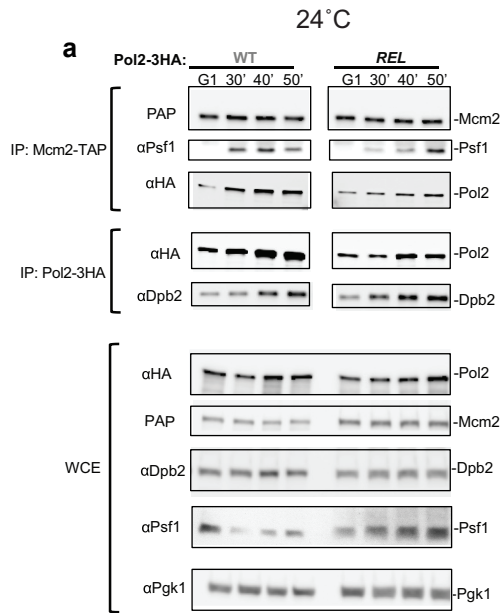


Figure 3-4. *pol2-REL* is defective in CMG formation and replisome assembly.

- a. Top, immunoblots showing the levels of Psf1 and Pol2 coimmunoprecipitated with TAP tagged Mcm2. Middle, levels of Dpb2 coimmunoprecipitated with HA tagged Pol2. bottom, immunoblots showing Pol2, Mcm2, Dpb2, Psf1, and Pgk1 protein levels in whole cell lysate. Pgk1 level serves as a loading control.
- b. Ratio of copurified Psf1 versus Mcm2 in the top panel of (a) were calculated and normalized to the ratio of the 30 min sample of Pol2-WT. White bar: Pol2-WT, gray bar: *pol2-REL*.
- c. Same as b, expect that the copurified Pol2 level was used instead of Psf1 signals, and the ratio was normalized to that of the G1 sample of Pol2-WT.
- d. Same as (a), expect samples were collected at 37°C.
- e-f. The same as b and c, respectively. Except that all the values are corresponding to (d).

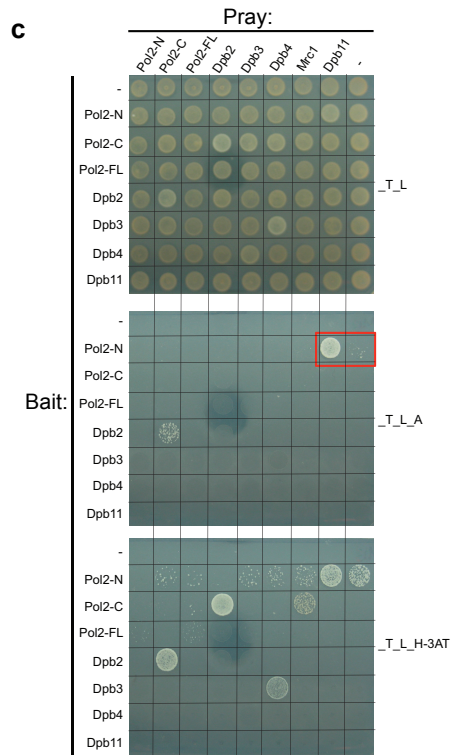
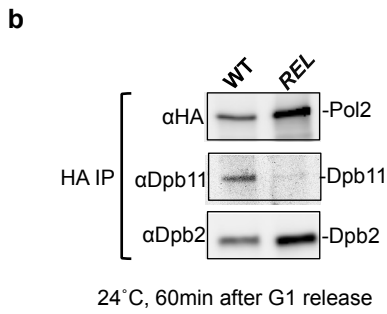
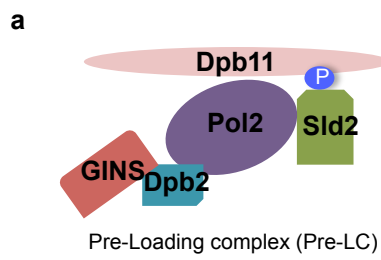


Figure 3-5. *pol2-REL* diminishes Pol2-Dpb11 interaction.

- a. Schematic of the pre-LC. P: CDK dependent phosphorylation at T84 of Sld2. Note that the Dpb3 and Dpb4 subunits of Pol ϵ are not essential for pre-LC formation and are not shown for simplicity.
- b. Immunoblots showing Dpb11 and Dpb2 levels coimmunoprecipitated with HA tagged Pol2. Both Pol2-WT and *pol2-REL* cells were collected after 60 min after releasing from G1 into S phase at 24°C. Proteins were cross-linked by formaldehyde and Pol2-HA was immunoprecipitated by anti-HA conjugated beads.
- c. Yeast two hybrid assay detects interaction of Dpb11 with Pol2-N terminus but not Pol2-C terminus. Bait: plasmids containing DNA binding domain. Prey: plasmids containing activating domain. Pol2-N: N-terminus of Pol2; Pol2-C: C-terminus of Pol2; Pol2-FL: full length Pol2. _T_L: Tryptophan and leucine double-dropout plate for selection of cells contains both prey and bait plasmids. _T_L_A, lacking adenine, a stringent condition for selecting protein interaction. _T_L_H_3AT, lacking histidine and is complemented with 3mM 3AT (3-Amino-1,2,4-tiazole), a less stringent condition for selecting protein interaction compared to _T_L_A. Note that several known interactions were observed here: for example, Dpb2 with Pol2-C terminus and Dpb3-Dpb4 interactions.

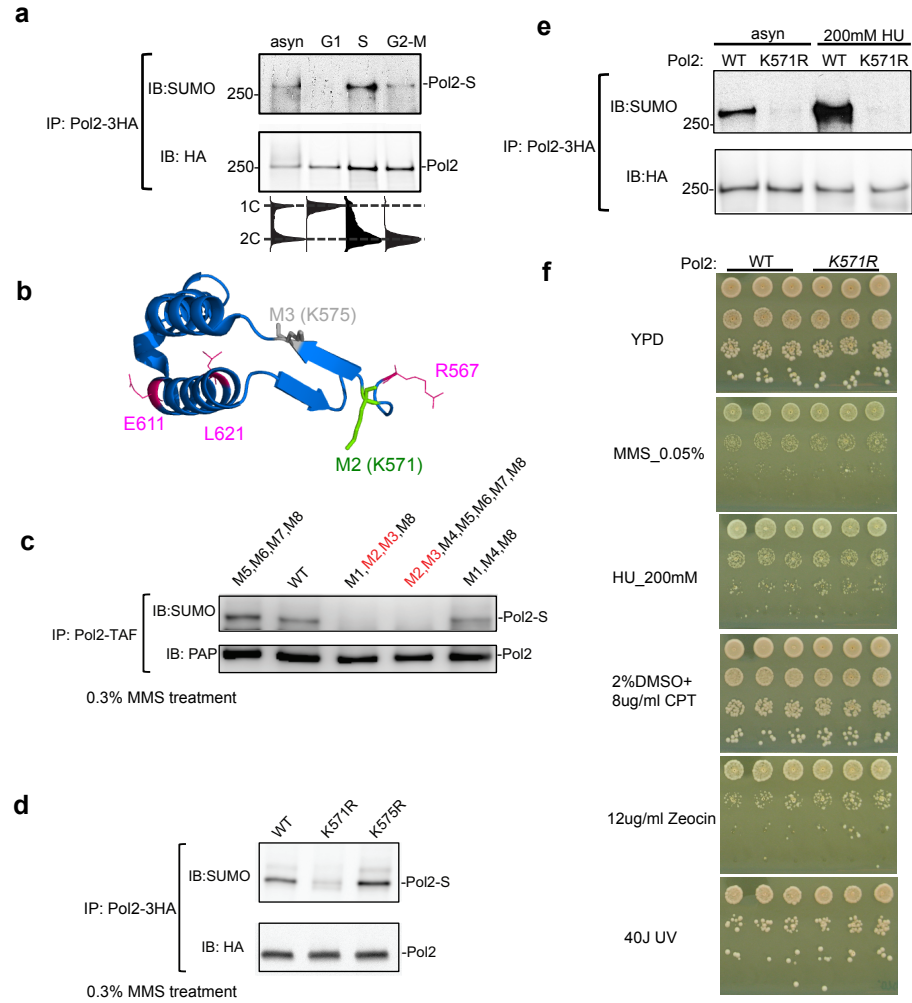


Figure 3-6. Pol2 sumoylation correlates with DNA replication and occurs at a single lysine on the NUD.

- a. Pol2 sumoylation status during the cell cycle. Cells were arrested in G1 phase and subsequently released into S phase, samples corresponding to different phases were collected. Flow cytometry analyses were plotted below. 1C and 2C indicate genome size.
- b. The location of M2 (K571, green stick) is located in a loop region, while M3 (K575, gray stick) is in the tail of a β sheet in NUD. *pol2-REL* mutations are labeled by red lines. PBD code: 4M8O.
- c. Eight consensus lysine sites (M1-M8) of Pol2 were mutated to arginines in combinations. Pol2 sumoylation was examined by immunoprecipitation of Pol2-TAF and subsequent western blotting using anti-SUMO antibody.
- d. K571R but not K575R mutation diminishes MMS induced Pol2 sumoylation. Note that Pol2 is tagged by 3HA.
- e. Pol2 K571R mutation reduces Pol2 sumoylation in both asynchronous cells and cells arrest in S phase by 200 mM HU.
- f. 10-fold serial dilutions of Pol2-WT and *pol2-K571R* cells were spotted on plates and grown at indicated temperatures for 36-48 hours before pictures were taken.

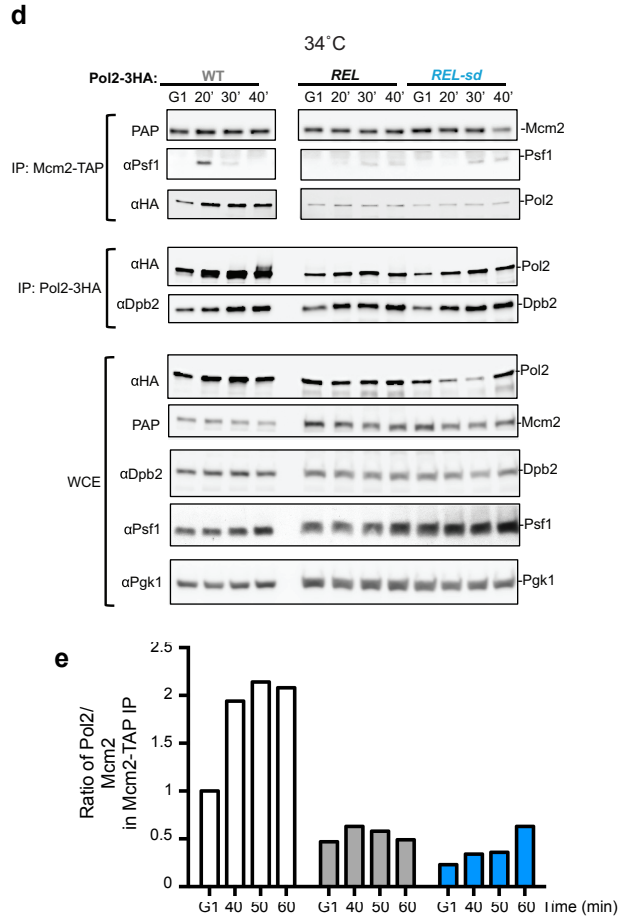
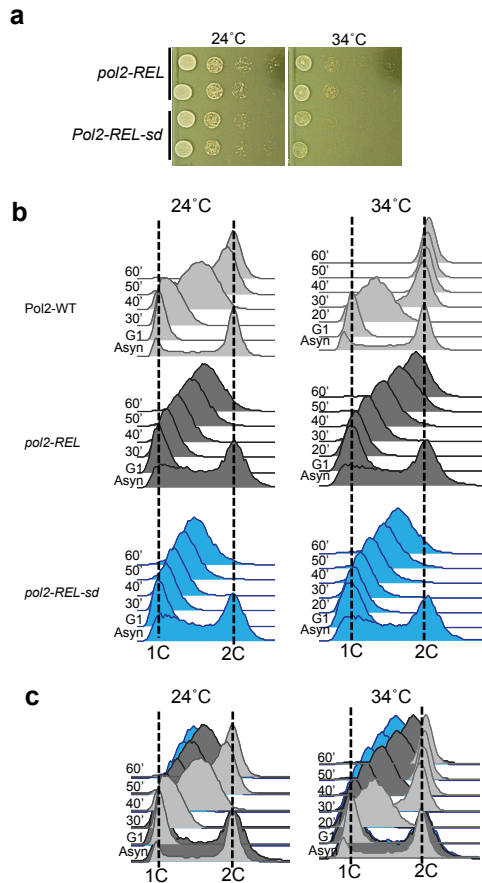


Figure 3-7. Pol2 sumoylation mutation exacerbates the replisome assembly defects caused by *pol2-REL*

- a. Pol2 sumoylation deficient mutation (K571R) exacerbates the growth defect of *pol2-REL* at semi-permissive temperature 34°C. *pol2-REL-sd*: *pol2-REL*+ K571R. 10-fold serial dilutions of cells were spotted on the plates and grown for 36-48 hour at indicated temperatures before pictures were taken.
- b. Replication profiles of Pol2-WT, *pol2-REL* and *pol2-REL-sd* cells were analyzed by flow cytometry. G1 synchronization and release were performed as in Figure 3-3c. 1C and 2C indicate genome size.
- c. The replication profiles of Pol2-WT, *pol2-REL*, and *pol2-REL-sd* in (b) were superimposed. Light grey: Pol2-WT; dark grey: *pol2-REL*; blue: *pol2-REL-sd*.
- d. CMG formation and replisome assembly were examined as in Figure 3-4a.
- e. Ratio of copurified Pol2 level versus Mcm2 signal were calculated and normalized to the ratio of the G1 sample of Pol2-WT. White bar: Pol2-WT; gray bar: *pol2-REL*; blue bar: *pol2-REL-sd*.

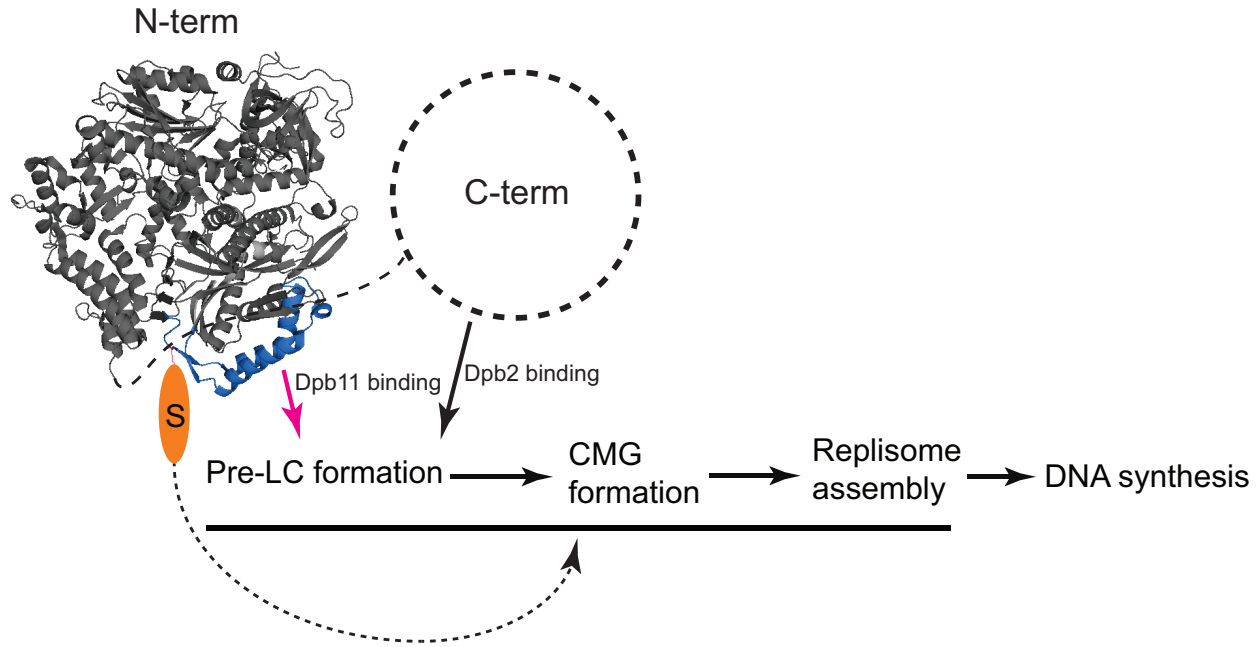


Figure 3-8. A working model of the function of the NUD and Pol2 sumoylation.

Crystal structure of yeast Pol2 N-terminus is shown, the C-terminus of Pol2 is indicated by a dashed circle. The NUD is labeled in blue, SUMO is marked in orange. During replication initiation, the NUD interacts with Dpb11 and the C-terminus of Pol2 interact with Dpb2, both interactions contribute to the pre-LC formation. Pre-LC subsequently leads to CMG formation and replisome assembly. Then DNA synthesis begins. Pol2 sumoylation likely takes place during pre-LC formation to replisome assembly, the precise timing is unknown. Pol2 sumoylation may promote replication initiation by affecting pre-LC, CMG or replisome assembly.

Chapter 4

Interplay between RPA sumoylation and the Mec1 checkpoint

Introduction

The DDR relies on PTMs to transduce signals and regulate multiple cellular processes. The best understood PTMs in the DDR are the Mec1/ATR and Tel1/ATM mediated phosphorylation events. In budding yeast, Mec1 is the primary checkpoint kinase and Tel1 has a minor role. Both the Mec1- and Tel1-mediated checkpoints are initiated by DNA damage sensor proteins. These proteins bind to common DNA structures generated from DNA lesions or stalled replication forks, such as ssDNA and DSBs. In the case of the Mec1-mediated checkpoint, several DNA damage sensor proteins can recruit Mec1 and its partner, Ddc2, to DNA lesion sites. The primary sensor protein is the ssDNA binding protein RPA, a trimeric complex composed of Rfa1-3 subunits. The N-terminal protein-protein interaction region of Rfa1 directly interacts with Ddc2, and this association recruits Mec1-Ddc2 to ssDNA regions (Zou and Elledge 2003; Ball et al. 2007). In addition, RPA interacts with and promotes the recruitment of two other factors that stimulate Mec1 kinase activity. These are the trimeric ring complex Rad17-Mec3-Ddc1 (or 9-1-1) and a DNA helicase-nuclease Dna2(Harrison and Haber 2006; Zou 2013). These multiple roles make the RPA coated ssDNA a critical upstream component in the Mec1-mediated checkpoint pathway.

A recent study has shown that the RPA-ssDNA filament also serves as a platform for DDIS(Chung and Zhao 2015). In this case, the C-terminal winged helix (WH) domain of the Rfa2 subunit binds and recruits the SUMO E3 ligase Siz2 to DNA lesion sites(Chung and Zhao 2015). The RPA-Siz2 interaction mediates some sumoylation

events after DNA damage and constitutes one branch of DDIS. This branch enables the sumoylation of RPA itself and recombinational repair proteins, including Rad52 and Rad59 (Psakhye and Jentsch 2012; Chung and Zhao 2015). A recent study suggests that sumoylation of these proteins has redundant roles in promoting homologous recombination (HR), such that lacking the sumoylation of a single protein does not affect HR at non-repetitive sequences (Psakhye and Jentsch 2012). This effect was termed as protein “group modification”, emphasizing the redundant nature of sumoylation on a group of functionally related substrates. However, in another context, Rad52 sumoylation alone can influence recombination at the repetitive rDNA locus, suggesting that “group modification” is a context dependent phenomenon (Torres-Rosell et al. 2007). The sumoylation of RPA and Rad59 has not been examined outside HR, thus it is unclear if their sumoylation has specific roles in other processes requiring RPA and Rad59.

Despite sharing a common DNA damage-sensing complex, RPA, the Mec1 checkpoint and DDIS are largely independent of each other (Cremona et al. 2012). Mec1 removal does not diminish DDIS, rather it increases sumoylation of certain substrates, likely due to increased levels of DNA damage in *mec1Δ* cells. On the other hand, reducing sumoylation can delay the Mec1 checkpoint activation, but does not abolish it. Further genetic data also support that the Mec1 checkpoint and DDIS make separate contributions to survival after DNA damage (Cremona et al. 2012). These findings suggest that while DDIS and the Mec1 checkpoint display a large degree of independence from one another, sumoylation can increase the robustness of the checkpoint. Additional support to this theory comes from a recent study in human cells, where the sumoylation of the Ddc2 homolog, ATRIP, was shown to promote the ATR-mediated checkpoint by targeting ATRIP to DNA damage sites and interacting with other

checkpoint proteins (Wu et al. 2014). This finding supports the idea of a SUMO-based enhancement of checkpoint activation. As the yeast Ddc2 protein has not been found to be sumoylated (Cremona et al. 2012), a positive crosstalk based on ATRIP sumoylation may be an event that appears late in evolution. The mechanism(s) that support SUMO-based enhancement of the Mec1 checkpoint in yeast are still a mystery. Such a mechanism may represent one means by which SUMO boosts the robustness of the Mec1 checkpoint.

As RPA uniquely supports both DDIS and the Mec1 checkpoint, and RPA is sumoylated, I examined whether its sumoylation can promote the Mec1 checkpoint and whether such a role is separable from the protein “group modification” wherein the sumoylation of RPA, Rad52, and Rad59 play redundant roles. I found that Rfa1 sumoylation was induced by several genotoxins that elicit checkpoint activation. I determined four sumoylation sites on Rfa1 and one on Rfa2. My genetic evidence showed that mutating these sites reduces the Mec1 checkpoint, but not the Tel1-mediated checkpoint. The biological effects of these mutants appear to be specific, as they do not affect other RPA-related processes, such as DNA end resection and replication. Consistent with a role of RPA sumoylation in promoting Mec1 functions, Rfa1 and Rfa2 sumoylation deficiencies sensitized another Rfa1 mutant towards the Top1 poison camptothecin (CPT). Together, my findings provide evidence that RPA sumoylation positively regulates activation of the Mec1 checkpoint. Based on these findings, I suggest that the crosstalk between DDIS and the Mec1 checkpoint in yeast is mediated by RPA, the common sensor of the two PTM pathways.

Results

Detection of Rfa1 and Rfa2 sumoylation

Previous reports have shown that after treating cells with the DNA alkylating agent MMS or the radiomimetic agent zeocin, Rfa1 sumoylation can be detected in cell extracts when using a denaturing protein preparation method (Psakhye and Jentsch 2012; Chung and Zhao 2015) (referred to as TCA method hereafter). Using the same extraction conditions, I detected three Rfa1 modification forms after MMS treatment (Figure 4-1a,1b). These forms were indeed the sumoylated forms of Rfa1 based on the following evidence. First, when I tagged endogenous SUMO with a hexa-histidine-Flag epitope (HF-SUMO), the modified Rfa1 bands showed an upshift compared to untagged SUMO (Figure 4-1a). Second, the intensity of these bands was diminished in cells lacking the SUMO E3 Siz2, the E3 that sumoylates Rfa1 (Psakhye and Jentsch 2012; Chung and Zhao 2015)(Figure 4-1b). Based on these criteria, I concluded that there are three Rfa1 sumoylation forms. Specifically, as mono-sumoylation typically results in a ~20 kDa upshift in mobility compared to the unmodified protein, the two bands indicated as Rfa1-Sa and Rfa1-Sb are likely to be mono-SUMO modified species (Figure 4-1a,1b). I note that multiple migration patterns for mono-sumoylated forms of a single protein are commonly seen, such as for PCNA, a processivity factor for the lagging strand polymerase Pol δ (Sacher et al. 2006; Karras and Jentsch 2010). This is likely because SUMO modification creates branched molecules, and SUMO modification at different positions on a substrate results in asymmetrically shaped branches, which can affect protein mobility in gels (more details later) (Figure 4-1c). A third modified Rfa1 band (Rfa1-S2) displayed a mobility shift of ~40 kDa, suggesting it represents a di-SUMO modified form of Rfa1 (Figure 4-1a,1b).

I could not detect modified Rfa2 in crude extracts, suggesting that Rfa2 sumoylation is less abundant compared to Rfa1. When Rfa2 was immunoprecipitated, I detected two sumoylated forms of this protein by western blot using a SUMO specific antibody (Figure 4-1d). The pattern of Rfa2 sumoylation is consistent with a previous report (Psakhye and Jentsch 2012). Rfa2-S had a characteristic ~20 kDa upshift compared to the unmodified band, consistent with a mono-sumoylated Rfa2 species, while Rfa2-S2 had ~40 kDa upshift, consistent with a di-sumoylated Rfa2 species (Figure 4-1d). Rfa3 sumoylation was seen by the Jentsch group (Psakhye and Jentsch 2012), but not by our lab, even after the protein was enriched by immunoprecipitation. Herein, I focus on Rfa1 and Rfa2 sumoylation.

Rfa1 sumoylation occurs under genotoxin treatments that activate Mec1

Besides MMS and zeocin, I also tested whether other genotoxins known to induce the Mec1 checkpoint lead to increased Rfa1 sumoylation. Indeed, I observed that Rfa1 is sumoylated in cells treated with UV, HU, or CPT (Figure 4-1e,1f). HU appeared to be more potent in inducing Rfa1 sumoylation compared with UV. The level of induction is likely related to the amount of ssDNA generated by the various DNA stress inducing agents. It is known that during HU treatment, large stretches of ssDNA are generated due to uncoupling of the replicative helicase and polymerase at hundreds of replication forks (Sogo et al. 2002; Byun et al. 2005; Feng et al. 2006). Regardless, my findings show that Rfa1 sumoylation occurs during multiple types of genotoxic conditions that activate Mec1.

The subsequent characterization of Rfa1 and Rfa2 sumoylation is mainly performed in MMS conditions. In addition, to gain a quantitative understanding of the amount of Rfa1 sumoylation, western blots were directly scanned using a scanner that

has a dynamic range of four orders of magnitude. This approach is used in most of the tests herein, unless otherwise indicated.

Confirming two major sites for Rfa1 sumoylation

In order to study the effects of Rfa1 and Rfa2 sumoylation, I aimed to determine their sumoylation sites. A previous report identified K170 and K427 as the sites for Rfa1 sumoylation based on mass spectrometry analysis of total sumoylated proteins from cells (Psakhye and Jentsch 2012). Mutating K170 and K427 to arginine noticeably reduced Rfa1 sumoylation consistent with the notion that they are the main sumoylation sites (Psakhye and Jentsch 2012). The authors also found that when combined with K170R and K427R, K133R further reduced Rfa1 sumoylation; however, K133 was not identified as sumoylation site in their mass spectrometry study.

In our independent study using *in vitro* sumoylated RPA as material for MS, I also identified K170 and K427 as sites of sumoylation in two out of four trials. To confirm that these are the *in vivo* sumoylation sites, I examined mutations of these sites. Because *mec1* Δ cells showed higher level of Rfa1 sumoylation (Figure 4-1b), I initially used these cells for my test. Specifically, *rfa1* Δ *mec1* Δ cells were supplemented with CEN-based plasmids expressing either WT Rfa1, *rfa1-K170R*, *rfa1-K427R*, or *rfa1-K170,427R* driven by the Rfa1 endogenous promoter. I assessed Rfa1 sumoylation by the TCA method after 0.02% MMS treatment. In cells containing *rfa1-K170R*, the intensity of Rfa1-Sa band reduced by ~80%, and that of the Rfa1-S2 band reduced 50%, while the intensity of Rfa1-Sb did not change (Figure 4-2a). This result suggests that K170 sumoylation is mainly responsible for the Rfa1-Sa form and part of the di-sumoylated form. In the *rfa1-K427R* mutant, the intensity of Rfa2-Sb band reduced

~60% and that of -S2 band intensity declined 20% while that of Rfa2-Sa did not change (Figure 4-2a). This result suggests that K427 sumoylation is mainly responsible for the Rfa1-Sb form and part of the di-sumoylated forms. When K170 and K427 were both mutated to arginine, total Rfa1 sumoylation level was reduced by 75% (Figure 4-2a). These results suggest that 1) sumoylation of K170 and K427 are mainly responsible for Rfa1-Sa and -Sb species, respectively; 2) the residual 25% Rfa1 sumoylation in *rfa1-K170, 427R* is due to additional sumoylation sites.

K133 and K494 are not responsible for Rfa1 sumoylation

In our mass spectrometry analyses, aside from K170 and K427, we also detected K133 and K494 in one of the four trials. I then evaluated these two sites in the *rfa1-K170, 427R* double mutant to see if further reduction of Rfa1 sumoylation level occurred. When the sumoylation level of *rfa1-K133,170,427R* was compared to that of *rfa1-K170,427R*, no further reduction in Rfa1 sumoylation level was detected (Figure 4-2b). Similarly, mutating K494 to arginine did not further reduce the Rfa1 sumoylation level in *rfa1-K170,427R* (Figure 4-2c). These results indicate that K133 and K494 do not contribute to Rfa1 sumoylation in the absence of the two major Rfa1 sumoylation sites.

Rationale for identifying candidate sites for residual Rfa1 sumoylation

The above results indicate that the sites of residual Rfa1 sumoylation were not recovered by our mass spectrometry analyses. This could be due to a number of reasons: their sumoylation may occur at lower frequency than at K170 and K427 (Figure 4-2a), or their sumoylation may require additional factors not included in the *in vitro* sumoylation reactions, or they may be in regions that are sparse for lysine and arginine

residues for trypsin digestion and are thus poorly recovered. To circumvent these issues, I used a candidate approach to determine the additional sumoylation sites.

As mentioned above, the migration patterns of the sumoylated forms on gels in principle can be influenced by the position of the conjugation. For example, when a SUMO moiety is conjugated at different distances to the ends of a protein, the resultant branched molecules have different shapes and will have different mobilities in SDS-PAGE. Indeed, K170 and K427 are different distances to the ends of Rfa1 (Figure 4-1c). Rfa1 mono-sumoylated at K170 or K427 are observed at different positions on SDS-PAGE (Figure 4-2a). Similar findings have been seen for PCNA and Rad52 (Sacher et al. 2006; Karras and Jentsch 2010).

The above phenomenon provides a strategy for finding candidate lysines responsible for residual sumoylation, considering that residual Rfa1 sumoylated forms run at the same positions as K170 and K427 sumoylation forms (Figure 4-2a). I thus hypothesized that the sites of residual sumoylation are likely around K170 and K427, or at their corresponding symmetrical sites from the other end of Rfa1. As it is not known how close these sites should be in order to run at very similar position, an arbitrary 20aa radius was employed for identifying residual Rfa1 sumoylation sites. Residues that fit these criteria for the Rfa1-Sa band are K180, K442, and K463, and for the Rfa1-Sb band are K411, K417, K200, K206, and K210. Since it has been proposed that sumoylation tends to take place in less structured loop regions (Gareau and Lima 2010), K180, K411 and K417 were tested first.

Identification of two additional sites of Rfa1 sumoylation

I tested K180R, K411R, and K417R mutations in the *rfa1-K170,427R* background. The K180R mutation abolished the residual Rfa1-Sa band in *rfa1-K170,427R*, while the intensity of Rfa1-Sb band did not decrease (Figure 4-2d, lane 5-8). This result suggests that both K170 and K180 are responsible for the Rfa1-Sa band. Similarly, K411R reduced the Rfa1-Sb band intensity in *rfa1-K170,180,427R* background without affecting Rfa1-Sa band intensity (Figure 4-2d, lane 6-10), indicating that K411 contributes the residual sumoylation of the Rfa1-Sb band. The total sumoylation level of *rfa1-K170,180,411,427R* (*rfa1-4KR*) is reduced by 90% compared to WT, this is a further reduction of 15% compared to the *rfa1-K170,427R* mutant (Figure 4-2d, right panel). I found that K417R did not further reduce the sumoylation of *rfa1-4KR* (data not shown), suggesting that K417 does not contribute significantly to Rfa1 sumoylation. Sumoylation of the *rfa1-K170,427R*, *rfa1-K170,180,427R*, and *rfa1-K170,180,411,427R* mutations discussed above was first tested in *mec1Δ* cells and then confirmed in WT cells. Considering *rfa1-4KR* still has residual Rfa1-Sb band (Figure 4-2d, lane 9-10), additional sumoylation sites may exist, perhaps K200, K206, and/or K210. Since *rfa1-4KR* reduces Rfa1 sumoylation by 90%, it was used for phenotypic studies discussed in subsequent sections of this chapter. It is worth noting that when the major sumoylation sites K170 and K427 are mutated, a novel sumoylation band appears between the Sa and Sb bands (Figure 4-2b, 2d, indicated by *). It is likely that some minor sumoylation events take place when the major sites for Rfa1 sumoylation are missing.

Among the four sumoylation sites on Rfa1, K427 and K170 conform to consensus [ΨKX(D/E)] and reverse consensus sumoylation sites [(D/E)XKΨ], respectively (Figure 4-2e). K180 and K411 are non-consensus sequences (Figure 4-

2e). This is consistent with the report that 50% of sumoylation takes place on consensus or reverse consensus sites (Lamoliatte et al. 2014).

Determining Rfa2 sumoylation sites

As K199 has been reported to be the Rfa2 sumoylation site, a single K199R mutation was generated at the endogenous Rfa2 locus with no addition of tag or selection marker by the URA-based pop-in-pop-out method (Reid et al. 2002). The resultant clean *rfa2-K199R* mutant had an undetectable level of Rfa2 sumoylation after 0.02% MMS treatment (Figure 4-2f). This result is consistent with the previous study showing that K199 is the sumoylation site of Rfa2 (Psakhye and Jentsch 2012).

Properties of RPA sumoylation sites

RPA is well studied at the structural and biochemical levels and is highly conserved among species (Wold 1997; Oakley and Patrick 2010; Fan and Pavletich 2012). Rfa1 is composed of three ssDNA binding domains, termed DbdA-C (Fan and Pavletich 2012) (Figure 4-3). In addition, it has an N-terminal domain that interacts with proteins such as Ddc2, the binding partner of Mec1 (Figure 4-3a). These domains are joined together by less structured linker regions. I note that, except for K411, the Rfa1 sumoylation sites are located within these linker regions (Fan and Pavletich 2012) (Figure 4-3). This fits with the previous observation that sumoylation sites tend to be within less structured regions (Gareau and Lima 2010). Similarly, K199 of Rfa2 is located outside its well-structured ssDNA-binding domain (dbdD) (Fan and Pavletich 2012) (Figure 4-3). Upon sequence comparison among RPA homologs, I noticed that the five sumoylation sites on Rfa1 and Rfa2 are only conserved in closely related yeast species, but not in human or *S. pombe* (Figure 4-2e). Human RPA has been reported to be sumoylated though the

sumoylation sites are located in the dbdC, indicating that although the sumoylation sites are not conserved, the sumoylation event is (Dou et al. 2010). This phenomenon is commonly found for other proteins (Eladad et al. 2005; Sacher et al. 2006; Lu et al. 2010; Saito et al. 2010). The non-conservation of sumoylation sites also indicates that mutating this lysine *per se* is unlikely to disrupt the critical function of RPA in DNA binding.

rfa1-4KR rescues srs2 Δ defects caused by persistent Mec1 checkpoint

After I determined Rfa1 sumoylation sites, I moved on to examine whether *rfa1-4KR* affected the Mec1 checkpoint. As described in the introduction, previous findings suggested a role of SUMO in boosting, but not controlling, the Mec1 checkpoint function (Cremona et al. 2012). Thus, if RPA sumoylation does contribute to this effect, I would expect a moderate decrease of checkpoint levels when RPA sumoylation is reduced. Previously characterized point mutations that partially affect Mec1 checkpoint functions do not tend to be hypersensitive to DNA damaging agents by themselves (Pike et al. 2003; Puddu et al. 2008; Kumar and Burgers 2013). I also found that *rfa1-4KR* grew like WT and was not sensitive to DNA damaging drugs tested (Figure 4-4a).

Next I used a sensitive genetic approach to probe the effect of *rfa1-4KR* on the Mec1 checkpoint. It is known that mild checkpoint defects can suppress mutants with persistent checkpoint activation (Vaze et al. 2002; Ohouo et al. 2013; Gobbini et al. 2015). In particular, *srs2 Δ* cells exhibit persistent Mec1 checkpoint activation, and such a defect causes sensitivity to genotoxins (Vaze et al. 2002; Yeung and Durocher 2011). I found that *rfa1-4KR* improved the resistance of *srs2 Δ* cells on media containing CPT (Figure 4-4b). This suppression is specific to *srs2 Δ* , since *rfa1-4KR* did not affect the

CPT sensitivity of *sae2* Δ (Figure 4-4c), which has been attributed to persistent Tel1 checkpoint activation (Gobbini et al. 2015).

***rfa1-4KR* augments suppression of *srs2* Δ by another *rfa1* allele**

As the observed suppression of *srs2* Δ by *rfa1-4KR* is mild, I asked whether *rfa1-4KR* could enhance a similar suppressive effect of other *rfa1* alleles. Specifically, I noticed that the *rfa1-K494R* allele, which did not reduce *in vivo* Rfa1 sumoylation (Figure 4-2c), suppressed *srs2* Δ sensitivity to CPT (Figure 4-4d). Based on this genetic finding, it is possible that *rfa1-K494R* is mildly defective in checkpoint function, though this has yet to be formally tested. K494 is one of the 52 residues of Rfa1 that contribute to DNA interaction based on structural studies (Figure 4-5). This residue is located in dbdC (Figure 4-3a, 3b and -4f), which has weaker DNA binding activity compared to dbdA and dbdB (Brill and Bastin-Shanower 1998; Lao et al. 1999). Mutation of K494 to arginine is expected to have a subtle effect on RPA ssDNA binding activity, though formal testing is needed to confirm this. Genetically, *rfa1-K494R* grew like WT and was only mildly sensitive to a high dose of CPT (Figure 4-4a).

I generated the *rfa1-5KR* allele by simultaneously mutating the four sumoylation sites and K494 to arginine. Interestingly, *rfa1-5KR* suppressed the DNA damage sensitivity of *srs2* Δ better than either *rfa1-K494R* or *rfa1-4KR* alone (Figure 4-4d). This effect of *rfa1-5KR* is specific to *srs2* Δ , since *rfa1-5KR* did not suppress the CPT sensitivity of *sae2* Δ (Figure 4-4e). This finding suggests that *rfa1-4KR* can enhance the suppression of *srs2* Δ by the K494R mutation. Consistent with the stronger effect of *rfa1-5KR* in *srs2* Δ suppression, this allele was 100-times more sensitive to CPT than *rfa1-K494R* or *rfa1-4KR* (Figure 4-4a). The sensitivity of *rfa1-5KR* appeared to be specific to

CPT, as it behaved like WT cells when treated with other DNA stress agents, such as MMS, HU, and zeocin.

rfa1-5KR leads to reduced Rad53 phosphorylation levels in srs2Δ cells

As indicated above, one interpretation of the observed genetic suppression is that *rfa1-4KR* and *rfa1-5KR* are defective in the Mec1 checkpoint. To directly test this idea, I examined Rad53 phosphorylation, a critical indicator of Mec1 checkpoint activation. If *rfa1-5KR* suppressed the CPT sensitivity of *srs2Δ* by reducing checkpoint activation, it would reduce the Rad53 phosphorylation levels in *srs2Δ* cells. To test this, I arrested both *srs2Δ* and *srs2Δ rfa1-5KR* cells in G1 phase, and then released the cells into CPT containing media for 0.5-12.5 hrs (Figure 4-6a). *srs2Δ* cells exhibited persistent Rad53 phosphorylation even at 12.5 hrs (Figure 4-6a). However, *srs2Δ rfa1-5KR* cells showed much less Rad53 phosphorylation at multiple time points (Figure 4-6b). The differences between the two strains were not due to different cell cycle distributions (Figure 4-6a, right panel). These results provide molecular support to my hypothesis that *rfa1-5KR* has a defective Mec1-mediated checkpoint.

I also used genetic approaches to test my hypothesis. If *rfa1-5KR* suppression of *srs2Δ* is mediated by the Mec1 checkpoint, then the suppression should be lost when Mec1 is removed. Indeed, *rfa1-5KR* failed to suppress *srs2Δ* in a *mec1Δ* background (Figure 4-6c). Our controls showed that *mec1Δ* and *srs2Δ* cells were not sensitive to CPT at the dosage used, and *mec1Δ srs2Δ* cells were sensitive, indicating that Mec1 and Srs2 have non-overlapping functions (Figure 4-6c). In addition, *mec1Δ rfa1-5KR* cells behaved like *mec1Δ* in their sensitivity to CPT (Figure 4-6d). Therefore, the lack of suppression of *srs2Δ* by *mec1Δ rfa1-5KR* is not because *mec1Δ rfa1-5KR* cells are

hypersensitive to CPT. Similarly, *mec1Δ rfa1-4KR* also behaved like *mec1Δ* in terms of CPT sensitivity, suggesting that Rfa1 and Mec1 are epistatic (Figure 4-6d).

It remains to be tested whether *rfa1-K494R* and *rfa1-4KR* have reduced Rad53 phosphorylation levels in the *srs2Δ* background, and whether such an effect is less severe than *rfa1-5KR*. I also plan to test if *rfa1-K494R*, *rfa1-4KR*, and *rfa1-5KR* have reduced Rad53 phosphorylation level in Srs2 WT background under DNA damaging conditions, especially after CPT treatment, since *rfa1-K494R* and *rfa1-5KR* demonstrated CPT specific sensitivity. These experiments are ongoing in the lab.

Rfa2 sumoylation deficient mutant behaves similarly to rfa1-4KR

The Rfa2 sumoylation deficient mutant *rfa2-K199R* behaved similarly to *rfa1-4KR* in suppression of *srs2Δ* CPT sensitivity (Figure 4-7a). In addition, this suppression by *rfa2-K199R* was additive with *rfa1-4KR* or *rfa1-5KR* (Figure 4-7a). One interpretation of this genetic data is that sumoylation of Rfa1 and Rfa2 additively affect the Mec1 checkpoint. Future work examining Rad53 phosphorylation will test this idea directly.

Consistent with an additive relationship with *rfa1-5KR*, *rfa2-K199R* enhanced the CPT sensitivity of *rfa1-K494R* and *rfa1-5KR*, while *rfa2-K199R* itself grew like WT and was not sensitive to the genotoxins tested (Figure 4-7b). However, unlike *rfa1-5KR*, which did not affect Rfa1 protein level, *rfa2-K199R* had 30% lower Rfa2 protein level compared to WT (Figure 4-7c-7e). It is not clear if the phenotypes of *rfa2-K199R* are due to lack of sumoylation, reduced protein level, or a combination of both. Experiments that correct the low protein level seen in *rfa2-K199R* are underway to further evaluate the effect of loss of Rfa2 sumoylation.

Loss of Rad52 and Rad59 sumoylation do not confer *srs2*Δ suppression

An earlier study suggested that the sumoylation of RPA, Rad52, and Rad59 share similar functions in HR (Psakhye and Jentsch 2012). This conclusion is based on the lack of DNA damage sensitivity of individual sumoylation site mutants and reduced HR levels at non-repetitive sequences when all sumoylation sites are mutated (Psakhye and Jentsch 2012). However, another study has shown that Rad52 sumoylation itself already affects rDNA repeat stability (Torres-Rosell et al. 2007). Thus it is likely that the sumoylation of these Siz2 substrates have redundant functions in some situations but distinct roles under other situations. To test this idea, I asked whether Rad52 and Rad59 sumoylation mutants also suppress *srs2*Δ defects. Rad52 is known to be sumoylated at three lysines (K43, K44, and K253) and Rad59 at two (K207 and K228) (Sacher et al. 2006; Altmannova et al. 2010; Psakhye and Jentsch 2012). I made K-R substitutions for each protein and found that these mutants failed to suppress *srs2*Δ CPT sensitivity both by themselves and in combination (Figure 4-7f). This finding suggests that the suppression of *srs2*Δ CPT sensitivity by Rfa1 and Rfa2 sumoylation site mutants is not due to a reduction of a function shared with Rad52 and Rad59. Thus, even though RPA, Rad52, and Rad59 share an E3 ligase, Siz2, and may have redundant functions in HR, sumoylation of each also has distinct roles.

***rfa1-5KR* does not affect DNA end resection**

Rfa1 has multiple roles in Mec1 checkpoint activation, including promoting DNA resection. Here I directly tested DNA resection by a physical assay. I examined *rfa1-5KR* in this assay, since it has the greatest defect in checkpoint activation among *rfa1-4KR*, *rfa1-K494R*, and *rfa1-5KR*. A single DSB was generated by HO endonuclease cleavage, and resection was monitored by the progressive disappearance of restriction fragments

flanking the cut site (Figure 4-8a). As shown in Figure 4-8a-d, the disappearance of two fragments 0.7kb and 3kb away from the break were monitored by southern blot. The intensity of the two fragments was normalized to loading control Dnl4 and the value at 30 min after HO induction was set as 100%. No significant difference in the kinetics of disappearance of either fragment was detected compared to WT strains, indicating that *rfa1-5KR* and, by extension, *rfa1-4KR* and *rfa1-K494R* are proficient for DNA resection after a single HO cut. The *rfa1-4KR* and *rfa1-K494R* alleles will be directly tested in this resection assay to confirm my findings. I conclude that Rfa1 sumoylation does not affect DNA resection.

Discussion

Potential mechanisms by which RPA sumoylation regulates the Mec1 checkpoint

What are the mechanisms by which RPA sumoylation deficient mutants could reduce Mec1 checkpoint activation? Aside from DNA resection, RPA contributes to the Mec1 checkpoint by two means. First, RPA's interaction with ssDNA is important both for checkpoint function and for other DNA transactions, such as replication and repair. Whether RPA sumoylation deficient mutants affect its ssDNA binding will be tested in the future by electrophoretic mobility shift assay (EMSA) and an assay for microhomology-mediated end joining (MMEJ). MMEJ is acutely sensitive to RPA defects in ssDNA binding, therefore if *rfa1-4KR* is defective for ssDNA binding, it would not be able to prevent annealing, and an increased incidence of MMEJ events would be observed (Deng et al. 2014). Second, RPA contributes to checkpoint activation by binding to the Mec1 partner Ddc2 and other factors critical for the activation of Mec1, including the 9-1-1 complex and Dna2 (Bae et al. 2001; Bae et al. 2003; Zou and Elledge 2003; Yang and

Zou 2006; Ball et al. 2007; Zhou et al. 2015). These protein-protein interactions appear to contribute more to checkpoint activation than ssDNA binding does. In addition, a common effect of sumoylation is to promote protein-protein interactions (Sarangi and Zhao 2015). Furthermore, previous studies suggest the presence of two SUMO interaction motifs (SIMs) in Mec1, and that Dna2 interacts with SUMO (Makhnevych et al. 2009; Psakhye and Jentsch 2012). Together this supports a model where RPA sumoylation promotes its interaction with Mec1 and/or Dna2. This hypothesis will be tested by examining whether sumoylated Rfa1 binds Mec1 and/or Dna2 better than unmodified Rfa1. As introduced in Chapter 2, SuOn tagging or SUMO fusion could be used to increase or mimic Rfa1 sumoylation (Almedawar et al. 2012; Wei and Zhao 2016a). The interaction between Mec1 or Dna2 with Rfa1-SuOn and/or Rfa1-SUMO could also be tested by yeast two hybrid and co-immunoprecipitation.

Generate new *Rfa2* and *Rfa3* sumoylation deficient alleles

While *rfa1-4KR* did not affect protein levels, *rfa2-K199R* had 30% less Rfa2 protein level than WT (Figure 4-7e). Currently I cannot exclude whether this reduction of protein level contributes to *rfa2-K199R* phenotypes. I am in the process of testing this by increasing Rfa2 transcription or translation levels so that *rfa2-K199R* is expressed at the WT level. It is also possible that reduced Rfa2 sumoylation is a cause of low protein level, which could be tested by examining the Rfa2 expression level in *siz2Δ* cells. If *siz2Δ* and *rfa2-K199R* have similar Rfa2 protein levels, then Rfa2 sumoylation may indeed affect its stability.

While current efforts failed to detect Rfa3 sumoylation, I plan to use a more sensitive Ni-NTA pull down method to verify whether the protein is indeed sumoylated (Cremona et al. 2012). A previous report has shown that K46 is the main sumoylation

site of Rfa3 (Psakhye and Jentsch 2012). It is of interest to confirm this site and generate an Rfa3 sumoylation deficient mutant to test whether it behaves similarly to Rfa1 and Rfa2 sumoylation deficient mutants. In addition, if the sumoylation of all three subunits of RPA play redundant roles, combined sumoylation deficient mutants of all three RPA subunits would exhibit stronger defects.

It is worth noting that a caveat of using RPA sumoylation deficient mutants generated by mutating lysine residues to arginine is the possibility that the lysines *per se* have structural roles, and thus the phenotypes observed may reflect structural roles of these residues rather than the loss of protein sumoylation. As mentioned before, none of sumoylation sites mapped in Rfa1 and Rfa2 are evolutionarily conserved, it is the sumoylation events that are conserved, indicating that these lysines may not be critical for structural purposes. Since this reasoning does rule out the effect of mutating these lysines *per se*, a rescue of the defects of these sumoylation deficient mutants by SUMO fusion would provide strong evidence for the importance of RPA sumoylation.

Why do *rfa1-4KR* and *rfa1-K494R* specifically cause CPT sensitivity?

rfa1-4KR and *rfa1-K494R* are synergistically sensitive to treatment with CPT, but not other genotoxic agents (Figures 4-4a). These are the only known RPA alleles that exhibit a unique CPT sensitivity. One interpretation is that a mildly defective Mec1 checkpoint is particularly a problem under CPT conditions (Model 1). Alternatively, these RPA mutants may affect a repair process specific for CPT, which is the removal of Top1 covalently bound to the 3' end of DNA (Model 2). If Model 1 is correct, then other mutants mildly defective in the Mec1 checkpoint should also be more sensitive to CPT than other types of genotoxins. This test is in progress.

With respect to Model 2, I found that *rfa1-4KR* and *rfa1-5KR* increase *tdp1Δ rad1Δ* sensitivity to CPT (Figure 4-8e). This suggests that RPA sumoylation does not affect Tdp1- and Rad1-mediated Top1 removal. I have not yet tested if other Top1 removal pathways, such as those mediated by Mus81 and MRX, are related to RPA sumoylation. Aside from these genetic tests, I plan to perform a physical assay to directly monitor the kinetics of Top1-DNA conjugate disappearance. Together, these approaches will clarify the effect of *rfa1-4KR* and *rfa1-K494R* in Top1-DNA conjugate removal.

Multiple functions of RPA sumoylation

Our results reveal a potential role for RPA sumoylation in promoting the Mec1 checkpoint and exclude effects on DNA resection. As RPA is involved in almost all DNA related transactions through DNA binding and interaction with a dozen proteins belonging to different processes, it is possible that RPA sumoylation may influence additional pathways other than checkpoint activation. Our findings do suggest that the role of RPA sumoylation in checkpoint activation is different from the group effect seen in HR where sumoylation of RPA, Rad52, and Rad59 play redundant roles (Psakhye and Jentsch 2012). The nature of this redundancy is not completely clear, though increasing protein-protein interaction has been proposed since Rad59 associates with a sumoylated form of RPA (Psakhye and Jentsch 2012). A similar finding was made in human cells. Human Rfa1 is sumoylated at two sites (K449 and K577) that are different from yeast Rfa1 (Dou et al. 2010). In addition, these sites are located in dbdC, a different location compared to yeast. Sumoylated RPA was shown to promote Rad51 interaction and HR (Dou et al. 2010). In yeast, it has not been reported whether sumoylated RPA interacts with Rad51, although Rad51 does contain a SIM and interacts with sumoylated Rad52 (Bergink et al. 2013). If sumoylated RPA shows an enhanced interaction with

Rad51 and promotes Rad51 recruitment, then *rfa1-4KR* and the *rad51-SIM* mutant, which does not bind SUMO, should be epistatic in terms of suppression of the DNA damage sensitivity of *srs2Δ*. This possibility is currently being tested. However, as *rfa1-5KR* also improves the DNA damage resistance of other mutants with persistent checkpoint, such as *rtt107Δ* (data not shown), it may have a general effect on Mec1 function rather than specifically increasing binding to Rad51. As many replication proteins also interact with RPA and contain SIMs, I plan to examine whether RPA sumoylation affects replication under DNA damaging conditions.

Strategies for identification of sumoylation sites

The mapping of Rfa1 residual sumoylation sites revealed several general rules and strategies for sumoylation site identification. First, mono-sumoylation of a protein at different sites can lead to distinct electrophoretic mobilities, potentially due to formation of asymmetrically branched molecules. This has previously been demonstrated for PCNA and Rad52 sumoylation (Sacher et al. 2006; Karras and Jentsch 2010), and now is shown for Rfa1 sumoylation in this study. This property could potentially be used to map residual sumoylation site(s) on other proteins. If the residual sumoylated band migrates very close to a band with a known sumoylation site, then the residual sumoylation site is probably very close to the known site or a corresponding position from the other end of the protein. Using this method, K180 and K411 were identified to be responsible for residual Rfa1 sumoylation. Second, consistent with the literature, four out of the five sumoylation sites I mapped on RPA are located within less well-structured loop regions, this is likely due to the fact that the acceptor lysine and SUMO need to align properly during the SUMO conjugation process, therefore a local conformation change around the sumoylation site may be needed. Third, three out of the five sumoylation sites I mapped are consensus [ΨKX(D/E)] or reverse consensus sites

[(D/E)XKΨ] (Figure 4-2e). It has been reported that only about half of known sumoylation sites are consensus sites (Lamoliatte et al. 2014). To this end, mass spectrometry analysis is critical for mapping sumoylation at non-consensus sites. One main obstacle for mass spectrometry analysis is the low recovery of SUMO containing peptides. For a given protein, usually less than 1% is sumoylated at steady state (Geiss-Friedlander and Melchior 2007a; Sarangi and Zhao 2015). For a mono-sumoylated protein molecule, usually just one peptide that contains remnant SUMO is generated after digestion with sequence specific proteases. In addition, remnant SUMO conjugated branch molecules are difficult to be detected in mass spectrometry, due to their irregular structure (Knuesel et al. 2005; Wohlschlegel et al. 2006). Three main methods can be used to overcome this obstacle: i) generating large amounts of sumoylated protein by in vitro sumoylation, although in vitro sumoylation sometimes generates false positive results and must be validated by in vivo mutagenesis studies (Wilson and Heaton 2008); ii) enriching remnant SUMO conjugated peptides by a specific antibody recognizing the GG-isopeptide structure (Impens et al. 2014; Tammsalu et al. 2015), iii) using an engineered SUMO to reduce the size of the remnant SUMO conjugate after digestion with sequence specific proteases (Knuesel et al. 2005; Wohlschlegel et al. 2006), for example the SUMO-I96R mutation will generate a SUMO molecule that leaves a remnant GG conjugated to peptides instead of EQIGG, making this new branch molecule easier to be recovered in mass spectrometry analysis.

Methods and Materials

Yeast strains and techniques

Standard procedures were used in cell growth and medium preparation. Strains were isogenic to W1588-4C, a *RAD5* derivative of W303 (*MATa ade2-1 can1-100 ura3-1 his3-11,15 leu2-3,112 trp1-1 rad5-535*)(Zhao and Blobel 2005b). Strains and their usage in specific figure panels are listed in table 3. Rfa1 and Rfa2 mutant alleles used in Figures 4-1d, 4-2f, and 4-4-8, were generated using URA3-based pop-in-pop-out method as previously described (Reid et al. 2002). Mutations were generated at their endogenous loci and proteins were expressed from their own promoters, no tag or selection marker was present. All alleles were verified by sequencing. Yeast spotting assays were performed with standard procedures. All genetic and biochemical experiments were performed with two different spore clones for each genotype.

Detection of Rfa1 sumoylation, Rfa1 protein level, and Rad53 phosphorylation.

2×10^8 cells were collected and lysed by bead-beating in the presence of 20% TCA. The pellet was recovered by centrifugation and incubated with 1X laemmli buffer at 95°C for 5 min. During western blotting, anti-Rfa1 antibody was used to detect sumoylated and unmodified Rfa1.

Detection of Rfa2 sumoylation.

Detection of Rfa2 sumoylation in Figure 4-1d and 4-2f was performed as previously described (Zhao and Blobel 2005b). In brief, 5×10^8 cells were harvested and disrupted by bead-beating under denaturing conditions. Whole cell lysates were cleared by centrifugation and supernatant was incubated with anti-Rfa2 antibody conjugated beads

for 2 h at 4°C. The beads were then washed and the eluents were subjected to SDS-PAGE and western blotting with antibodies against SUMO (Zhao and Blobel 2005b) to detect sumoylated Rfa2 bands. Unmodified Rfa2 was detected by anti-Rfa2.

DSB resection assay.

Southern blot-based DSB resection assays were performed as previously described⁸⁸. A DSB at the *MAT a* locus was introduced by galactose-induced HO endonuclease expression during the time course in asynchronous cultures (Figure 4-8a-8c). Samples were collected at the indicated time points. Genomic DNA was isolated and an aliquot was subjected to XbaI and StyI digestion. Digested DNA was then subjected to native agarose gel electrophoresis, transferred to Hybond XL membranes (GE Healthcare), and subsequently hybridized with two radiolabeled DNA probes, 0.7 kb and 3.0 kb away from the HO cut site respectively. Dnl4 probe was used to indicate loading. The proportion of unresected DNA at each time point was calculated as the ratio of the signal intensity at that time point to that at 30 min after HO induction and then normalized to the Dnl4 signal. The values at 30 min were set to 100%.

Immunoblotting analysis and antibodies.

Protein samples were resolved on 3-8% or 4-20% gradient gels (Life Technologies and Bio-Rad) and transferred to 0.2- μ m nitrocellulose membrane (G5678144, GE). Antibodies used were anti-Rfa1 and anti-Rfa2 (gifts from S. Brill), and anti-Rad53 (sc-6749, Santa Cruz). For quantification purposes, membranes were scanned with a Fujifilm LAS-3000 luminescent image analyzer, which has a linear dynamic range of 10^4 . Quantification of blots and generation of figures was performed with ImageGauge and Photoshop.

Table 3: Strains and plasmids used in this study

All strains are isogenic to W1588-4C (a RAD5 derivative of W303: MATa ade2-1 can1-100 his3-11,15 leu2-3,112 trp1-1 ura3-1). One strain is listed for each genotype, and two were used in experiments.

| Strain | Genotype |
|-----------|---|
| X3579-11d | MAT a HF-Smt3::LEU2 |
| T193-7c | MAT a siz2Δ::KAN |
| G13 | MAT a mec1Δ::TRP1 sml1Δ::HIS3 |
| X4767-5c | MAT a rfa2-K199R |
| T1387-t19 | mec1Δ::TRP1 sml1Δ::HIS3 rfa1Δ::TRP1 pRS416-Rfa1 |
| T1965 | mec1Δ::TRP1 sml1Δ::HIS3 rfa1Δ::TRP1 pRS416-rfa1-K427R |
| T1964 | mec1Δ::TRP1 sml1Δ::HIS3 rfa1Δ::TRP1 pRS416-rfa1-K170R |
| T1389-t12 | mec1Δ::TRP1 sml1Δ::HIS3 rfa1Δ::TRP1 pRS416-rfa1-K170,427R |
| T1390-4c | mec1Δ::TRP1 sml1Δ::HIS3 rfa1Δ::TRP1 pRS416-rfa1-K133,170,427R |
| T1966 | mec1Δ::TRP1 sml1Δ::HIS3 rfa1Δ::TRP1 pRS416-rfa1-K170,427,494R |
| T1391-10c | mec1Δ::TRP1 sml1Δ::HIS3 rfa1Δ::TRP1 pRS416-rfa1-K170,180,411,427R |
| T1393-19a | mec1Δ::TRP1 sml1Δ::HIS3 rfa1Δ::TRP1 pRS416-rfa1-K170,180,411,427R |
| X5029-16d | MATa srs2Δ::HIS3 |
| X5828-3c | MATa srs2Δ::HIS3 rfa1-K170,180,411,427R |
| X5031-8b | sae2Δ::KAN |
| X5031-8c | sae2Δ::KAN rfa1-K170,180,411,427R |
| X5027-4a | MATalpha srs2Δ::HIS3 rfa1-494R |
| X5029-17c | MATa srs2Δ::HIS3 rfa1-K170,180,411,427,494R |
| X5032-3c | sae2Δ::KAN rfa1-K170,180,411,427,494R |
| Z417-17 | rfa1-K170,180,411,427R |
| Z418-15 | rfa1-K170,180,411,427,494R |
| Z419-1a | rfa1-494R |
| X5148-11d | mec1Δ::TRP1 sml1Δ::HIS3 srs2Δ::HIS |
| X5148-10d | mec1Δ::TRP1 sml1Δ::HIS3 srs2Δ::HIS rfa1-K170,180,411,427,494R |
| X5022-4c | mec1Δ::TRP1 sml1Δ::HIS3 rfa1-K170,180,411,427R |
| X5023-9b | mec1Δ::TRP1 sml1Δ::HIS3 rfa1-K170,180,411,427,494R |
| X5446-5a | srs2Δ::HIS3 rfa2-K199R |
| X5447-3a | srs2Δ::HIS3 rfa2-K199R rfa1-K170,180,411,427R |
| X5446-18a | srs2Δ::HIS3 rfa2-K199R rfa1-K170,180,411,427,494R |
| X6075-7a | rfa2-K199R rfa1-K170,180,411,427R |
| X5016-2c | rfa2-K199R rfa1-K170,180,411,427,494R |
| X5014-9d | rfa2-K199R rfa1-K494R |
| X5448-3c | srs2Δ::HIS3 rad52-K43,44,253R |
| X5448-10d | srs2Δ::HIS3 rad59-K207,228R |
| X5448-5c | MATalpha srs2Δ::HIS3 rad52-K43,44,253R rad59-K207,228R |
| X5555-29b | MATa Ade3::Gal-HO hmlΔ hmrΔ |

| | |
|----------------|--|
| X6245-B-17b | MATa Ade3::Gal-HO hmlΔ hmrΔ rfa1-K170,180,411,427,494R |
| X5025-6a | tdp1Δ::KAN rad1Δ::LEU2 |
| X5025-2b | tdp1Δ::KAN rad1Δ::LEU2 rfa1-K170,180,411,427R |
| X5025-4d | tdp1Δ::KAN rad1Δ::LEU2 rfa1-K170,180,411,427,494R |
| | |
| <i>Plasmid</i> | <i>Genotype</i> |
| pXZ578 | pRS416-Rfa1 |
| pXZ580 | pRS416-rfa1-K170R |
| pXZ581 | pRS416-rfa1-K427R |
| pXZ583 | pRS416-rfa1-K170,427R |
| pXZ594 | pRS416-rfa1-K133,170,427R |
| pXZ584 | pRS416-rfa1-K170,427,494R |
| pXZ623 | pRS416-rfa1-K170,180,411,427R |

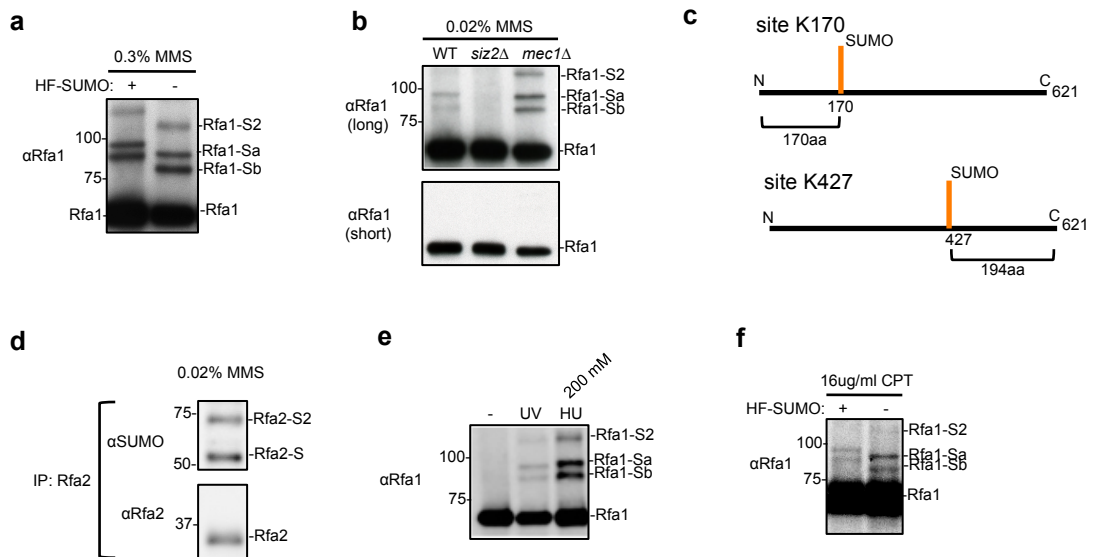


Figure 4-1. Characterization of the sumoylation status of Rfa1 and Rfa2.

- Immunoblots showing Rfa1 sumoylation in 0.3% MMS. HF-SUMO, His6-Flag-tagged SUMO. Rfa1-Sa, -Sb, mono sumoylated Rfa1 species. Rfa1-S2, di-sumoylated Rfa1 species. Molecular weight is shown at the left side of the blot.
- Rfa1 sumoylation is reduced in SUMO E3 *siz2Δ* mutant and increased in *mec1Δ* mutant in 0.02% MMS. Both long and short exposures of the same blot are shown.
- Mono-sumoylation at different lysine sites may generate asymmetrical branched molecules.
- Immunoblots showing Rfa2 sumoylation in 0.02% MMS treatment. Rfa2-S: mono-sumoylated Rfa2; Rfa2-S2: di-sumoylated Rfa2.
- e-f. Rfa1 sumoylation is observed under various condition, including UV, HU, and CPT.

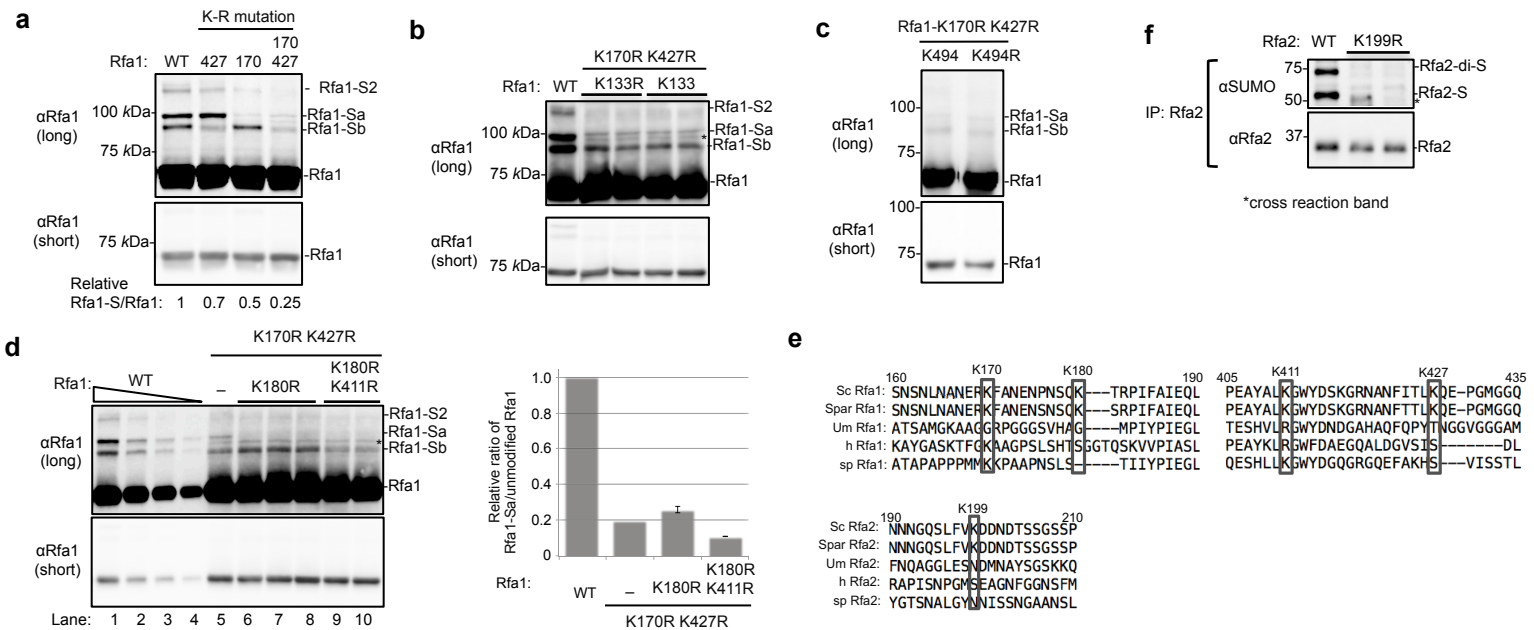


Figure 4-2. Determination of the sumoylation sites on Rfa1

- Mutating K170 and K427 reduces Rfa1 sumoylation. K170R and K427R decrease the level of different Rfa1-sumoylation bands. The K170,427R double mutation reduces Rfa1 sumoylation by 75%. Relative sumoylated Rfa1 versus unmodified Rfa1 was quantified by dividing the total signal of sumoylated Rfa1 by the signal of unmodified Rfa1 from the short exposure, this value was normalized to the value of the first lane.
- K133R does not reduce Rfa1 sumoylation when K170 and K427 are mutated. * indicates an additional Rfa1 sumoylation band detected when K170 and K427 are mutated.
- K494R does not reduce Rfa1 sumoylation when K170 and K427 are mutated.
- K180R and K411R reduce the Rfa1-Sa and -Sb bands, respectively. Mutating all four lysines reduced Rfa1 sumoylation by 90%. The relative ratio of sumoylated Rfa1 versus unmodified Rfa1 was quantified and plotted on the right.
- All five sumoylation sites of Rfa1 and Rfa2 are conserved in closed related yeast species, but not in human or *S. pombe*.
- rfa2-K199R* reduces Rfa2 sumoylation.

Note: all experiments were done in *mec1Δ sml1Δ* cells +0.02% MMS, except in (f), WT cells were used and under 0.02% MMS treatment.

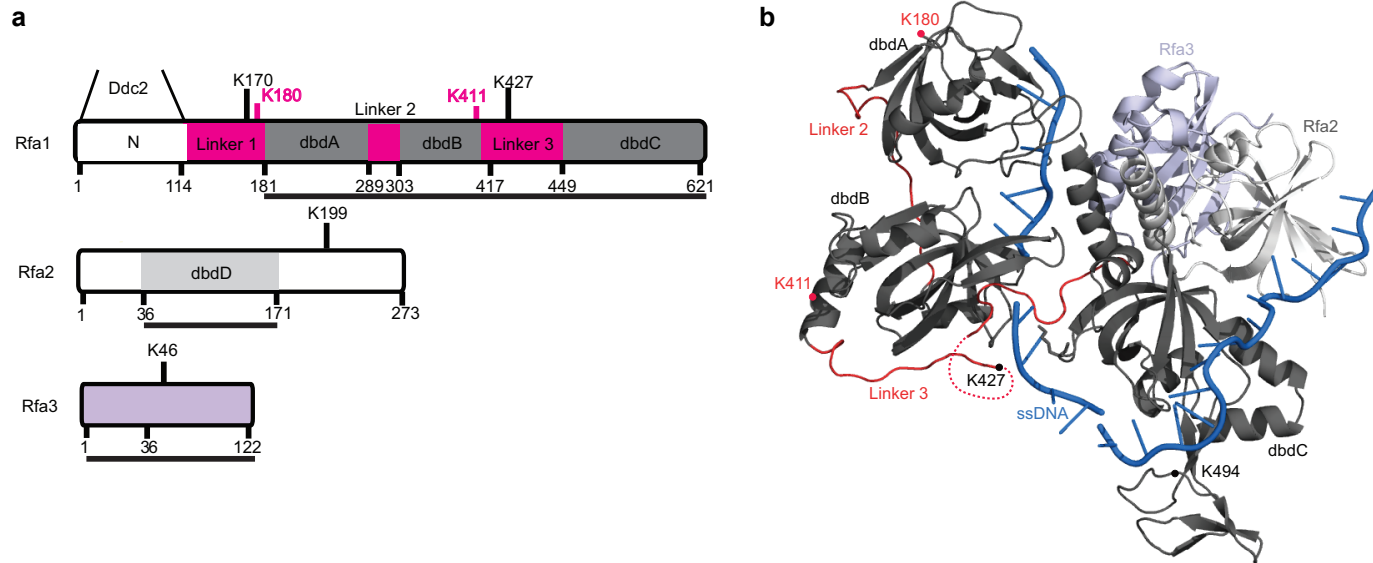


Figure 4-3. The domain composition and structure of the RPA complex

- Schematics of budding yeast RPA protein domains, based on the crystal structure of RPA of another yeast species *Ustilago maydis* in (b). Rfa1 contains three DNA binding domains (dbdA-C, dark grey), a N-terminal protein interaction domain binds to yeast ATRIP homolog Ddc2 (white), and three linker regions (red). Rfa2 contains one DNA binding domains (dbdD, light grey), and Rfa3 is in light purple. Horizontal black lines indicate the corresponding parts of *Ustilago maydis* RPA proteins used for crystallography studies in (b). four lysine residues K170, K427, K199 and K46 indicated reported RPA sumoylation sites. K180 and K411 highlighted indicate two additional sumoylation sites.
- Crystal structure of *Ustilago maydis* RPA in complex with ssDNA. The colors of domains correspond to those in (a) ssDNA is blue. Location of sumoylation sites are indicated. The K170 residue of Rfa1 and the K199 residue of Rfa2 are not included in the structure. The K46 residue of Rfa3 is not visible from this angle.

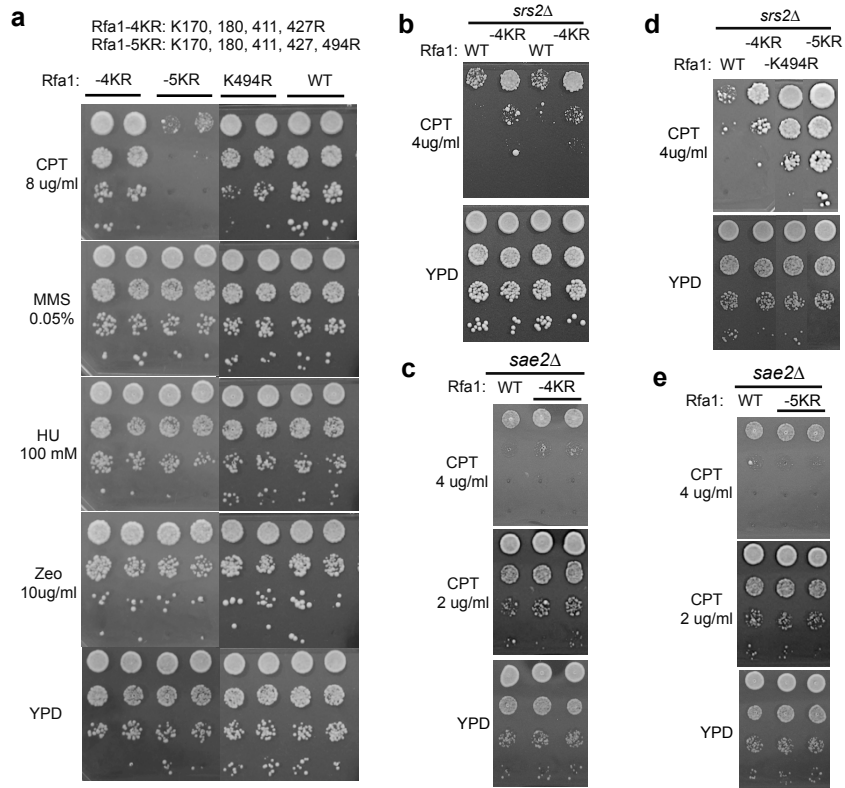
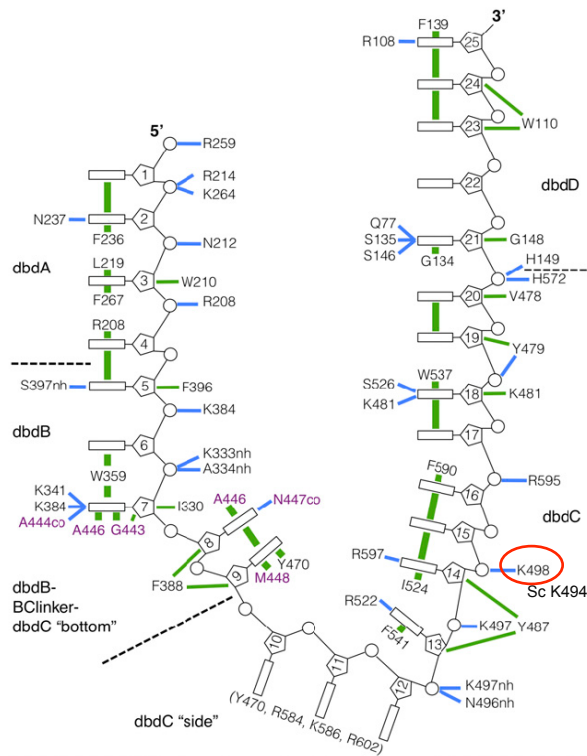


Figure 4-4. Rfa1 sumoylation deficient mutant is defective in Mec1 mediated checkpoint activation.

- a. Rfa1 sumoylation deficient mutant *rfa1-4KR* supports WT growth and is resistant to genotoxins. Combination of *rfa1-4KR* and *rfa1-K494R* (*rfa1-5KR*) leads to specific CPT sensitivity. Note *rfa1-K494R* is only mildly sensitive to 8 ug/ml CPT and *rfa1-4KR* is not sensitive to CPT.
- b-c. *rfa1-4KR* suppresses the CPT sensitivity of *srs2Δ* but not *sae2Δ*.
- d. *rfa1-K494R* suppresses the CPT sensitivity of *srs2Δ*.
- e. *rfa1-5KR* does not suppress the CPT sensitivity of *sae2Δ*.



Source: Fan and Pavletich, 2012*

Figure 4-5. Rfa1 K494 contacts DNA.

Schematic representation of *Ustilago maydis* RPA interaction with ssDNA. Blue lines indicate hydrogen bond and electrostatic interactions between RPA side chains and ssDNA phosphate (circles) and bases (rectangles). Green lines indicate van der Waals contacts to base or ribose groups as well as stacking between adjacent bases (green lines connecting rectangles). The boundaries of the four dbds are indicated by dashed lines. K494 in budding yeast corresponds to *Ustilago maydis* Rfa1 K498 and is highlighted in red circle.

*Reprinted from Fan, J. & Pavletich, N.P. (2012) Structure and conformational change of a replication protein A heterotrimer bound to ssDNA. *Genes Dev* **26**, 2337-2347

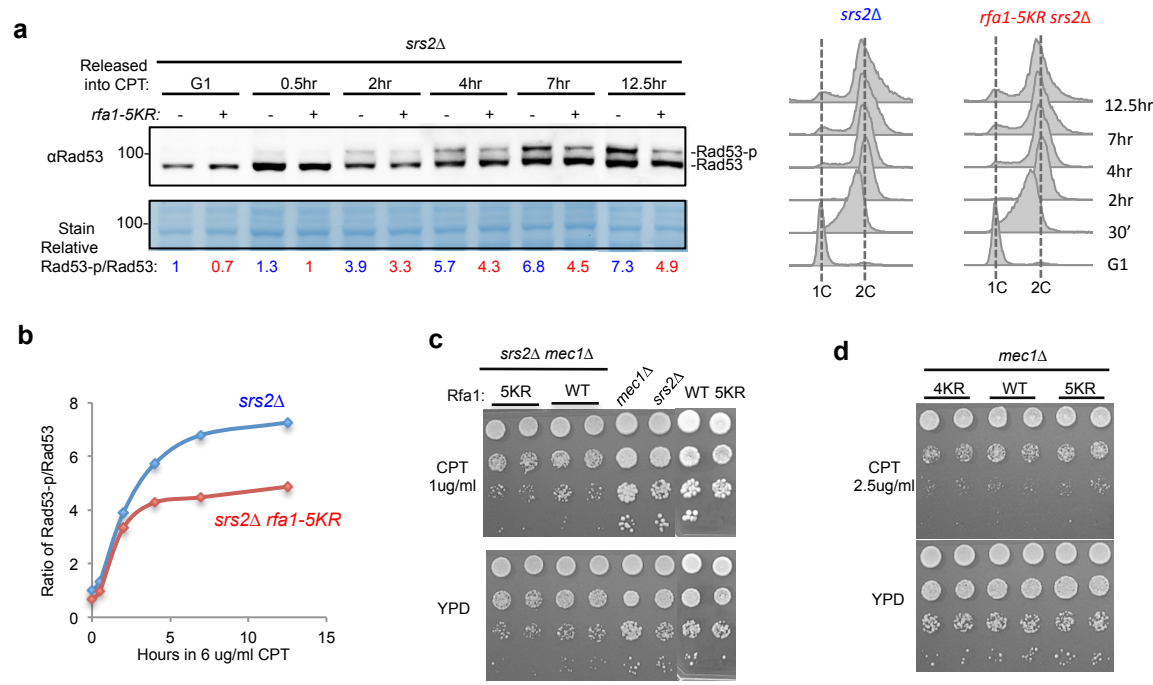


Figure 4-6. *rfa1-5KR* has decreased phosphorylation of Rad53 under CPT treatment conditions.

- a. *rfa1-5KR* has reduced Rad53 phosphorylation in *srs2Δ* cells upon CPT treatment. Cells were first arrested in G1 by alpha factor, then released into S phase in media containing 6 ug/ml CPT. Cells were harvested at indicated time points and both phosphorylated and unmodified Rad53 were detected by western blotting using Rad53 specific antibody. Ratio of Rad53 phosphorylation signals to those of unmodified Rad53 was quantified, with the value of the first lane set to 1. Stain was shown to indicate equal loading. Flow cytometry profiles shows cell cycle progression (right). 1C and 2C indicate the genome size.
- b. Ratio of Rad53 phosphorylation signals to those of unmodified Rad53 from (a) was plotted.
- c. *rfa1-5KR* did not suppress *srs2Δ* CPT sensitivity in the absence of Mec1. 10-fold serial dilutions of cells of indicated genotypes were spotted onto plates. Note that 1 ug/ml CPT was used due to the extreme sensitivity of *srs1Δ mec1Δ* cell to higher concentrations of CPT.
- d. *rfa1-4KR* and *-5KR* do no increase *mec1Δ* sensitivity to CPT. Note that 2.5 ug/ml CPT was used due to the sensitivity of *mec1Δ* cells to higher concentrations of CPT.

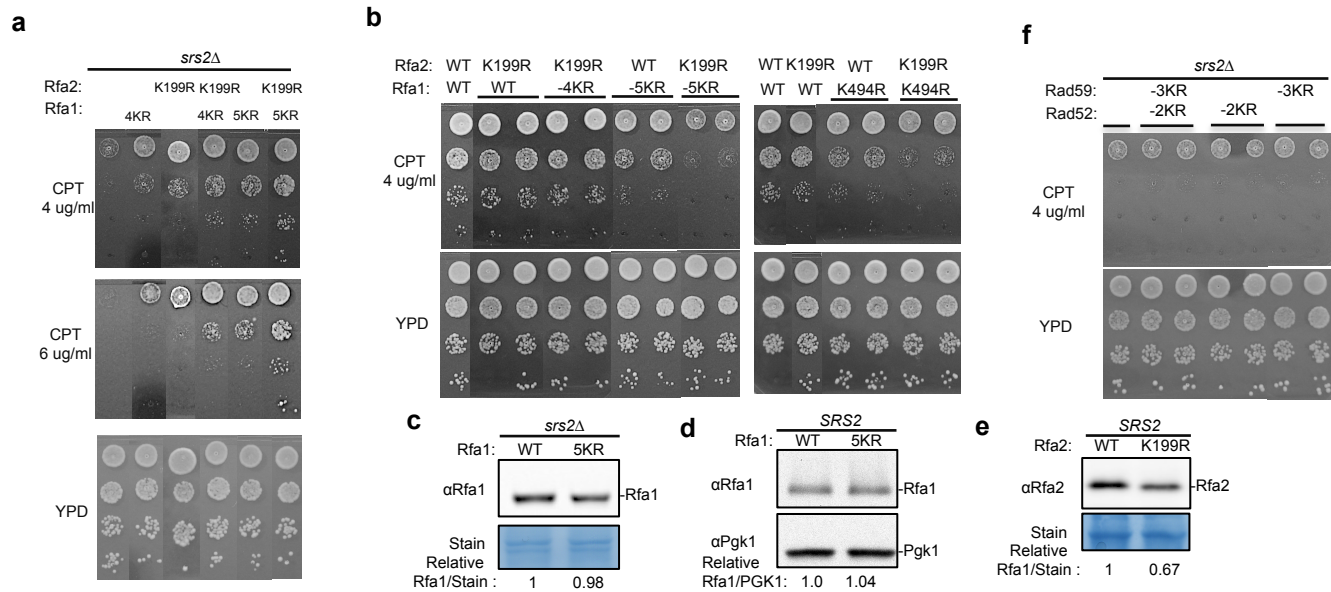


Figure 4-7. Rfa2 sumoylation mutant phenocopies Rfa1 sumoylation deficient mutant.

- a. *rfa2-K199R* suppresses the CPT sensitivity of *srs2Δ* and confers additional suppression when combined with *rfa1-4KR* or *rfa1-5KR*.
- b. *rfa2-K199R* is not CPT sensitive, but becomes hyper-sensitive to CPT when combined with *rfa1 K494R* or *rfa1-5KR*.
- c-d. Protein levels of *rfa1-5KR* were detected by western blotting.
- e. Protein levels of *rfa2-K199R* were detected by western blotting.
- f. Rad52 and Rad59 sumoylation deficient mutants do not suppress the CPT sensitivity of *srs2Δ*.

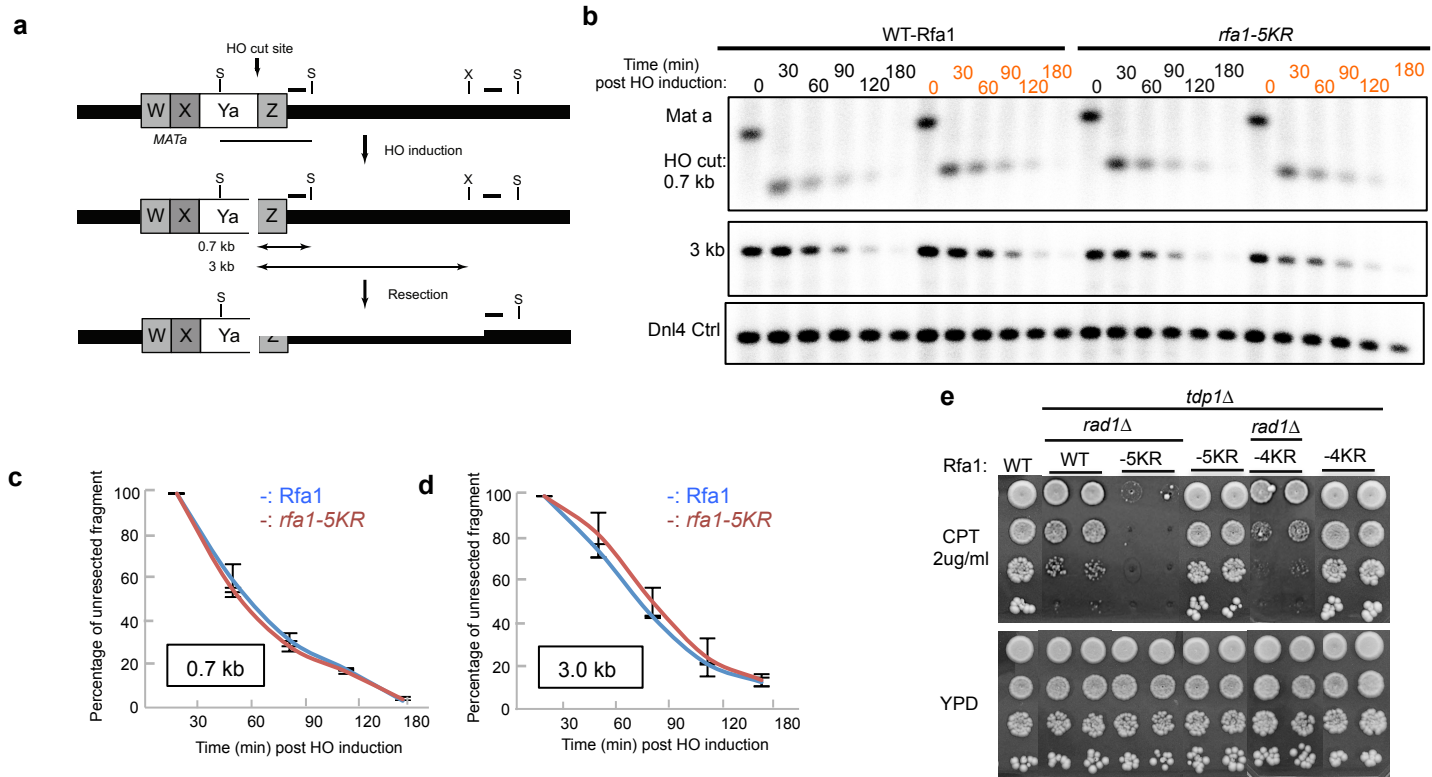


Figure 4-8. *rfa1-5KR* mutant shows proficient DSB resection, and exacerbates the CPT sensitivity of mutants specifically defective in CPT repair pathway.

- a. Schema of the *Mat a* locus on chromosome III and the assay to examine resection of an HO-induced single DSB. 5'-3' resection of DNA eliminates the *Styl* (S) and *XbaI* (X) restriction sites and results in the disappearance of the *Styl*/*XbaI* digestion fragments. Horizontal lines indicate the probes used for Southern blotting to detect the fragments 0.7 kb and 3 kb away from the HO cut site, respectively.
- b-d. Southern blot (b) and quantification (c-d) showing the kinetics of the disappearance of 2 fragments 0.7kb (top panel) and 3kb (middle panel) away from the HO cut. *Dnl4* signal (bottom panel) indicates equal loading. Two independent isolates are shown for each genotype. Quantification shows the ratios of 0.7kb (left) and 3kb (right) fragment signals to the *Dnl4* signal, with the ratio at 30 min set to 100%.
- e. *rfa1-4KR* and *-5KR* sensitize the CPT sensitivity of *rad1Δ tdp1Δ*, which is defective in removal of Top1 from DNA.

Chapter 5

Conclusions and Perspectives

Summary and conclusions

Genome stability relies on proper DNA replication initiation and capacity for response to DNA damage. My thesis addresses how these processes are regulated at molecular levels by studying three proteins, the replicative DNA helicase MCM, DNA polymerase epsilon, and ssDNA binding protein RPA. My work suggests that the sumoylation of MCM negatively regulates replication initiation by recruiting a phosphatase that reverses Mcm4 phosphorylation, which is required for MCM activation. These findings provide a mechanism that potentially prevents premature origin firing and/or re-replication. My work also shows that the NUD in Pol2 is essential for replication initiation by promoting the formation of the pre-loading complex. In addition, Pol2 was sumoylated at a single lysine on the NUD to promote replisome assembly. Finally, my study on RPA revealed a crosstalk between two branches of the DNA damage response by showing that RPA sumoylation promotes optimal DNA damage checkpoint activation. This chapter discusses the implications of these findings and addresses the remaining outstanding questions.

Emerging roles for SUMO-based regulation of DNA replication

Inhibitory effects of sumoylation on replication initiation

Several reports suggest that my findings of a negative effect of sumoylation on origin firing in budding yeast is likely conserved across species. In *Xenopus* egg extracts, it has been noted that reducing sumoylation by either expression of a dominant negative SUMO E2, or addition of SUMO specific proteases, leads to increased origin firing as

measured by a DNA fiber assay (Bonne-Andrea et al. 2013). While this observation indicates that sumoylation inhibits origin firing in *Xenopus*, the underlying mechanism remains unclear. Because MCM is sumoylated in both *Xenopus* and human cells (Golebiowski et al. 2009; Hendriks et al. 2014; Ma et al. 2014; Tammsalu et al. 2014), it is possible that MCM sumoylation in these organisms also inhibits replication initiation. Support for this notion comes from a report showing that the pattern of human MCM4 sumoylation during the cell cycle is similar to that of yeast Mcm2-6 subunits (Schimmel et al. 2014). Specifically, human MCM4 sumoylation levels peak in G1 phase, decline in S phase, and increase again during G2/M phase (Schimmel et al. 2014). Considering that PP1 and DDK-mediated MCM regulation is conserved from yeast to humans (Wotton and Shore 1997; Lee et al. 2003a; Cho et al. 2006; Masai et al. 2006; Montagnoli et al. 2006; Tsuji et al. 2006; Cornacchia et al. 2012; Hayano et al. 2012; Yamazaki et al. 2012), it is possible that MCM sumoylation can also influence these pathways, leading to inhibition of replication initiation. Direct interrogation of these pathways will clarify the role of MCM sumoylation in higher eukaryotes. Another important question to be addressed is whether MCM sumoylation provides mechanisms to enforce proper replication timing and thus prevent premature origin firing or re-replication. Such a role would predict that deregulation of MCM sumoylation can lead to increased genetic alterations promoting tumorigenesis. A finding in line with this idea is that overexpression of the SUMO specific protease SENP1 is associated with progression of human prostate and thyroid cancers (Jacques et al. 2005; Cheng et al. 2006b). Delineation of the underlying mechanisms of this association will shed light on whether deregulation of MCM sumoylation is directly linked to cancer progression.

A positive role for sumoylation on replication initiation

While MCM sumoylation negatively affects replication initiation, my data on Pol2 sumoylation suggest that this modification has a stimulatory role in replication initiation by promoting replisome assembly. The opposing effects of sumoylation on replication initiation through different substrates may appear to be contradictory at first glance, but in fact they serve the same purpose in ensuring accurate replication initiation. MCM sumoylation occurs during origin licensing (G1 phase), preceding Pol2 sumoylation, which takes place in S phase. MCM sumoylation acts to prevent premature origin firing in G1, while Pol2 sumoylation helps to recruit Pol2 and other components of the pre-LC to the loaded MCM. Thus, by affecting different steps of replication, these two sequential sumoylation events can better ensure accurate and efficient replication initiation. It remains unknown how Pol2 sumoylation promotes replisome assembly, we speculate that this role entails regulating the NUD functions. We also note that since MCM and Pol2 sumoylation can be up-regulated during replication stress, their sumoylation may affect replication beyond replication initiation. Several other proteins involved in replication initiation and progression are also SUMO substrates, including the ORC complex and CDK (Golebiowski et al. 2009; Elrouby and Coupland 2010; Cremona et al. 2012; Bonne-Andrea et al. 2013; Hendriks et al. 2014; Ma et al. 2014; Tammsalu et al. 2014), thus much remains to be understood about the additional roles of sumoylation in replication.

SUMO and replication progression

Several studies have suggested a role for sumoylation during replication progression, particularly under replication stress situations. In budding yeast, reduction of sumoylation, by SUMO E3 ligase deficiency, impairs replication when cells are treated

with the DNA alkylating agent MMS (Cremona et al. 2012). A recent study further showed under MMS conditions that the SUMO E3 ligase, Mms21, of the conserved Smc5/6 complex may collaborate with the scaffold protein Rtt107 to promote sumoylation of Mcm6 and Pol2 (Hang et al. 2015). Based on the physical interaction of Rtt107 with both the Smc5/6 complex and the SUMO substrates, Mcm6 and Pol2 (Hang et al. 2015), it is possible that Rtt107 serves as a bridging factor in sumoylation. It has been shown that deficiency in Rtt107 or Smc5/6 impairs replication progression, especially at regions containing large replicons, and does not affect origin firing (Hang et al. 2015). It is likely that Rtt107 and Smc5/6 promote replication progression by modulating the sumoylation of replisome components, particularly Pol2 and Mcm6. While my data suggest that Pol2 and MCM sumoylation affects origin firing under unperturbed replication conditions, further studies are needed to understand whether their sumoylation occurs at the same sites under DNA damaging conditions. In addition, it will be important to determine how these sumoylation events exert different effects during replication initiation and progression.

Understanding of how sumoylation affects replication progression in higher eukaryotes will benefit from the iPOND technique (isolation of protein on nascent DNA chains). In human cells, when proteins recovered from iPOND were subjected to mass spectrometry, it was found that SUMO was enriched within nascent chromatin containing replisomes, while ubiquitin molecules were enriched in mature chromatin (Lopez-Contreras et al. 2013). A follow-up study showed that the SUMO deubiquitinase, USP7, contributes to the establishment of this SUMO-high and ubiquitin-low nascent chromatin environment (Lecona et al. 2016). USP7 can deubiquitinate SUMO2 *in vitro* and *in vivo*, and is associated with nascent chromatin and MCM4 (Lecona et al. 2016). These findings support a model that USP7 removes ubiquitin from SUMO2 molecules that are

conjugated to replisome components in the nascent chromatin. Consistent with this model, USP7 impairment leads to redistribution of sumoylated proteins from nascent to mature chromatin, correlates with reduction of fork speed and origin firing, and increases DNA damage checkpoint activation (Lecona et al. 2016). Taken together, these findings support the notion that enrichment of SUMO and reduction of ubiquitin at, or near, replisomes can be advantageous for replication progression. Further investigation is needed to provide mechanistic insights into the relevant SUMO substrates and their biological effects. Previous studies and our work here have suggested several relevant candidate substrates for SUMO-based regulation, such as Pol2, MCM, human polymerase delta subunit POL3, and PCNA, the processivity factor for polymerase delta (Hoegge et al. 2002; Papouli et al. 2005; Golebiowski et al. 2009; Cremona et al. 2012).

Low levels of sumoylation can lead to robust biological effects

A common theme of protein sumoylation is that only a small population of substrates are sumoylated at a given time (Geiss-Friedlander and Melchior 2007b; Sarangi and Zhao 2015). This is the case for both MCM and Pol2. We estimate that few MCM that are loaded on origins are sumoylated. While this might be a slight under-estimation considering that desumoylation is difficult to prevent during protein preparation, it remains important to address how a small population of sumoylated protein generates significant biological effects. In general, three models can be considered. As has been suggested before, the sumoylation and desumoylation cycle is highly dynamic (Li and Hochstrasser 1999; Hay 2005; Geiss-Friedlander and Melchior 2007b). As such, many more molecules of substrates undergo sumoylation than are measured by static sumoylation levels. It is possible that once a protein is modified by SUMO, it can generate a biological consequence that cannot be reversed even when the sumo is later

removed from the protein. This idea was suggested in the field and described in detail by Ronald Hay over 10 years ago (Hay 2005). Several findings have provided support for this model. For example, the DNA repair nuclease Rad1 is sumoylated only during or after its action at DNA lesions and this modification results in its dissociation from DNA, which helps the subsequent repair step to take place (Sarangi et al. 2014b; Sarangi and Zhao 2015). As Rad1 is desumoylated once it disassociates from DNA, static levels of Rad1 sumoylation are quite low (Sarangi et al. 2014b). In this case, sumoylated protein achieves a biological effect without accumulating high level of the modified form (Sarangi et al. 2014b).

A second model to explain the biological effects associated with low level sumoylation is related to the recruitment of enzymes. It is known that a common effect of sumoylation is to recruit proteins through SUMO-SIM interaction (Geiss-Friedlander and Melchior 2007b; Gareau and Lima 2010). When the recruited proteins are enzymes, even a small amount could catalyze multiple reactions. Consequently, a small percentage of modification can lead to a significant biological effect. In the case of MCM, sumoylation promotes the recruitment of the enzyme PP1. As replication origins can exist in clusters, increased PP1 levels at a few origins can influence more origins within the cluster. Another example wherein SUMO facilitates enzyme recruitment to achieve biological effect is the sumoylation of PCNA (Papouli et al. 2005; Armstrong et al. 2012). In this case, PCNA sumoylation recruits an anti-recombinase Srs2, the helicase activity of which is responsible for removing Rad51 filament from DNA (Krejci et al. 2003; Veaute et al. 2003; Dupaigne et al. 2008), thus preventing potentially harmful HR. In addition, many sumoylated substrates recruit the SUMO targeted ubiquitin E3 ligase (STUBL), RNF4, which promotes proteasome mediated degradation of the sumoylated substrate. One example is the misfolded mutant Ataxin-1, which forms pathogenic

aggregation and leads to a fetal neurological disorder spinocerebellar ataxia type 1 (SCA1) (Guo et al. 2014). Aggregated mutant Ataxin-1 is sumoylated by the PML SUMO E3 ligase, subsequently polyubiquitinated by RNF4 and degraded by the proteasome (Guo et al. 2014).

A third means by which low level sumoylation can generate biological effects is through simultaneous targeting of multiple components in a pathway, thus influencing a process in a collaborative manner. For example, loss of sumoylation of RPA, Rad52 and Rad59 individually has subtle effect on HR, however, loss of sumoylation of these substrates altogether generates a stronger defect in HR (Psakhye and Jentsch 2012). Similarly, simultaneous lack of sumoylation of DNA resection factors Sae2 and the MRX complex exhibits stronger resection defects than the removal of either alone (Sarangi et al. 2015).

Crosstalk between sumoylation and other types of PTMs

It remains to be seen how SUMO-based regulation are integrated with other types of protein modifications. Several studies have shown that multiple PTMs can influence each other in different ways. In the case of sumoylation and phosphorylation, both antagonistic and collaborative relationships have been identified (Geiss-Friedlander and Melchior 2007b; Gareau and Lima 2010).

In the case of MCM, its sumoylation inhibits Mcm4 phosphorylation, while Mcm4 hyperphosphorylation correlates with diminished MCM sumoylation. Thus, these two PTMs appear to disfavor each other. While my work provides a plausible scenario for how sumoylation reduces Mcm4 phosphorylation through PP1 recruitment, we have yet to investigate whether MCM phosphorylation or DDK can directly affect MCM

sumoylation. Among several scenarios, one interesting possibility is that DDK phosphorylates MCM and recruits the SUMO protease Ulp2, which we have shown can reverse MCM sumoylation. It is possible that after MCM loading but before CMG formation, MCM sumoylation is favored over MCM phosphorylation because of low DDK levels, and sumoylation further elicits a negative regulation on DDK-mediated MCM phosphorylation. Thus, as a consequence, origin firing is prevented during G1. As cells enter S phase, increased DDK levels override PP1 function and may lead to MCM desumoylation. Consequently, the combined effects of these events favor origin firing.

Phosphorylation of a protein has also been found to be stimulatory with regard to its sumoylation. FEN1 is a flap endonuclease that promotes the maturation of the okazaki fragments where phosphorylation at site S187 on FEN1 during S phase is required for its sumoylation (Guo et al. 2012). Indeed, the non-phosphorylatable FEN1 (S187A) abolishes FEN1 sumoylation (Guo et al. 2012). In this case, the cascade of PTMs does not stop here, as sumoylated FEN1 triggers its ubiquitination and proteasome mediated degradation, presumably by recruiting a SIM-containing ubiquitin E3 ligase PRP19 (Guo et al. 2012). The timely degradation of FEN1 mediated by this PTM cascade is critical to maintain genome stability, as its deregulation leads to cell cycle delay and polyploidy (Guo et al. 2012).

My study of RPA sumoylation suggests that this modification can stimulate the Mec1 checkpoint pathway favoring phosphorylation of many Mec1 substrates. Activation of the Mec1 DNA damage checkpoint and DDIS are two generally independent processes that promote cell survival upon DNA damage (Cremona et al. 2012). However, reducing sumoylation can delay the Mec1 checkpoint activation, suggesting that sumoylation can increase the robustness of the Mec1 checkpoint

activation (Cremona et al. 2012). Our findings indicate that RPA sumoylation likely promotes activation of the Mec1 checkpoint by increasing RPA association with either Mec1 or its activating factor Dna2 via SUMO-SIM binding. While this hypothesis remains to be tested, a similar finding comes from a recent study in human cells. It was found that the sumoylation of the Ddc2 homolog, ATRIP, can promote ATR checkpoint activation by targeting ATRIP to DNA damage sites and promoting its interaction with other checkpoint proteins (Wu et al. 2014). In both cases, sumoylation of either RPA (yeast) or ATRIP (human) provides a means for sumoylation to positively influence phosphorylation of substrates by checkpoint kinase.

The function of Pol2 in replication initiation

My thesis also provides insights into the function of Pol2 NUD. Our data suggest that the NUD is essential and contributes to the pre-LC formation, likely via binding with Dpb11. Considering Pol2-C terminus was previously shown to have similar function by mediating Dpb2 interaction (Johansson et al. 2011; Sengupta et al. 2013), we propose that Pol2 N- and C-termini contribute to the pre-LC formation by promoting binding to Dpb11 and Dpb2, respectively.

Our finding that the NUD is essential was initially surprising, as deleting the Pol2 N-terminus (*pol2-ΔN*) only leads to slow cell growth, not lethality (Dua et al. 1999; Kesti et al. 1999). Thus we are left to wonder why mutation of the NUD is lethal yet a *pol2-ΔN* is not? One possibility is that the N-terminal half of Pol2 is inhibitory for the pre-LC formation. In this scenario, NUD interaction with Dpb11 would be required to alleviate this inhibition to promote the pre-LC formation. Deletion of the entire N-terminal half would bypass the role of NUD, rendering the *pol2-ΔN* cells viable. Future experiments,

such as examination of the pre-LC formation using purified recombinant proteins, including different fragments of Pol2, will clarify if this hypothesis is correct.

Conclusions and future perspectives

My thesis has provided several novel insights into the mechanisms underlying replication initiation and the DNA damage response. First, my findings showed that sumoylation affects different steps of DNA replication to ensure timing and efficiency of origin firing. Sumoylation of MCM inhibited origin firing by counteracting DDK mediated phosphorylation of MCM, while sumoylation of Pol2 occurs in a stage after MCM sumoylation and promotes replisome assembly. In addition, I uncovered the role of the NUD of Pol2 in the pre-LC formation, a key step in replication initiation. These findings add to our understanding of the intricate molecular mechanisms regulating origin firing. Lastly, the identification of RPA sumoylation provided the missing link between sumoylation and Mec1-mediated checkpoint activation.

While these and other studies provide insight into several long-standing questions, our journey to understand the roles of SUMO in replication, and how it integrates with other PTMs, in both replication and DNA repair is still at its beginning. Many outstanding questions remain in efforts to uncover the underlying molecular mechanisms regulating DNA replication and repair. Here are a few of these questions and ideas extended from my thesis.

Is the function of MCM sumoylation conserved in higher eukaryotic cells? The sumoylation of MCM is conserved from yeast to human (Golebiowski et al. 2009; Elrouby and Coupland 2010; Cremona et al. 2012; Ma et al. 2014), and the pattern of MCM sumoylation is conserved in human (Schimmel et al. 2014). While this similarity

suggests a conserved function for MCM sumoylation, we are still a few steps away to extend our findings to humans. In addition, my findings indicate that MCM sumoylation has roles other than counteracting DDK mediated MCM phosphorylation. Since all MCM subunits are sumoylated, it is possible that their sumoylation has distinct roles. Mapping the sumoylation sites on all MCM subunits will be required to further delineate the function of sumoylation of individual MCM subunits.

Moving forward, it will be interesting to determine the biological consequences of deregulated MCM sumoylation. Based on my findings, we favor the idea that deregulation of MCM sumoylation can lead to deregulation of the timing of origin firing and re-replication. As cells employ multiple mechanisms to ensure the timing of origin firing and prevent re-replication, it is possible that MCM sumoylation is redundant with these other mechanisms (Nguyen et al. 2001; Blow and Dutta 2005; Arias and Walter 2007). This hypothesis remains to be tested.

How is sumoylation and desumoylation of MCM regulated? The recruitment of the SUMO enzymes and SUMO specific proteases is likely at the center of the regulation of the MCM sumoylation cycle. It has been shown that DDK specifically targets loaded MCM via direct binding to Mcm2 and Mcm4 subunits (Sheu and Stillman 2006; Bruck and Kaplan 2009; Ramer et al. 2013; Bruck and Kaplan 2014). A similar mechanism may be employed by SUMO enzymes and proteases to target loaded MCM.

One outstanding question regarding Pol2 function is: How are its N- and C-termini coordinated to promote the pre-LC formation. The current paradigm suggests that the two termini of Pol2 act as independent entities, however, my findings indicate that the two termini likely promote the pre-LC formation in a coordinated manner.

Reconstitution of the pre-LC complex using purified proteins will help to elucidate the role of Pol2 in the pre-LC formation.

The molecular mechanism by which sumoylated RPA promotes the Mec1 checkpoint remains to be determined. While we show that RPA sumoylation plays a role in Mec1 checkpoint activation, it will be interesting to see if there are additional interplays between sumoylation and checkpoint activation.

Lastly, two intertwined processes, DNA replication and DNA repair, function in a highly coordinated manner. Indeed, DNA replication process can generate DNA damage and DNA damage can cause replication fork stalling and influence origin firing. Our understanding of how these two processes integrate with each other under different circumstances, for example, normal growth, DNA damaging conditions, and in diseases such as cancer cells, is still very limited. Proteins having dual functions in DNA replication and DNA repair, such as MCM, Pol2 and RPA are expected to be a key in this crosstalk between DNA replication and repair. Further analyses of such proteins will enrich our view of how genome integrity is maintained in eukaryotic cells.

REFERENCES

- Alcasabas AA, Osborn AJ, Bachant J, Hu F, Werler PJ, Bousset K, Furuya K, Diffley JF, Carr AM, Elledge SJ. 2001. Mrc1 transduces signals of DNA replication stress to activate Rad53. *Nat cell Biol* **3**: 958-965.
- Almedawar S, Colomina N, Bermudez-Lopez M, Pocino-Merino I, Torres-Rosell J. 2012. A SUMO-dependent step during establishment of sister chromatid cohesion. *Curr Biol* **22**: 1576-1581.
- Altmannova V, Eckert-Boulet N, Arneric M, Kolesar P, Chaloupkova R, Damborsky J, Sung P, Zhao X, Lisby M, Krejci L. 2010. Rad52 SUMOylation affects the efficiency of the DNA repair. *Nucleic Acids Res* **38**: 4708-4721.
- Arias EE, Walter JC. 2007. Strength in numbers: preventing rereplication via multiple mechanisms in eukaryotic cells. *Genes Dev* **21**: 497-518.
- Armstrong AA, Mohideen F, Lima CD. 2012. Recognition of SUMO-modified PCNA requires tandem receptor motifs in Srs2. *Nature* **483**: 59-63.
- Bae KH, Kim HS, Bae SH, Kang HY, Brill S, Seo YS. 2003. Bimodal interaction between replication-protein A and Dna2 is critical for Dna2 function both in vivo and in vitro. *Nucleic Acids Res* **31**: 3006-3015.
- Bae SH, Bae KH, Kim JA, Seo YS. 2001. RPA governs endonuclease switching during processing of Okazaki fragments in eukaryotes. *Nature* **412**: 456-461.
- Ball HL, Ehrhardt MR, Mordes DA, Glick GG, Chazin WJ, Cortez D. 2007. Function of a conserved checkpoint recruitment domain in ATRIP proteins. *Mol Cell Biol* **27**: 3367-3377.
- Bayer P, Arndt A, Metzger S, Mahajan R, Melchior F, Jaenicke R, Becker J. 1998. Structure determination of the small ubiquitin-related modifier SUMO-1. *J Mol Biol* **280**: 275-286.
- Bazzi M, Mantiero D, Trovesi C, Lucchini G, Longhese MP. 2010. Dephosphorylation of gamma H2A by Glc7/protein phosphatase 1 promotes recovery from inhibition of DNA replication. *Mol Cell Biol* **30**: 131-145.
- Bell SP, Dutta A. 2002. DNA replication in eukaryotic cells. *Annu Rev Biochem* **71**: 333-374.
- Bell SP, Kaguni JM. 2013. Helicase loading at chromosomal origins of replication. *Cold Spring Harb Perspect Biol* **5**: a010124
- Bell SP, Stillman B. 1992. ATP-dependent recognition of eukaryotic origins of DNA replication by a multiprotein complex. *Nature* **357**: 128-134.
- Bergink S, Ammon T, Kern M, Schermelleh L, Leonhardt H, Jentsch S. 2013. Role of Cdc48/p97 as a SUMO-targeted segregase curbing Rad51--Rad52 interaction. *Nat Cell Biol* **15**: 526-532.

- Bloom J, Cross FR. 2007. Novel Role for Cdc14 Sequestration: Cdc14 Dephosphorylates Factors That Promote DNA Replication. *Mol Cell Biol* **27**: 842-853.
- Blow JJ, Dutta A. 2005. Preventing re-replication of chromosomal DNA. *Nat Rev Mol Cell Biol* **6**: 476-486.
- Bochman ML, Bell SP, Schwacha A. 2008. Subunit organization of Mcm2-7 and the unequal role of active sites in ATP hydrolysis and viability. *Mol Cell Biol* **28**: 5865-5873.
- Bonne-Andrea C, Kahli M, Mechali F, Lemaitre J-M, Bossis G, Coux O. 2013. SUMO2/3 modification of cyclin E contributes to the control of replication origin firing. *Nat Commun* **4**: 1850.
- Brill SJ, Bastin-Shanower S. 1998. Identification and characterization of the fourth single-stranded-DNA binding domain of replication protein A. *Mol Cell Biol* **18**: 7225-7234.
- Bruck I, Kaplan D. 2009. Dbf4-Cdc7 phosphorylation of Mcm2 is required for cell growth. *J Biol Chem* **284**: 28823-28831.
- Bruck I, Kaplan DL. 2011. Origin single-stranded DNA releases Sld3 protein from the Mcm2-7 complex, allowing the GINS tetramer to bind the Mcm2-7 complex. *J Biol Chem* **286**: 18602-18613.
- Bruck I, Kaplan DL. 2014. The Dbf4-Cdc7 kinase promotes Mcm2-7 ring opening to allow for single-stranded DNA extrusion and helicase assembly. *J Biol Chem* **290**: 1210-1221.
- Bylebyl GR, Belichenko I, Johnson ES. 2003. The SUMO isopeptidase Ulp2 prevents accumulation of SUMO chains in yeast. *J Biol Chem* **278**: 44113-44120.
- Byun TS, Pacek M, Yee MC, Walter JC, Cimprich KA. 2005. Functional uncoupling of MCM helicase and DNA polymerase activities activates the ATR-dependent checkpoint. *Genes Dev* **19**: 1040-1052.
- Calzada A, Sánchez M, Sánchez E, Bueno A. 2000. The stability of the Cdc6 protein is regulated by cyclin-dependent kinase/cyclin B complexes in *Saccharomyces cerevisiae*. *J Biol Chem* **275**: 9734-9741.
- Cannavo E, Cejka P. 2014. Sae2 promotes dsDNA endonuclease activity within Mre11-Rad50-Xrs2 to resect DNA breaks. *Nature* **514**: 122-125.
- Cejka P, Cannavo E, Polaczek P, Masuda-Sasa T, Pokharel S, Campbell JL, Kowalczykowski SC. 2010. DNA end resection by Dna2-Sgs1-RPA and its stimulation by Top3-Rmi1 and Mre11-Rad50-Xrs2. *Nature* **467**: 112-116.
- Cerami E, Gao J, Dogrusoz U, Gross BE, Sumer SO, Aksoy BA, Jacobsen A, Byrne CJ, Heuer ML, Larsson E et al. 2012. The cBio cancer genomics portal: an open platform for exploring multidimensional cancer genomics data. *Cancer Discov* **2**: 401-404.

- Chapman JW, Johnston LH. 1989. The yeast gene, DBF4, essential for entry into S phase is cell cycle regulated. *Exp Cell Res* **180**: 419-428.
- Chen H, Lisby M, Symington LS. 2013. RPA Coordinates DNA End Resection and Prevents Formation of DNA Hairpins. *Mol Cell* **50**: 589-600.
- Chen S, Bell SP. 2011. CDK prevents Mcm2-7 helicase loading by inhibiting Cdt1 interaction with Orc6. *Genes Dev* **25**: 363-372.
- Chen SH, Zhou H. 2009. Reconstitution of Rad53 activation by Mec1 through adaptor protein Mrc1. *J Biol Chem* **284**: 18593-18604.
- Cheng CH, Lo YH, Liang SS, Ti SC, Lin FM, Yeh CH, Huang HY, Wang TF. 2006a. SUMO modifications control assembly of synaptonemal complex and polycomplex in meiosis of *Saccharomyces cerevisiae*. *Genes Dev* **20**: 2067-2081.
- Cheng J, Bawa T, Lee P, Gong L, Yeh ET. 2006b. Role of desumoylation in the development of prostate cancer. *Neoplasia* **8**: 667-676.
- Cheng LA, Collyer T, Hardy CFJ. 1999. Cell cycle regulation of DNA replication initiator factor Dbf4p. *Mol Cell Biol* **19**: 4270-4278.
- Cho W-H, Lee Y-J, Kong S-I, Hurwitz J, Lee J-K. 2006. CDC7 kinase phosphorylates serine residues adjacent to acidic amino acids in the minichromosome maintenance 2 protein. *Proc Natl Acad Sci USA* **103**: 11521-11526.
- Chung I, Zhao X. 2015. DNA break-induced sumoylation is enabled by collaboration between a SUMO ligase and the ssDNA-binding complex RPA. *Genes Dev* **29**: 1593-1598.
- Clerici M, Mantiero D, Lucchini G, Longhese MP. 2005. The *Saccharomyces cerevisiae* Sae2 protein promotes resection and bridging of double strand break ends. *J Biol Chem* **280**: 38631-38638.
- Clerici M, Mantiero D, Lucchini G, Longhese MP. 2006. The *Saccharomyces cerevisiae* Sae2 protein negatively regulates DNA damage checkpoint signalling. *EMBO Rep* **7**: 212-218.
- Cocker JH, Piatti S, Santocanale C, Nasmyth K, Diffley JF. 1996. An essential role for the Cdc6 protein in forming the pre-replicative complexes of budding yeast. *Nature* **379**: 180-182.
- Cornacchia D, Dileep V, Quivy JP, Foti R, Tili F, Santarella-Mellwig R, Antony C, Almouzni G, Gilbert DM, Buonomo SBC. 2012. Mouse Rif1 is a key regulator of the replication-timing programme in mammalian cells. *EMBO J* **31**: 3678-3690.
- Costa A, Hood IV, Berger JM. 2013. Mechanisms for initiating cellular DNA replication. *Annu Rev Biochem* **82**: 25-54.

- Costa A, Ilves I, Tamberg N, Petojevic T, Nogales E, Botchan MR, Berger JM. 2011. The structural basis for MCM2-7 helicase activation by GINS and Cdc45. *Nat Struct Mol Biol* **18**: 471-477.
- Costa A, Renault L, Swuec P, Petojevic T, Pesavento JJ, Ilves I, MacLellan-Gibson K, Fleck RA, Botchan MR, Berger JM. 2014. DNA binding polarity, dimerization, and ATPase ring remodeling in the CMG helicase of the eukaryotic replisome. *eLife* **3**: e03273.
- Crabbe L, Thomas A, Pantesco V, De Vos J, Pasero P, Lengronne A. 2010. Analysis of replication profiles reveals key role of RFC-Ctf18 in yeast replication stress response. *Nat Struct Mol Biol* **17**: 1391-1397.
- Cremona CA, Sarangi P, Yang Y, Hang LE, Rahman S, Zhao X. 2012. Extensive DNA damage-induced sumoylation contributes to replication and repair and acts in addition to the mec1 checkpoint. *Mol Cell* **45**: 422-432.
- Crevel G, Ivetic A, Ohno K, Yamaguchi M, Cotterill S. 2001. Nearest neighbour analysis of MCM protein complexes in *Drosophila melanogaster*. *Nucleic Acids Res* **29**: 4834-4842.
- Davé A, Cooley C, Garg M, Bianchi A. 2014. Protein phosphatase 1 recruitment by Rif1 regulates DNA replication origin firing by counteracting DDK activity. *Cell Rep* **7**: 53-61.
- Davey MJ, Indiani C, O'Donnell M. 2003. Reconstitution of the Mcm2-7p heterohexamer, subunit arrangement, and ATP site architecture. *J Biol Chem* **278**: 4491-4499.
- Deegan TD, Yeeles JT, Diffley JF. 2016. Phosphopeptide binding by Sld3 links Dbf4-dependent kinase to MCM replicative helicase activation. *EMBO J* e201593552.
- Deem A, Keszthelyi A, Blackgrove T, Vayl A, Coffey B, Mathur R, Chabes A, Malkova A. 2011. Break-induced replication is highly inaccurate. *PLoS biology* **9**: e1000594.
- Deng C, Brown JA, You D, Brown JM. 2005. Multiple endonucleases function to repair covalent topoisomerase I complexes in *Saccharomyces cerevisiae*. *Genetics* **170**: 591-600.
- Deng SK, Gibb B, de Almeida MJ, Greene EC, Symington LS. 2014. RPA antagonizes microhomology-mediated repair of DNA double-strand breaks. *Nat Struct Mol Biol* **21**: 405-412.
- Desdouets C, Santocanale C, Drury LS, Perkins G, Foiani M, Plevani P, Diffley JF. 1998. Evidence for a Cdc6p-independent mitotic resetting event involving DNA polymerase alpha. *Embo J* **17**: 4139-4146.
- Dhingra N, Bruck I, Smith S, Ning B, Kaplan DL. 2015. Dpb11 protein helps control assembly of the Cdc45.Mcm2-7.GINS replication fork helicase. *J Biol Chem* **290**: 7586-7601.
- Diffley JF, Cocker JH. 1992. Protein-DNA interactions at a yeast replication origin. *Nature* **357**: 169-172.

- Diffley JF, Cocker JH, Dowell SJ, Rowley A. 1994. Two steps in the assembly of complexes at yeast replication origins in vivo. *Cell* **78**:303-316.
- Donovan S, Harwood J, Drury LS, Diffley JF. 1997. Cdc6p-dependent loading of Mcm proteins onto pre-replicative chromatin in budding yeast. *Proc Natl Acad Sci USA* **94**: 5611-5616.
- Dou H, Huang C, Singh M, Carpenter PB, Yeh ET. 2010. Regulation of DNA repair through deSUMOylation and SUMOylation of replication protein A complex. *Mol Cell* **39**: 333-345.
- Drury LS, Perkins G, Diffley JF. 1997. The Cdc4/34/53 pathway targets Cdc6p for proteolysis in budding yeast. *EMBO J* **16**: 5966-5976.
- . 2000. The cyclin-dependent kinase Cdc28p regulates distinct modes of Cdc6p proteolysis during the budding yeast cell cycle. *Curr Biol* **10**: 231-240.
- Dua R, Edwards S, Levy DL, Campbell JL. 2000. Subunit interactions within the *Saccharomyces cerevisiae* DNA polymerase epsilon (pol epsilon) complex. Demonstration of a dimeric pol epsilon. *J Biol Chem* **275**: 28816-28825.
- Dua R, Levy DL, Campbell JL. 1999. Analysis of the Essential Functions of the C-terminal Protein/Protein Interaction Domain of *Saccharomyces cerevisiae* pol epsilon and Its Unexpected Ability to Support Growth in the Absence of the DNA Polymerase Domain. *J Biol Chem* **274**: 22283-22288.
- Dupaigne P, Le Breton C, Fabre F, Gangloff S, Le Cam E, Veaute X. 2008. The Srs2 helicase activity is stimulated by Rad51 filaments on dsDNA: implications for crossover incidence during mitotic recombination. *Mol Cell* **29**: 243-254.
- Eladad S, Ye TZ, Hu P, Leversha M, Beresten S, Matunis MJ, Ellis NA. 2005. Intra-nuclear trafficking of the BLM helicase to DNA damage-induced foci is regulated by SUMO modification. *Hum Mol Genet* **14**: 1351-1365.
- Elrouby N, Coupland G. 2010. Proteome-wide screens for small ubiquitin-like modifier (SUMO) substrates identify *Arabidopsis* proteins implicated in diverse biological processes. *Proc Natl Acad Sci USA* **107**: 17415-17420.
- Elsasser S, Chi Y, Yang P, Campbell JL. 1999. Phosphorylation controls timing of Cdc6p destruction: A biochemical analysis. *Mol Biol Cell* **10**: 3263-3277.
- Elsasser S, Lou F, Wang B, Campbell JL, Jong A. 1996. Interaction between yeast Cdc6 protein and B-type cyclin/Cdc28 kinases. *Mol Biol Cell* **7**: 1723-1735.
- Falck J, Coates J, Jackson SP. 2005. Conserved modes of recruitment of ATM, ATR and DNA-PKcs to sites of DNA damage. *Nature* **434**: 605-611.
- Fan J, Pavletich NP. 2012. Structure and conformational change of a replication protein A heterotrimer bound to ssDNA. *Genes Dev* **26**: 2337-2347.

- Feng W, Collingwood D, Boeck ME, Fox LA, Alvino GM, Fangman WL, Raghuraman MK, Brewer BJ. 2006. Genomic mapping of single-stranded DNA in hydroxyurea-challenged yeasts identifies origins of replication. *Nat Cell Biol* **8**: 148-155.
- Fernández-Cid A, Riera A, Tognetti S, Herrera MC, Samel S, Evrin C, Winkler C, Gardenal E, Uhle S, Speck C. 2013. An ORC/Cdc6/MCM2-7 complex is formed in a multistep reaction to serve as a platform for MCM double-hexamer assembly. *Mol Cell* **50**: 577-588.
- Ferreira MG, Santocanale C, Drury LS, Diffley JFX. 2000. Dbf4p, an essential S phase-promoting factor, is targeted for degradation by the anaphase-promoting complex. *Mol Cell Biol* **20**: 242-248.
- Fragkos M, Ganier O, Coulombe P, Mechali M. 2015. DNA replication origin activation in space and time. *Nat Rev Mol Cell Biol* **16**: 360-374.
- Francis LI, Randell JCW, Takara TJ, Uchima L, Bell SP. 2009. Incorporation into the prereplicative complex activates the Mcm2-7 helicase for Cdc7-Dbf4 phosphorylation. *Genes Dev* **23**: 643-654.
- Friedman KL, Brewer BJ. 1995. Analysis of replication intermediates by two-dimensional agarose gel electrophoresis. *Meth Enzymol* **262**: 613-627.
- Frigola J, Remus D, Mehanna A, Diffley JFX. 2013. ATPase-dependent quality control of DNA replication origin licensing. *Nature* **495**: 339-343.
- Fukunaga K, Kwon Y, Sung P, Sugimoto K. 2011. Activation of protein kinase Tel1 through recognition of protein-bound DNA ends. *Mol Cell Biol* **31**: 1959-1971.
- Gaillard H, Garcia-Muse T, Aguilera A. 2015. Replication stress and cancer. *Nat rev Cancer* **15**: 276-289.
- Galanty Y, Belotserkovskaya R, Coates J, Polo S, Miller KM, Jackson SP. 2009. Mammalian SUMO E3-ligases PIAS1 and PIAS4 promote responses to DNA double-strand breaks. *Nature* **462**: 935-939.
- Gambus A, Jones RC, Sanchez-Diaz A, Kanemaki M, van Deursen F, Edmondson RD, Labib K. 2006. GINS maintains association of Cdc45 with MCM in replisome progression complexes at eukaryotic DNA replication forks. *Nat Cell Biol* **8**: 358-366.
- Gao J, Aksoy BA, Dogrusoz U, Dresdner G, Gross B, Sumer SO, Sun Y, Jacobsen A, Sinha R, Larsson E et al. 2013. Integrative analysis of complex cancer genomics and clinical profiles using the cBioPortal. *Sci Signal* **6**: pl1.
- Gareau JR, Lima CD. 2010. The SUMO pathway: emerging mechanisms that shape specificity, conjugation and recognition. *Nat Rev Mol cell biol* **11**: 861-871.
- Geiss-Friedlander R, Melchior F. 2007a. Concepts in sumoylation: a decade on. *Nat Rev Mol Cell Biol* **8**: 947-956.

- Geiss-Friedlander R, Melchior F. 2007b. Concepts in sumoylation: a decade on. *Nat Rev Mol Cell Biol* **8**: 947-956.
- Gilbert CS, Green CM, Lowndes NF. 2001. Budding yeast Rad9 is an ATP-dependent Rad53 activating machine. *Mol Cell* **8**: 129-136.
- Gobbini E, Villa M, Gnugnoli M, Menin L, Clerici M, Longhese MP. 2015. Sae2 Function at DNA Double-Strand Breaks Is Bypassed by Dampening Tel1 or Rad53 Activity. *PLoS genetics* **11**: e1005685.
- Golebiowski F, Matic I, Tatham MH, Cole C, Yin Y, Nakamura A, Cox J, Barton GJ, Mann M, Hay RT. 2009. System-wide changes to SUMO modifications in response to heat shock. *Sci Signal* **2**: ra24.
- Granata M, Lazzaro F, Novarina D, Panigada D, Puddu F, Abreu CM, Kumar R, Grenon M, Lowndes NF, Plevani P et al. 2010. Dynamics of Rad9 chromatin binding and checkpoint function are mediated by its dimerization and are cell cycle-regulated by CDK1 activity. *PLoS genetics* **6**.
- Guillemain G, Ma E, Mauger S, Miron S, Thai R, Guerois R, Ochsenbein F, Marsolier-Kergoat MC. 2007. Mechanisms of checkpoint kinase Rad53 inactivation after a double-strand break in *Saccharomyces cerevisiae*. *Mol Cell Biol* **27**: 3378-3389.
- Guo L, Giasson BI, Glavis-Bloom A, Brewer MD, Shorter J, Gitler AD, Yang X. 2014. A cellular system that degrades misfolded proteins and protects against neurodegeneration. *Mol Cell* **55**: 15-30.
- Guo Z, Kanjanapangka J, Liu N, Liu S, Liu C, Wu Z, Wang Y, Loh T, Kowolik C, Jamsen J et al. 2012. Sequential Posttranslational Modifications Program FEN1 Degradation during Cell-Cycle Progression. *Mol Cell* **47**: 444-456.
- Hammet A, Magill C, Heierhorst J, Jackson SP. 2007. Rad9 BRCT domain interaction with phosphorylated H2AX regulates the G1 checkpoint in budding yeast. *EMBO Rep* **8**: 851-857.
- Hang LE, Peng J, Tan W, Szakal B, Menolfi D, Sheng Z, Lobachev K, Branzei D, Feng W, Zhao X. 2015. Rtt107 Is a Multi-functional Scaffold Supporting Replication Progression with Partner SUMO and Ubiquitin Ligases. *Mol Cell* **60**: 268-279.
- Hardy CF, Dryga O, Seematter S, Pahl PM, Sclafani RA. 1997. mcm5/cdc46-bob1 bypasses the requirement for the S phase activator Cdc7p. *Proc Natl Acad Sci USA* **94**: 3151-3155.
- Harrison JC, Haber JE. 2006. Surviving the breakup: the DNA damage checkpoint. *Annu Rev Genet* **40**: 209-235.
- Havens KA, Guseman JM, Jang SS, Pierre-Jerome E, Bolten N, Klavins E, Nemhauser JL. 2012. A synthetic approach reveals extensive tunability of auxin signaling. *Plant Physiol* **160**: 135-142.

- Hawkins M, Retkute R, Muller CA, Saner N, Tanaka TU, de Moura AP, Nieduszynski CA. 2013. High-resolution replication profiles define the stochastic nature of genome replication initiation and termination. *Cell Rep* **5**: 1132-1141.
- Hay RT. 2005. SUMO: a history of modification. *Mol Cell* **18**: 1-12.
- Hayano M, Kanoh Y, Matsumoto S, Renard-Guillet C, Shirahige K, Masai H. 2012. Rif1 is a global regulator of timing of replication origin firing in fission yeast. *Genes Dev.* **26**: 137-150.
- Heller RC, Kang S, Lam WM, Chen S, Chan CS, Bell SP. 2011. Eukaryotic origin-dependent DNA replication in vitro reveals sequential action of DDK and S-CDK kinases. *Cell* **146**: 80-91.
- Hendriks IA, D'Souza RC, Yang B, Verlaan-de Vries M, Mann M, Vertegaal AC. 2014. Uncovering global SUMOylation signaling networks in a site-specific manner. *Nat Struct Mol Biol* **21**: 927-936.
- Hickey CM, Wilson NR, Hochstrasser M. 2012. Function and regulation of SUMO proteases. *Nat Rev Mol Cell Biol* **13**: 755-766.
- Hiraga S-I, Alvino GM, Chang F, Lian H-Y, Sridhar A, Kubota T, BREWER BJ, Weinreich M, Raghuraman MK, Donaldson AD. 2014. Rif1 controls DNA replication by directing Protein Phosphatase 1 to reverse Cdc7-mediated phosphorylation of the MCM complex. *Genes Dev* **28**: 372-383.
- Hoegge C, Pfander B, Moldovan G-L, Pyrowolakis G, Jentsch S. 2002. RAD6-dependent DNA repair is linked to modification of PCNA by ubiquitin and SUMO. *Nature* **419**: 135-141.
- Hogg M, Osterman P, Bylund GO, Ganai RA, Lundström E-B, Sauer-Eriksson AE, Johansson E. 2014. Structural basis for processive DNA synthesis by yeast DNA polymerase ϵ . *Nat Struct Mol Biol* **21**: 49-55.
- Ilves I, Petojevic T, Pesavento JJ, Botchan MR. 2010. Activation of the MCM2-7 helicase by association with Cdc45 and GINS proteins. *Mol Cell* **37**: 247-258.
- Impens F, Radoshevich L, Cossart P, Ribet D. 2014. Mapping of SUMO sites and analysis of SUMOylation changes induced by external stimuli. *Proc Natl Acad Sci USA* **111**: 12432-12437.
- Jackson AP, Laskey RA, Coleman N. 2014. Replication proteins and human disease. *Cold Spring Harb Perspect Biol* **6**: 327-342.
- Jacques C, Baris O, Prunier-Mirebeau D, Savagner F, Rodien P, Rohmer V, Franc B, Guyetant S, Malhiery Y, Reynier P. 2005. Two-step differential expression analysis reveals a new set of genes involved in thyroid oncocytic tumors. *J Clin Endocrinol Metab* **90**: 2314-2320.
- Johansson E, Speck C, Chabes A. 2011. A top-down view on DNA replication and recombination from 9,000 feet above sea level. *Genome Biol* **12**:304.

- Johnson ES. 2004. Protein modification by SUMO. *Annu Rev Biochem* **73**: 355-382.
- Johnson ES, Gupta AA. 2001. An E3-like factor that promotes SUMO conjugation to the yeast septins. *Cell* **106**: 735-744.
- Kang YH, Galal WC, Farina A, Tappin I, Hurwitz J. 2012. Properties of the human Cdc45/Mcm2-7/GINS helicase complex and its action with DNA polymerase epsilon in rolling circle DNA synthesis. *Proc Natl Acad Sci USA* **109**: 6042-6047.
- Kanter DM, Kaplan DL. 2011. Sld2 binds to origin single-stranded DNA and stimulates DNA annealing. *Nucleic Acids Res* **39**: 2580-2592.
- Karras GI, Jentsch S. 2010. The RAD6 DNA damage tolerance pathway operates uncoupled from the replication fork and is functional beyond S phase. *Cell* **141**: 255-267.
- Kelly TJ, Brown GW. 2000. Regulation of chromosome replication. *Annu Rev Biochem* **69**: 829-880.
- Kesti T, Flick K, Keranen S, Syvaaja JE, Wittenberg C. 1999. DNA polymerase epsilon catalytic domains are dispensable for DNA replication, DNA repair, and cell viability. *Mol Cell* **3**: 679-685.
- Klemm RD, Austin RJ, Bell SP. 1997. Coordinate binding of ATP and origin DNA regulates the ATPase activity of the origin recognition complex. *Cell* **88**: 493-502.
- Klemm RD, Bell SP. 2001. ATP bound to the origin recognition complex is important for preRC formation. *Proc Natl Acad Sci USA* **98**: 8361-8367.
- Klug H, Xaver M, Chaugule VK, Koidl S, Mittler G, Klein F, Pichler A. 2013. Ubc9 sumoylation controls SUMO chain formation and meiotic synapsis in *Saccharomyces cerevisiae*. *Mol Cell* **50**: 625-636.
- Knuesel M, Cheung HT, Hamady M, Barthel KK, Liu X. 2005. A method of mapping protein sumoylation sites by mass spectrometry using a modified small ubiquitin-like modifier 1 (SUMO-1) and a computational program. *Mol Cell Proteomics* **4**: 1626-1636.
- Krejci L, Van Komen S, Li Y, Villemain J, Reddy MS, Klein H, Ellenberger T, Sung P. 2003. DNA helicase Srs2 disrupts the Rad51 presynaptic filament. *Nature* **423**: 305-309.
- Kroetz MB, Su D, Hochstrasser M. 2009. Essential role of nuclear localization for yeast Ulp2 SUMO protease function. *Mol Biol Cell* **20**: 2196-2206.
- Kumar S, Burgers PM. 2013. Lagging strand maturation factor Dna2 is a component of the replication checkpoint initiation machinery. *Genes Dev.* **27**: 313-321.
- Labib K, Diffley JF, Kearsley SE. 1999. G1-phase and B-type cyclins exclude the DNA-replication factor Mcm4 from the nucleus. *Nat cell biol* **1**: 415-422.
- Labib K, Kearsley SE, Diffley JF. 2001. MCM2-7 proteins are essential components of prereplicative complexes that accumulate cooperatively in the nucleus during G1-phase

and are required to establish, but not maintain, the S-phase checkpoint. *Mol Biol Cell* **12**: 3658-3667.

Lamoliatte F, Caron D, Durette C, Mahrouche L, Maroui MA, Caron-Lizotte O, Bonneil E, Chelbi-Alix MK, Thibault P. 2014. Large-scale analysis of lysine SUMOylation by SUMO remnant immunoaffinity profiling. *Nat commun* **5**: 5409.

Langston LD, Zhang D, Yurieva O, Georgescu RE, Finkelstein J, Yao NY, Indiani C, O'Donnell ME. 2014. CMG helicase and DNA polymerase epsilon form a functional 15-subunit holoenzyme for eukaryotic leading-strand DNA replication. *Proc Natl Acad Sci USA* **111**: 15390-15395.

Lao Y, Lee CG, Wold MS. 1999. Replication protein A interactions with DNA. 2. Characterization of double-stranded DNA-binding/helix-destabilization activities and the role of the zinc-finger domain in DNA interactions. *Biochemistry* **38**: 3974-3984.

Lecona E, Fernandez-Capetillo O. 2014. Replication stress and cancer: it takes two to tango. *Exp Cell Res* **329**: 26-34.

Lecona E, Rodriguez-Acebes S, Specks J, Lopez-Contreras AJ, Ruppen I, Murga M, Munoz J, Mendez J, Fernandez-Capetillo O. 2016. USP7 is a SUMO deubiquitinase essential for DNA replication. *Nat Struct Mol Biol* **23**: 270-277.

Lee J-K, Seo Y-S, Hurwitz J. 2003a. The Cdc23 (Mcm10) protein is required for the phosphorylation of minichromosome maintenance complex by the Dfp1-Hsk1 kinase. *Proc Natl Acad Sci USA* **100**: 2334-2339.

Lee JH, Paull TT. 2004. Direct activation of the ATM protein kinase by the Mre11/Rad50/Nbs1 complex. *Science* **304**: 93-96.

-. 2005. ATM activation by DNA double-strand breaks through the Mre11-Rad50-Nbs1 complex. *Science* **308**: 551-554.

Lee SJ, Schwartz MF, Duong JK, Stern DF. 2003b. Rad53 phosphorylation site clusters are important for Rad53 regulation and signaling. *Mol Cell Biol* **23**: 6300-6314.

Lei M, Kawasaki Y, Young MR, Kihara M, Sugino A, Tye BK. 1997. Mcm2 is a target of regulation by Cdc7-Dbf4 during the initiation of DNA synthesis. *Genes Dev.* **11**: 3365-3374.

Lengsfeld BM, Rattray AJ, Bhaskara V, Ghirlando R, Paull TT. 2007. Sae2 is an endonuclease that processes hairpin DNA cooperatively with the Mre11/Rad50/Xrs2 complex. *Mol Cell* **28**: 638-651.

Leroy C, Lee SE, Vaze MB, Ochsenbein F, Guerois R, Haber JE, Marsolier-Kergoat MC. 2003. PP2C phosphatases Ptc2 and Ptc3 are required for DNA checkpoint inactivation after a double-strand break. *Mol Cell* **11**: 827-835.

Li SJ, Hochstrasser M. 1999. A new protease required for cell-cycle progression in yeast. *Nature* **398**: 246-251.

- . 2000. The yeast ULP2 (SMT4) gene encodes a novel protease specific for the ubiquitin-like Smt3 protein. *Mol Cell Biol* **20**: 2367-2377.
- Liang C, Weinreich M, Stillman B. 1995. ORC and Cdc6p interact and determine the frequency of initiation of DNA replication in the genome. *Cell* **81**: 667-676.
- Liku ME, Nguyen VQ, Rosales AW, Irie K, Li JJ. 2005. CDK phosphorylation of a novel NLS-NES module distributed between two subunits of the Mcm2-7 complex prevents chromosomal rereplication. *Mol Biol Cell* **16**: 5026-5039.
- Lisby M, Barlow JH, Burgess RC, Rothstein R. 2004. Choreography of the DNA damage response: spatiotemporal relationships among checkpoint and repair proteins. *Cell* **118**: 699-713.
- Lobachev KS, Gordenin DA, Resnick MA. 2002. The Mre11 complex is required for repair of hairpin-capped double-strand breaks and prevention of chromosome rearrangements. *Cell* **108**: 183-193.
- Lopez-Contreras AJ, Ruppen I, Nieto-Soler M, Murga M, Rodriguez-Acebes S, Remeseiro S, Rodrigo-Perez S, Rojas AM, Méndez J, Muñoz J et al. 2013. A Proteomic Characterization of Factors Enriched at Nascent DNA Molecules. *Cell Rep* **3**:1105-1116.
- Lopez-Mosqueda J, Maas NL, Jonsson ZO, Defazio-Eli LG, Wohlschlegel J, Toczyski DP. 2010. Damage-induced phosphorylation of Sld3 is important to block late origin firing. *Nature* **467**: 479-483.
- Lu CY, Tsai CH, Brill SJ, Teng SC. 2010. Sumoylation of the BLM ortholog, Sgs1, promotes telomere-telomere recombination in budding yeast. *Nucleic Acids Res* **38**: 488-498.
- Ma L, Aslanian A, Sun H, Jin M, Shi Y, Yates JR, 3rd, Hunter T. 2014. Identification of small ubiquitin-like modifier substrates with diverse functions using the *Xenopus* egg extract system. *Mol Cell proteomics* **13**: 1659-1675.
- Macheret M, Halazonetis TD. 2015. DNA replication stress as a hallmark of cancer. *Annu Rev Pathol* **10**: 425-448.
- Makhnevych T, Sydorskyy Y, Xin X, Srikumar T, Vizeacoumar FJ, Jeram SM, Li Z, Bahr S, Andrews BJ, Boone C et al. 2009. Global map of SUMO function revealed by protein-protein interaction and genetic networks. *Mol Cell* **33**: 124-135.
- Mantiero D, Mackenzie A, Donaldson A, Zegerman P. 2011. Limiting replication initiation factors execute the temporal programme of origin firing in budding yeast. *EMBOJ* **30**: 4805-4814.
- Maric M, Maculins T, De Piccoli G, Labib K. 2014. Cdc48 and a ubiquitin ligase drive disassembly of the CMG helicase at the end of DNA replication. *Science* **346**: 1253596.
- Masai H, Matsumoto S, You Z, Yoshizawa-Sugata N, Oda M. 2010. Eukaryotic chromosome DNA replication: where, when, and how? *Annu Rev Biochem* **79**: 89-130.

- Masai H, Taniyama C, Ogino K, Matsui E, Kakusho N, Matsumoto S, Kim J-M, Ishii A, Tanaka T, Kobayashi T et al. 2006. Phosphorylation of MCM4 by Cdc7 kinase facilitates its interaction with Cdc45 on the chromatin. *J Biol Chem* **281**: 39249-39261.
- Masumoto H, Muramatsu S, Kamimura Y, Araki H. 2002. S-Cdk-dependent phosphorylation of Sld2 essential for chromosomal DNA replication in budding yeast. *Nature* **415**: 651-655.
- Mattarocci S, Shyian M, Lemmens L, Damay P, Altintas DM, Shi T, Bartholomew CR, Thomä NH, Hardy CFJ, Shore D. 2014. Rif1 controls DNA replication timing in yeast through the PP1 phosphatase Glc7. *Cell Rep* **7**: 62-69.
- Mimitou EP, Symington LS. 2008. Sae2, Exo1 and Sgs1 collaborate in DNA double-strand break processing. *Nature* **455**: 770-774.
- Montagnoli A, Valsasina B, Brotherton D, Troiani S, Rainoldi S, Tenca P, Molinari A, Santocanale C. 2006. Identification of Mcm2 phosphorylation sites by S-phase-regulating kinases. *J Biol Chem* **281**: 10281-10290.
- Mordes DA, Nam EA, Cortez D. 2008. Dpb11 activates the Mec1-Ddc2 complex. *Proc Natl Acad Sci USA* **105**: 18730-18734.
- Morohashi H, Maculins T, Labib K. 2009. The amino-terminal TPR domain of Dia2 tethers SCF(Dia2) to the replisome progression complex. *Curr Biol* **19**: 1943-1949.
- Morris JR, Boutell C, Keppler M, Densham R, Weekes D, Alamshah A, Butler L, Galanty Y, Pangon L, Kiuchi T et al. 2009. The SUMO modification pathway is involved in the BRCA1 response to genotoxic stress. *Nature* **462**: 886-U877.
- Mossesso E, Lima CD. 2000a. Ulp1-SUMO crystal structure and genetic analysis reveal conserved interactions and a regulatory element essential for cell growth in yeast. *Mol Cell* **5**: 865-876.
- Mossesso E, Lima CD. 2000b. Ulp1-SUMO crystal structure and genetic analysis reveal conserved interactions and a regulatory element essential for cell growth in yeast. *Mol Cell* **5**: 865-876.
- Moyer SE, Lewis PW, Botchan MR. 2006a. Isolation of the Cdc45/Mcm2-7/GINS (CMG) complex, a candidate for the eukaryotic DNA replication fork helicase. *Proc Natl Acad Sci USA* **103**: 10236-10241.
- Moyer SE, Lewis PW, Botchan MR. 2006b. Isolation of the Cdc45/Mcm2-7/GINS (CMG) complex, a candidate for the eukaryotic DNA replication fork helicase. *Proc Natl Acad Sci USA* **103**: 10236-10241.
- Murakami H, Keeney S. 2014. Temporospatial coordination of meiotic DNA replication and recombination via DDK recruitment to replisomes. *Cell* **158**: 861-873.
- Muramatsu S, Hirai K, Tak Y-S, Kamimura Y, Araki H. 2010. CDK-dependent complex formation between replication proteins Dpb11, Sld2, Pol (epsilon), and GINS in budding yeast. *Genes Dev* **24**: 602-612.

- Nakada D, Matsumoto K, Sugimoto K. 2003. ATM-related Tel1 associates with double-strand breaks through an Xrs2-dependent mechanism. *Genes Dev* **17**: 1957-1962.
- Navadgi-Patil VM, Burgers PM. 2008. Yeast DNA replication protein Dpb11 activates the Mec1/ATR checkpoint kinase. *J Biol Chem* **283**: 35853-35859.
- . 2009. The unstructured C-terminal tail of the 9-1-1 clamp subunit Ddc1 activates Mec1/ATR via two distinct mechanisms. *Mol Cell* **36**: 743-753.
- Navas TA, Zhou Z, Elledge SJ. 1995. DNA polymerase epsilon links the DNA replication machinery to the S phase checkpoint. *Cell* **80**: 29-39.
- Neale MJ, Pan J, Keeney S. 2005. Endonucleolytic processing of covalent protein-linked DNA double-strand breaks. *Nature* **436**: 1053-1057.
- Nguyen VQ, Co C, Irie K, Li JJ. 2000. Clb/Cdc28 kinases promote nuclear export of the replication initiator proteins Mcm2-7. *Curr Biol* **10**: 195-205.
- Nguyen VQ, Co C, Li JJ. 2001. Cyclin-dependent kinases prevent DNA re-replication through multiple mechanisms. *Nature* **411**: 1068-1073.
- Nick McElhinny SA, Gordenin DA, Stith CM, Burgers PMJ, Kunkel TA. 2008. Division of Labor at the Eukaryotic Replication Fork. *Mol Cell* **30**: 137-144.
- Nicolette ML, Lee K, Guo Z, Rani M, Chow JM, Lee SE, Paull TT. 2010. Mre11-Rad50-Xrs2 and Sae2 promote 5' strand resection of DNA double-strand breaks. *Nat Struct Mol Biol* **17**: 1478-1485.
- Nimonkar AV, Genschel J, Kinoshita E, Polaczek P, Campbell JL, Wyman C, Modrich P, Kowalczykowski SC. 2011. BLM-DNA2-RPA-MRN and EXO1-BLM-RPA-MRN constitute two DNA end resection machineries for human DNA break repair. *Genes Dev.* **25**: 350-362.
- Nishimura K, Fukagawa T, Takisawa H, Kakimoto T, Kanemaki M. 2009. An auxin-based degron system for the rapid depletion of proteins in nonplant cells. *Nat Methods* **6**: 917-922.
- Niu H, Chung WH, Zhu Z, Kwon Y, Zhao W, Chi P, Prakash R, Seong C, Liu D, Lu L et al. 2010. Mechanism of the ATP-dependent DNA end-resection machinery from *Saccharomyces cerevisiae*. *Nature* **467**: 108-111.
- O'Neill BM, Szyjka SJ, Lis ET, Bailey AO, Yates JR, Aparicio OM, Romesberg FE. 2007. Pph3-Psy2 is a phosphatase complex required for Rad53 dephosphorylation and replication fork restart during recovery from DNA damage. *Proc Natl Acad Sci USA* **104**: 9290-9295.
- Oakley GG, Patrick SM. 2010. Replication protein A: directing traffic at the intersection of replication and repair. *Front in biosci* **15**: 883-900.

- Ohouo PY, Bastos de Oliveira FM, Liu Y, Ma CJ, Smolka MB. 2013. DNA-repair scaffolds dampen checkpoint signalling by counteracting the adaptor Rad9. *Nature* **493**: 120-124.
- Osborn AJ, Elledge SJ. 2003. Mrc1 is a replication fork component whose phosphorylation in response to DNA replication stress activates Rad53. *Genes Dev* **17**: 1755-1767.
- Oshiro G, Owens JC, Shellman Y, Sclafani RA, Li JJ. 1999. Cell cycle control of Cdc7p kinase activity through regulation of Dbf4p stability. *Mol Cell Biol* **19**: 4888-4896.
- Pacek M, Tutter AV, Kubota Y, Takisawa H, Walter JC. 2006. Localization of MCM2-7, Cdc45, and GINS to the site of DNA unwinding during eukaryotic DNA replication. *Mol Cell* **21**: 581-587.
- Panse VG, Kuster B, Gerstberger T, Hurt E. 2003. Unconventional tethering of Ulp1 to the transport channel of the nuclear pore complex by karyopherins. *Nat Cell Biol* **5**: 21-27.
- Papouli E, Chen S, Davies AA, Huttner D, Krejci L, Sung P, Ulrich HD. 2005. Crosstalk between SUMO and Ubiquitin on PCNA Is Mediated by Recruitment of the Helicase Srs2p. *Mol Cell* **19**: 123-133.
- Perkins G, Drury LS, Diffley JF. 2001. Separate SCF(CDC4) recognition elements target Cdc6 for proteolysis in S phase and mitosis. *EMBO J* **20**: 4836-4845.
- Pfander B, Diffley JF. 2011. Dpb11 coordinates Mec1 kinase activation with cell cycle-regulated Rad9 recruitment. *EMBO J* **30**: 4897-4907.
- Pike BL, Yongkiettrakul S, Tsai MD, Heierhorst J. 2003. Diverse but overlapping functions of the two forkhead-associated (FHA) domains in Rad53 checkpoint kinase activation. *J Biol Chem* **278**: 30421-30424.
- Poh WT, Chadha GS, Gillespie PJ, Kaldis P, Blow JJ. 2014. Xenopus Cdc7 executes its essential function early in S phase and is counteracted by checkpoint-regulated protein phosphatase 1. *Open Biol* **4**: 130138.
- Priego Moreno S, Bailey R, Champion N, Herron S, Gambus A. 2014. Polyubiquitylation drives replisome disassembly at the termination of DNA replication. *Science* **346**: 477-481.
- Psakhye I, Jentsch S. 2012. Protein Group Modification and Synergy in the SUMO Pathway as Exemplified in DNA Repair. *Cell* **151**: 807-820.
- Puddu F, Granata M, Di Nola L, Balestrini A, Piergiovanni G, Lazzaro F, Giannattasio M, Plevani P, Muzi-Falconi M. 2008. Phosphorylation of the budding yeast 9-1-1 complex is required for Dpb11 function in the full activation of the UV-induced DNA damage checkpoint. *Mol Cell Biol* **28**: 4782-4793.

- Ramer MD, Suman ES, Richter H, Stanger K, Spranger M, Bieberstein N, Duncker BP. 2013. Dbf4 and Cdc7 proteins promote DNA replication through interactions with distinct Mcm2-7 protein subunits. *J Biol Chem* **288**: 14926-14935.
- Randell JCW, Bowers JL, Rodríguez HK, Bell SP. 2006. Sequential ATP hydrolysis by Cdc6 and ORC directs loading of the Mcm2-7 helicase. *Mol Cell* **21**: 29-39.
- Randell JCW, Fan A, Chan C, Francis LI, Heller RC, Galani K, Bell SP. 2010. Mec1 is one of multiple kinases that prime the Mcm2-7 helicase for phosphorylation by Cdc7. *Mol Cell* **40**: 353-363.
- Rao H, Stillman B. 1995. The origin recognition complex interacts with a bipartite DNA binding site within yeast replicators. *Proc Natl Acad Sci USA* **92**: 2224-2228.
- Reid RJ, Lisby M, Rothstein R. 2002. Cloning-free genome alterations in *Saccharomyces cerevisiae* using adaptamer-mediated PCR. *Methods Enzymol* **350**: 258-277.
- Remus D, Diffley JFX. 2009. Eukaryotic DNA replication control: lock and load, then fire. *Curr Opin Cell Biol* **21**: 771-777.
- Rowley A, Cocker JH, Harwood J, Diffley JF. 1995. Initiation complex assembly at budding yeast replication origins begins with the recognition of a bipartite sequence by limiting amounts of the initiator, ORC. *EMBO J* **14**: 2631-2641.
- Sabate R, Espargaro A, Grana-Montes R, Reverter D, Ventura S. 2012. Native structure protects SUMO proteins from aggregation into amyloid fibrils. *Biomacromolecules* **13**: 1916-1926.
- Sacher M, Pfander B, Hoegge C, Jentsch S. 2006. Control of Rad52 recombination activity by double-strand break-induced SUMO modification. *Nat Cell Biol* **8**: 1284-1290.
- Saito K, Kagawa W, Suzuki T, Suzuki H, Yokoyama S, Saitoh H, Tashiro S, Dohmae N, Kurumizaka H. 2010. The putative nuclear localization signal of the human RAD52 protein is a potential sumoylation site. *J Biochem* **147**: 833-842.
- Sakofsky CJ, Roberts SA, Malc E, Mieczkowski PA, Resnick MA, Gordenin DA, Malkova A. 2014. Break-induced replication is a source of mutation clusters underlying kataegis. *Cell Rep* **7**: 1640-1648.
- Samel SA, Fernandez-Cid A, Sun J, Riera A, Tognetti S, Herrera MC, Li H, Speck C. 2014. A unique DNA entry gate serves for regulated loading of the eukaryotic replicative helicase MCM2-7 onto DNA. *Genes Dev* **28**: 1653-1666.
- Sánchez M, Calzada A, Bueno A. 1999. The Cdc6 protein is ubiquitinated in vivo for proteolysis in *Saccharomyces cerevisiae*. *J Biol Chem* **274**: 9092-9097.
- Sarangi P, Altmannova V, Holland C, Bartosova Z, Hao F, Anrather D, Ammerer G, Lee SE, Krejci L, Zhao X. 2014a. A versatile scaffold contributes to damage survival via sumoylation and nuclease interactions. *Cell Rep* **9**: 143-152.

- Sarangi P, Bartosova Z, Altmannova V, Holland C, Chavdarova M, Lee SE, Krejci L, Zhao X. 2014b. Sumoylation of the Rad1 nuclease promotes DNA repair and regulates its DNA association. *Nucleic Acids Res* **42**: 6393-6404.
- Sarangi P, Steinacher R, Altmannova V, Fu Q, Paull TT, Krejci L, Whitby MC, Zhao X. 2015. Sumoylation influences DNA break repair partly by increasing the solubility of a conserved end resection protein. *PLoS genetics* **11**: e1004899.
- Sarangi P, Zhao X. 2015. SUMO-mediated regulation of DNA damage repair and responses. *Trends Biochem Sci* **40**: 233-242.
- Schepers A, Diffley JF. 2001. Mutational analysis of conserved sequence motifs in the budding yeast Cdc6 protein. *J Mol Biol* **308**: 597-608.
- Schimmel J, Eifler K, Sigurethsson JO, Cuijpers SA, Hendriks IA, Verlaan-de Vries M, Kelstrup CD, Francavilla C, Medema RH, Olsen JV et al. 2014. Uncovering SUMOylation dynamics during cell-cycle progression reveals FoxM1 as a key mitotic SUMO target protein. *Mol Cell* **53**: 1053-1066.
- Schwartz DC, Felberbaum R, Hochstrasser M. 2007. The Ulp2 SUMO Protease Is Required for Cell Division following Termination of the DNA Damage Checkpoint. *Mol Cell Biol* **27**: 6948-6961.
- Schwartz MF, Duong JK, Sun Z, Morrow JS, Pradhan D, Stern DF. 2002. Rad9 phosphorylation sites couple Rad53 to the *Saccharomyces cerevisiae* DNA damage checkpoint. *Mol Cell* **9**: 1055-1065.
- Sclafani RA, Holzen TM. 2007. Cell Cycle Regulation of DNA Replication. *Annu Rev Genet* **41**: 237-280.
- Sengupta S, van Deursen F, De Piccoli G, Labib K. 2013. Dpb2 Integrates the Leading-Strand DNA Polymerase into the Eukaryotic Replisome. *Curr Biol* **23**:543-552
- Shanbhag NM, Rafalska-Metcalf IU, Balane-Bolivar C, Janicki SM, Greenberg RA. 2010. ATM-Dependent Chromatin Changes Silence Transcription In cis to DNA Double-Strand Breaks. *Cell* **141**: 970-981.
- Shcherbakova PV, Pavlov YI, Chilkova O, Rogozin IB, Johansson E, Kunkel TA. 2003. Unique error signature of the four-subunit yeast DNA polymerase epsilon. *J Biol Chem* **278**: 43770-43780.
- Sheu Y-J, Stillman B. 2006. Cdc7-Dbf4 phosphorylates MCM proteins via a docking site-mediated mechanism to promote S phase progression. *Mol Cell* **24**: 101-113.
- . 2010. The Dbf4-Cdc7 kinase promotes S phase by alleviating an inhibitory activity in Mcm4. *Nature* **463**: 113-117.
- Sheu YJ, Kinney JB, Lengronne A, Pasero P, Stillman B. 2014. Domain within the helicase subunit Mcm4 integrates multiple kinase signals to control DNA replication initiation and fork progression. *Proc Natl Acad Sci USA* **111**: E1899-1908.

- Sogo JM, Lopes M, Foiani M. 2002. Fork reversal and ssDNA accumulation at stalled replication forks owing to checkpoint defects. *Science* **297**: 599-602.
- Speck C, Chen Z, Li H, Stillman B. 2005. ATPase-dependent cooperative binding of ORC and Cdc6 to origin DNA. *Nat Struct Mol Biol* **12**: 965-971.
- Strunnikov AV, Aravind L, Koonin EV. 2001. *Saccharomyces cerevisiae* SMT4 encodes an evolutionarily conserved protease with a role in chromosome condensation regulation. *Genetics* **158**: 95-107.
- Sun J, Evrin C, Samel SA, Fernández-Cid A, Riera A, Kawakami H, Stillman B, Speck C, Li H. 2013. Cryo-EM structure of a helicase loading intermediate containing ORC-Cdc6-Cdt1-MCM2-7 bound to DNA. *Nat Struct Mol Biol* **20**: 944-951.
- Sun J, Shi Y, Georgescu RE, Yuan Z, Chait BT, Li H, O'Donnell ME. 2015. The architecture of a eukaryotic replisome. *Nat Struct Mol Biol* **22**: 976-982.
- Sung MK, Lim G, Yi DG, Chang YJ, Yang EB, Lee K, Huh WK. 2013. Genome-wide bimolecular fluorescence complementation analysis of SUMO interactome in yeast. *Genome Res* **23**: 736-746.
- Szyjka SJ, Aparicio JG, Viggiani CJ, Knott S, Xu W, Tavare S, Aparicio OM. 2008. Rad53 regulates replication fork restart after DNA damage in *Saccharomyces cerevisiae*. *Genes Dev*. **22**: 1906-1920.
- Tak Y-S, Tanaka Y, Endo S, Kamimura Y, Araki H. 2006. A CDK-catalysed regulatory phosphorylation for formation of the DNA replication complex Sld2-Dpb11. *EMBO J* **25**: 1987-1996.
- Takahashi Y, Dulev S, Liu XP, Hiller NJ, Zhao XL, Strunnikov A. 2008. Cooperation of Sumoylated Chromosomal Proteins in rDNA Maintenance. *PLoS Genet* **4**: 12.
- Takahashi Y, Toh-e A, Kikuchi Y. 2001. A novel factor required for the SUMO1/Smt3 conjugation of yeast septins. *Gene* **275**: 223-231.
- Tammsalu T, Matic I, Jaffray EG, Ibrahim AF, Tatham MH, Hay RT. 2015. Proteome-wide identification of SUMO modification sites by mass spectrometry. *Nat Protoc* **10**: 1374-1388.
- Tammsalu T, Matic I, Jaffray EG, Ibrahim AFM, Tatham MH, Hay RT. 2014. Proteome-wide identification of SUMO2 modification sites. *Sci signal* **7**: rs2.
- Tanaka S, Nakato R, Katou Y, Shirahige K, Araki H. 2011. Origin association of Sld3, Sld7, and Cdc45 proteins is a key step for determination of origin-firing timing. *Curr Biol* **21**: 2055-2063.
- Tanaka S, Umemori T, Hirai K, Muramatsu S, Kamimura Y, Araki H. 2007. CDK-dependent phosphorylation of Sld2 and Sld3 initiates DNA replication in budding yeast. *Nature* **445**: 328-332.

- Torres-Rosell J, Sunjevaric I, De Piccoli G, Sacher M, Eckert-Boulet N, Reid R, Jentsch S, Rothstein R, Aragon L, Lisby M. 2007. The Smc5-Smc6 complex and SUMO modification of Rad52 regulates recombinational repair at the ribosomal gene locus. *Nat Cell Biol* **9**: 923-931.
- Tsuji T, Ficarro SB, Jiang W. 2006. Essential role of phosphorylation of MCM2 by Cdc7/Dbf4 in the initiation of DNA replication in mammalian cells. *Mol Biol Cell* **17**: 4459-4472.
- Ulrich HD, Davies AA. 2009. In vivo detection and characterization of sumoylation targets in *Saccharomyces cerevisiae*. *Methods Mol Biol* **497**: 81-103.
- Vaze MB, Pelliccioli A, Lee SE, Ira G, Liberi G, Arbel-Eden A, Foiani M, Haber JE. 2002. Recovery from checkpoint-mediated arrest after repair of a double-strand break requires Srs2 helicase. *Mol Cell* **10**: 373-385.
- Veaute X, Jeusset J, Soustelle C, Kowalczykowski SC, Le Cam E, Fabre F. 2003. The Srs2 helicase prevents recombination by disrupting Rad51 nucleoprotein filaments. *Nature* **423**: 309-312.
- Visintin R, Craig K, Hwang ES, Prinz S, Tyers M, Amon A. 1998. The phosphatase Cdc14 triggers mitotic exit by reversal of Cdk-dependent phosphorylation. *Mol Cell* **2**: 709-718.
- Vogelstein B, Papadopoulos N, Velculescu VE, Zhou S, Diaz LA, Jr., Kinzler KW. 2013. Cancer genome landscapes. *Science* **339**: 1546-1558.
- Wei L, Zhao X. 2016a. A new MCM modification cycle regulates DNA replication initiation. *Nat Struct Mol Biol* **23**: 209-216.
- Wei L, Zhao X. 2016b. The Initiation of DNA Replication in Eukaryotes, Editors: Kaplan, Daniel L., Chapter 18: Role of Posttranslational Modifications in Replication Initiation Springer International Publishing, ISBN 978-3-319-24696-3.
- Weinert TA, Hartwell LH. 1988. The RAD9 gene controls the cell cycle response to DNA damage in *Saccharomyces cerevisiae*. *Science* **241**: 317-322.
- Weinreich M, Stillman B. 1999. Cdc7p-Dbf4p kinase binds to chromatin during S phase and is regulated by both the APC and the RAD53 checkpoint pathway. *EMBO J* **18**: 5334-5346.
- Wilmes GM, Archambault V, Austin RJ, Jacobson MD, Bell SP, Cross FR. 2004. Interaction of the S-phase cyclin Clb5 with an 'RXL' docking sequence in the initiator protein Orc6 provides an origin-localized replication control switch. *Genes Dev* **18**: 981-991.
- Wilson VG, Heaton PR. 2008. Ubiquitin proteolytic system: focus on SUMO. *Expert Rev proteomics* **5**: 121-135.

- Wohlschlegel JA, Johnson ES, Reed SI, Yates JR, 3rd. 2006. Improved identification of SUMO attachment sites using C-terminal SUMO mutants and tailored protease digestion strategies. *J Proteome Res* **5**: 761-770.
- Wold MS. 1997. Replication protein A: a heterotrimeric, single-stranded DNA-binding protein required for eukaryotic DNA metabolism. *Annu Rev Biochem* **66**: 61-92.
- Wotton D, Shore D. 1997. A novel Rap1p-interacting factor, Rif2p, cooperates with Rif1p to regulate telomere length in *Saccharomyces cerevisiae*. *Genes Dev* **11**: 748-760.
- Wu CS, Ouyang J, Mori E, Nguyen HD, Marechal A, Hallet A, Chen DJ, Zou L. 2014. SUMOylation of ATRIP potentiates DNA damage signaling by boosting multiple protein interactions in the ATR pathway. *Genes Dev*. **28**: 1472-1484.
- Yamazaki S, Ishii A, Kanoh Y, Oda M, Nishito Y, Masai H. 2012. Rif1 regulates the replication timing domains on the human genome. *EMBO J* **31**: 3667-3677.
- Yang XH, Zou L. 2006. Recruitment of ATR-ATRIP, Rad17, and 9-1-1 complexes to DNA damage. *Methods enzymol* **409**: 118-131.
- Yeeles JT, Deegan TD, Janska A, Early A, Diffley JF. 2015. Regulated eukaryotic DNA replication origin firing with purified proteins. *Nature* **519**: 431-435.
- Yeung M, Durocher D. 2011. Srs2 enables checkpoint recovery by promoting disassembly of DNA damage foci from chromatin. *DNA repair* **10**: 1213-1222.
- Yuan Z, Bai L, Sun J, Georgescu R, Liu J, O'Donnell ME, Li H. 2016. Structure of the eukaryotic replicative CMG helicase suggests a pumpjack motion for translocation. *Nat Struct Mol Biol* **23**: 217-224.
- Zegerman P, Diffley JFX. 2007. Phosphorylation of Sld2 and Sld3 by cyclin-dependent kinases promotes DNA replication in budding yeast. *Nature* **445**: 281-285.
- . 2010. Checkpoint-dependent inhibition of DNA replication initiation by Sld3 and Dbf4 phosphorylation. *Nature* **467**: 474-478.
- Zhao X, Blobel G. 2005a. A SUMO ligase is part of a nuclear multiprotein complex that affects DNA repair and chromosomal organization. *Proc Natl Acad Sci USA* **102**: 4777-4782.
- . 2005b. A SUMO ligase is part of a nuclear multiprotein complex that affects DNA repair and chromosomal organization. *Proc Natl Acad Sci USA* **102**: 4777-4782.
- Zhou C, Pourmal S, Pavletich NP. 2015. Dna2 nuclease-helicase structure, mechanism and regulation by Rpa. *eLife* **4**.
- Zhu Z, Chung WH, Shim EY, Lee SE, Ira G. 2008. Sgs1 helicase and two nucleases Dna2 and Exo1 resect DNA double-strand break ends. *Cell* **134**: 981-994.
- Zou L. 2013. Four pillars of the S-phase checkpoint. *Genes Dev* **27**: 227-233.

Zou L, Elledge SJ. 2003. Sensing DNA damage through ATRIP recognition of RPA-ssDNA complexes. *Science* **300**: 1542-1548.